Acta Horticulturae et Regiotecturae 2
Nitra, Slovaca Universitas Agriculturae Nitriae, 2019, pp. 56–60

DIFFERENCES IN WATER VAPOR ADSORPTION-DESORPTION OF NON AGED AND 3-YEAR AGED BIOCHAR IN SANDY SPODOSOLS

Eugene BALASHOV*, Irina MUKHINA, Elena RIZHIYA

Agrophysical Research Institute, St. Petersburg, Russia

Ageing of biochars in soil affects their surface properties and can cause changes in water vapor adsorption-desorption processes. Measurements of hygroscopic water contents and corresponding water potentials of non aged and 3-year aged biochars as well as of sandy soils with medium and high quality were carried out during 5 cycles of water vapor adsorption-desorption processes at a room temperature of 23.5 °C. The results showed a significantly lower content of maximum hygroscopic water in the aged biochars than that in the non aged biochar at the end of water vapor adsorption processes at high air humidity. A significantly higher affinity of the high quality soil to water vapor resulted in insignificant differences in the maximum hygroscopic water content and in significant changes in the corresponding water potentials as compared to the same properties of the soil with medium quality. Minimum content of hygroscopic water was significantly lower in the non aged biochar than in the aged biochars at the end of the water desorption processes at ambient laboratory atmosphere. There were insignificant differences in minimum contents of hygroscopic water and in the corresponding water potentials of the aged biochars from soils with medium and high quality.

Keywords: biochar, ageing, water vapor adsorption-desorption

In current conditions of climate change soils can be subjected to impacts of extreme weather factors and anthropogenic treatments which can lead to unfavorable changes in the indicators of their quality and sustainability. Apart from rational application of organic and mineral fertilizers, agricultural use of biochar is a promising way of sustainable and environmental management of soils (Lehmann et al., 2011).

Biochar is a product of the incomplete combustion of agricultural and forest waste. Organic matter of biochar includes amorphous and crystalline aromatic structures and, therefore, is resistant to biotic and abiotic mineralization (Keiluweit et al., 2010). Biochar is being produced in the process of slow (hours) and fast (minutes) pyrolysis of biomass without access of oxygen at high temperatures of 300–900 °C. Carbon content in biochar can exceed 80% depending on technological conditions of pyrolysis and feedstock type (Lehmann et al., 2011). Technological conditions of pyrolysis and type of feedstock result in different properties of biochar.

Incorporation of biochar into arable soils can lead to enhancing carbon sequestration, improvement of physical, physico-chemical, biological soil properties and to decreasing N_2O emission from soils (El-Naggar et al., 2019; Horák, 2015).

The recalcitrant nature of biochar does not mean that it remains unchanged when ageing in soils. The quantification of changes in the surface properties of biochar while ageing in soils is a crucial aim of current research. An oxidation of biochar in soils can lead to an increase in a density of oxygen-containing functional groups (OFGs) on its surface. The high density of polar OFGs (carboxyl, carbonyl and phenolic hydroxyl) on the biochar surface can increase its affinity to water molecules, nutrients and organic pollutants.

Current hydrophysical studies of biochars are mainly focused on measurements of their water retention curves and available water contents at high matric potentials (>-15 MPa) using pressure plate chambers (Marshall et al., 2019). Less attention has been paid to the assessment of water vapor adsorption-desorption characteristics of biochar surface while ageing in soils. Scientific information on these processes is needed for better understanding of temporal changes in the surface structural properties of aged biochars.

The objective of this study was to quantify the changes in water vapor adsorption-desorption characteristics of biochar after 3-year ageing in sandy Spodosols with medium and high quality.

Material and methods

The study was carried out at the Menkovo experimental station of the Agrophysical Research Institute in the St. Petersburg region of Russia (59° 34′ N, 30° 08′ E). The studied soil was classified as sandy Spodosol and contained 91.7% sand, 5.2% silt, and 3.1% clay particles. In early May of 2012 a small-scale field experiment was established with

Contact address: Assoc. prof. Eugene Balashov, PhD, Agrophysical Research Institute, Department of Soil Physics, Physical Chemistry and Biophysics, 14 Grazhdansky prospekt, St. Petersburg, 195220, Russia, e-mail: Eugene_Balashov@yahoo.co.uk

forty bottomless plastic buckets (30 cm in height and 30 cm in diameter). Empty buckets were dug into the 0–25 cm plough layers at an area of 5 m^2. Afterwards, samples of soils with medium (MQ) and high (HQ) quality (resulting from different soil management for the previous ten years) collected from the 0–25 cm layers were placed in the buckets at a bulk density of 1.2 $g.cm^{-3}$. The experiment included four treatments: control (no biochar, no N-fertilizer), biochar (12 $t.ha^{-1}$), N-fertilizer (90 $kg.ha^{-1}$.N) and biochar (12 $t.ha^{-1}$) + N-fertilizer (90 $kg.ha^{-1}$.N). The mineral N-fertilizer used in the experiment was ammonium nitrate (NH_4NO_3). There were five randomized replicates of each treatment for the HQ and MQ soils.

During growing seasons (May – September) of 2012 – 2014 the average air temperature was 14.3 °C, 15.5 °C, and 14.9 °C, respectively, while the total amount of precipitation for the periods reached 630 mm, 465 mm and 320 mm, respectively.

The MQ soil had acidic reaction (pH_{KCl} 5.6), contained 18.0 $g.C.kg^{-1}$ soil of soil organic matter (SOM), 1.6 $g.N.kg^{-1}$ soil of total N and 10.5 $mg.N.kg^{-1}$ soil of mineral nitrogen. The HQ soil had neutral reaction (pH_{KCl} 6.5) and contained 23.0 $g.C.kg^{-1}$ soil of SOM, 1.9 $g.N.kg^{-1}$ soil of total N and 47.7 $mg.N.kg^{-1}$ soil of mineral nitrogen. Spring barley (*Hordeum vulgare* L.) was grown on the experimental plot in 2012 and perennial grasses (*Phleum pratense* L. and *Trifolium pratense* L.) – in 2013 and 2014. The N fertilizers and biochar were mixed with topsoil layers (0–10 cm) at the beginning of the experiment. A particle size of the incorporated biochar was 2–5 mm. A fresh slow pyrolysis biochar was produced from small birch logs and branches in a controlled kiln at temperature of the pyrolysis of 650 °C. Afterwards, the produced biochar (or non aged biochar) was oxidated in air conditions during one year. Chemical and physical properties of the non aged biochar were: total carbon content – 825.5 $g.C.kg^{-1}$, total N content – 5.7 $g.N.kg^{-1}$, C/N ratio – 145, pH_{H_2O} – 7.0, moisture content –1.92% and ash content – 0.23%. All the soil chemical and physical analyses were conducted by standard and traditional methods used in Russian soil science laboratories (Rastvorova et al., 1995).

In September of 2014, bulk MQ and HQ soil samples and biochar particles of 2–5 mm were collected from experimental plots with the control and biochar (12 $t.ha^{-1}$) treatments. Air-dried soil samples were sieved through sieves of 3 mm and 5 mm to receive 3–5 mm soil fraction. Afterwards, these soil and biochar samples were stored for 5 years in hermetically sealed plastic vessels without access of oxygen at a room temperature of 20 °C. It was assumed that these storage conditions could not result in any significant changes in the surface and physicochemical properties of the soil and biochar samples. The 3–5 mm size fractions of the soils and 2–5 mm size fractions of the biochar were used in our study.

Before the beginning of water vapor adsorption-desorption measurements, all the plastic vessels were opened and all the soil and biochar samples were kept at a room temperature of 23.5 °C and at an ambient laboratory atmosphere for one day to achieve an equilibrium content of hygroscopic water in the samples.

A dewpoint potentiameter (WP4-T, Decagon Devices, Inc., Pullman, WA, USA) was used to measure water potentials of the biochar and soil samples. Weight of biochar and soil samples was equal to 0.5 g and 2 g, respectively. Five cycles of water vapor adsorption-desorption processes were carried out for the biochar and soil samples. During the 24 h adsorption process, the samples were saturated by water vapor in plastic vapor-tight vessels (100 cm^3) over distilled water at 95–98% relative air humidity (p/p_o) up to equilibrium maximum hygroscopic water content (HWC_{max}). The measurements of water potentials and weights of the biochar and soil samples were carried out immediately after the end of the adsorption process. Afterwards, the desorption process included several subsequent measurements (every 30–60 minutes) of the water potentials and weights of biochar and soil samples until the samples were reaching equilibrium minimum hygroscopic water content (HWC_{min}). After the end of the fifth cycle of adsorption-desorption process the biochar and soil samples were dried at 105 °C and their moisture content was calculated. These data are presented in the hygroscopic water retention curves. The same sample (both for the biochar and the soils) was used in the five subsequent cycles of water vapor adsorption-desorption processes.

Means and standard deviations were calculated for HWC_{min} and HWC_{max} of all the studied samples after the five cycles of water vapor adsorption-desorption processes. The results were subjected to the analysis of variance (one-way ANOVA) at $P \leq 0.05$. Strength of associations between sets of the parameters was assessed with Pearson correlation coefficients at $P \leq 0.05$.

Results and discussion

Fresh biochar is usually hydrophobic, but if its surface was oxidized by air or water molecules, biochar becomes more hydrophilic and accessible to stronger chemical interactions with soil minerals with subsequent physical occlusion in organo-mineral fractions (Lehmann et al., 2011).

Our results showed that the highest values of HWC_{max} were observed in the non aged biochar – 14.07% ±0.37% (of weight). The ageing of biochar in the MQ and HQ soils resulted in a decrease of HWC_{max} to 10.33% ±0.17% and 10.52% ±0.65%, respectively. There were no significant differences between the HWC_{max} of the aged biochars from the MQ and HQ soils, but the differences between the values of HWC_{max} in the non aged biochar and the two aged biochars were statistically significant (P <0.001).

The HWC_{max} of MQ and HQ soils showed lower values (2.86% ±0.14% and 4.39% ±0.89%, respectively) than those of the aged biochars. Because the clay content and mineralogical composition of the MQ and HQ soils were similar, the significant (P <0.05) differences in the HWC_{max} of MQ and HQ soils could be attributed to those in the SOM content (18.0 $g.C.kg^{-1}$ soil and 23.0 $g.C.kg^{-1}$ soil, respectively). The higher hydrophilicity of HQ soil did not result in any significant changes in the hydrophilicity of the aged biochar compared to that of the aged biochar from MQ soil.

After the end of the water vapor adsorption processes values of the biochars and soils water potentials relatively well reflected the above-mentioned differences in their HWC_{max}. The water potentials were equal to: –5.5 MPa ±

–1.3 MPa (non aged biochar), –9.8 MPa ± –1.4 MPa (aged biochar from HQ soil), –7.2 MPa ± –0.8 MPa (aged biochar from MQ soil), –5.2 MPa ± –0.6 MPa (HQ soil) and –8.1 MPa ± –2.3 MPa (MQ soil). Significant differences in water potentials were observed between the non aged biochar and aged biochar from MQ soil (P <0.05). Water potentials of the MQ and HQ soils also demonstrated significant differences in water potential (P <0.001). The ageing of biochars in the soils led to a stronger association of hygroscopic water with biochar surfaces at HWC_{max} compared to non aged biochar.

During the adsorption process at low p/p_o water molecules form bonds with OFGs and previously adsorbed water molecules, and then form separate and convex water clusters on an adsorbent surface. If p/p0 increases up to high values (>50%), such water clusters grow and fill in micropores of an adsorbent. At p/p_o between the formation of the initial water clusters and the condensation, water clusters in micropores may grow and coalesce as a result of hydrogen bonding formation between them. The adsorption rates are fastest at low air humidity and are slowest at condensation. In mesopores (at p/p_o 80–90%) larger clusters form bridges, and the growth of clusters prior to bridging requires a higher chemical potential and therefore, water adsorption occurs progressively from smaller to larger pores (Liu et al., 2017).

The HWC_{max} depends on the density of OFGs and the volume and size of pores available for water vapor adsorption at a given p/p0. Among the OFGs, carboxyl groups demonstrate the highest affinity towards water molecules (Brennan et al., 2001). Water molecules tend to cluster around carboxyl groups, regardless of the presence of carbonyl or hydroxyl functional groups. At the pore filling stage the rates of water uptake are inversely proportional to the pore sizes.

The 3-year ageing of biochar in both soils had probably caused a decrease in the density of OFGs on the biochar surface and in the available volume of pores because of their blocking by clay particles. Mineralogical composition of the soil clay particles was mainly presented by quartz and potassium feldspar with a low affinity to water molecules (Boitsova et al., 2015).

The results of the studies of the water desorption process from HWC_{max} to HWC_{min} demonstrated a higher water retention of the HQ soil than that of the MQ soil (Figure 1).

There were significant (P <0.001) differences between hygroscopic water retention curves of the HQ and MQ soils. If the whole desorption process was considered, mean values of corresponding water potentials of the HQ (-98.1 MPa) and MQ (-96.7 MPa) soils showed only insignificant differences. Pearson correlation coefficient between hygroscopic water retention curves of the HQ and MQ soil was equal to 0.98 (P <0.001). The results showed that desorption processes of hygroscopic water from both soils probably occurred from pores of similar size. The significant differences between hygroscopic water retention curves could be mainly induced by the differences in hydrophilic SOM contents between the HQ and MQ soils. There were significant (P <0.05) differences between mean values of HWC_{min} of the HQ (1.42% ±0.17%) and MQ (1.16% ±0.03%) soils. The mean values of HWC_{min} corresponded to mean water potentials of –190.5 MPa ± –13.3 MPa for HQ soil and –186.0 MPa ± –14.4 MPa for MQ soil. According to Do et al. (2009), the desorption process of hygroscopic water in activated carbons resulted from the decomposition of the larger (superclusters) to smaller clusters before they are desorbed from the micropores. A magnitude of desorption process depends on a number of superclusters in the pores and on their volumes and sizes.

The magnitude of decreasing water potentials was smaller at the initial stage (from HWC_{max}) of desorption process for the non aged biochar than for the aged biochar. For instance, during the first 30 min of desorption a decrease in water potentials reached –70 MPa for non aged biochar and –130 MPa for aged biochars. Further temporal stages of desorption (down to HWC_{min}) were characterized by the lower magnitude of decrease in water potentials of the aged biochars compared to non aged biochar. The differences in the magnitudes of decreasing water potentials could be attributed to higher volumes of emptying pores in non aged biochar.

During the desorption process mean values of corresponding water potentials were equal to –109.8 MPa

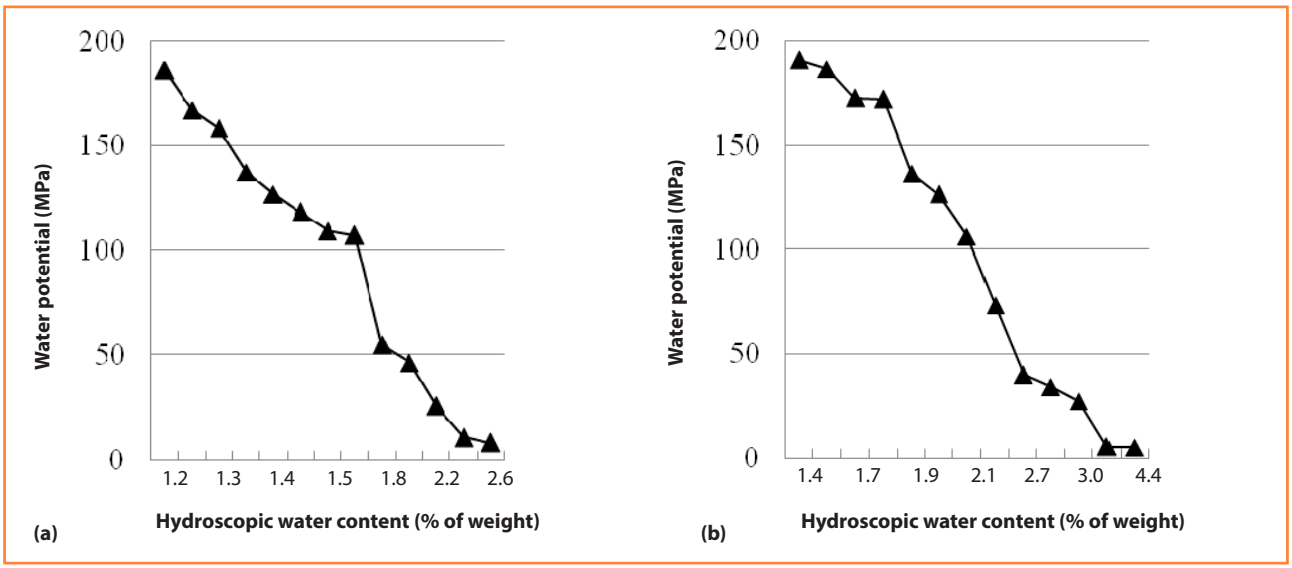

Figure 1 Hygroscopic water retention curves of sandy Spodosols with (a) medium and (b) high quality

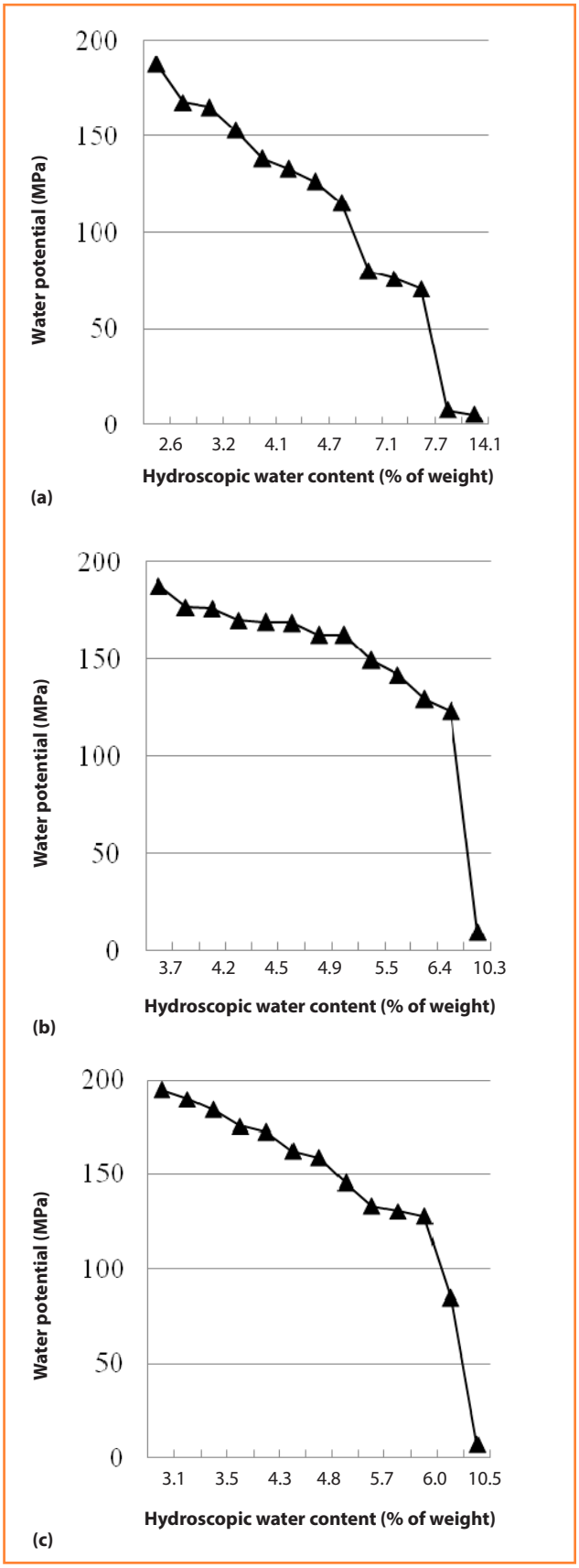

Figure 2 Hygroscopic water retention curves of (a) non aged biochar, (b) aged biochar from soil with high quality and (c) medium quality

(non aged biochar), –148.3 MPa (aged biochar from HQ soil) and –143.6 MPa (aged biochar from MQ soil). There were significant differences in the mean water potentials of the non aged biochar and the aged biochars from the HQ soil (P <0.01) and MQ soil (P <0.001).

There were insignificant differences between the water retention curves of the studied biochars during the desorption processes. However two aged biochars retained more hygroscopic water than non aged biochar at the same corresponding water potentials (Fig. 2). Desorption rates of hygroscopic water were lower from the aged biochars than from the non aged biochar which probably had higher volumes of pores. Therefore a decrease in the same amount of desorbed hygroscopic water corresponded to a higher difference in water potentials of the non aged biochar compared to two aged biochars.

Mean values of HWC_{min} and corresponding water potentials for the biochars were equal to: 2.61% ±0.08% (–187.6 MPa ± –4.4 MPa) for non aged biochar, 3.75% ±0.09% (–187.7 MPa ± –1.8 MPa) for aged biochar from HQ soil and 3.14% ±0.12% (–194.8 MPa ± –5.2 MPa) for aged biochar from MQ soil. There were significant differences (P <0.001) in HWC_{min} between all biochars. Significant differences in water potentials were observed for the aged biochar from MQ soil versus HQ soil (P <0.05) and versus the non aged biochar (P <0.05).

By subtracting the values of HWC_{min} from HWC_{max}, the absolute amounts of adsorbed water can be calculated for all the biochars and soils during their saturation at high values of p/p_o. These amount of adsorbed water ranged in the following decreasing order: 114.6 $g.kg^{-1}$ ±3.2 $g.kg^{-1}$ (non aged biochar), 73.7 $g.kg^{-1}$ ±5.9 $g.kg^{-1}$ (aged biochar from MQ soil), 65.8 g ±1.4 $g.kg^{-1}$ (aged biochar from HQ soil), 29.7 $g.kg^{-1}$ ±8.7 $g.kg^{-1}$ (HQ soil), 14.0 $g.kg^{-1}$ ±1.6 $g.kg^{-1}$ (MQ soil). These data showed that the improvement of soil quality had significantly (P <0.05) promoted the affinity of the soil to water vapor, probably as a result of increase in the content of hydrophilic SOM. The significant changes in the water vapor adsorption by the HQ soil did not contribute to the similar changes in the aged biochar. In opposite, as compared to the non aged biochar, both aged biochars demonstrated a significant decrease (P <0.001) in the absolute amounts of adsorbed water.

Conclusions

The 3-year ageing of biochar in the soils with medium and high quality caused a significant (P <0.05 and P <0.01) decrease in their maximum hygroscopic water content as compared to that of the non aged biochar. A significantly (P <0.05) higher hydrophilicity of the soil with high quality compared to the soil with medium quality did not contribute to any significant increase in the soil maximum hygroscopic water content. The ageing of biochar in both soils could cause a decrease in the density of the biochar oxygen-containing functional groups and in the available volume of pores as a result of their blocking by clay particles with low affinity to water vapor.

The 3-year ageing of biochars in both soils resulted in a significant (P <0.001) increase in their minimum hygroscopic water content compared to that of the non aged biochar after finishing the process of hygroscopic

water desorption. The desorption rates of hygroscopic water were lower from two aged biochars than those from the non aged biochar which probably had higher volumes of micro- and mesopores.

Acknowledgement

This study was supported by the Russian Foundation for Basic Research (grant No. 19-016-00038-A).

References

BOITSOVA, L. – ZINCZUK, E. – NEPRIMEROVA, S. – BALASHOV, E. 2015. Distribution of total and clay-associated organic matter in profiles of arable loamy sand Spodosol. In Folia Oecologica, vol. 42, 2015, no. 1, pp. 1–9. ISSN 1336-5266.

BRENNAN, J. K. – BANDOSZ, T. J. – THOMSON, K. T. – GUBBINS, K. E. 2001. Water in porous carbons. In Colloids and Surfaces A: Physicochemical and engineering aspects, vol. 187, 2001, pp. 539–568. ISSN 0927-7757.

DO, D. D. – JUNPIROM, S. – DO, H. D. 2009. A new adsorption-desorption model for water adsorption in activated carbon. In Carbon, vol. 47, 2009, no. 6, pp. 1466–1473. ISSN 0016-7061.

EL-NAGGAR, A. – LEE, S. S. – RINKLEBE, J. – FAROOQ, M. – SONG, H. – SARMAH, A. K. – ZIMMERMAN, A. R. – AHMAD, M. – SHAHEEN, S.M. – OK, Y. S. 2019. Biochar application to low fertility soils: A review of current status, and future prospects. In Geoderma, vol. 337, 2019, pp. 536–554. ISSN 0016-7061.

HORÁK, J. 2015. Testing biochar as a possible way to ameliorate slightly acidic soil at the research field located in the Danubian lowland. In Acta Horticulturae et Regiotecturae, vol. 18, 2015, no. 1, pp. 20–24. ISSN 1338-5259.

KEILUWEIT, M. – NICO, P. S. – JOHNSON, M. G. – KLEBER, M. 2010. Dynamic molecular structure of plant biomass-derived black carbon (biochar). In Environmental Science & Technology, vol. 44, 2010, no. 4, pp. 1247–1253. ISSN 0013-936X.

LEHMANN, J. – RILLIG, M. C. – THIES, J. – MASIELLO, C. A. – HOKADAY, W. C. – CROWLEY, D. 2011. Biochar effects on soil biota-a review. In Soil Biology and Biochemistry, vol. 43, 2011, no. 9, pp. 1812–1836. ISSN 0038-0717.

LIU, L. – TAN, S. J. – HORIKAWA, T. – DO, D. D. – NICHOLSON, D. – LIU, J. 2017. Water adsorption on carbon – A review. In Advances in Colloid and Interface Science, vol. 250, 2017, pp. 64–78. ISSN 0001-8686.

MARSHALL, J. – MUHLACK, R. – MORTON, B. J. – DUNNIGAN, L. – CHITTLEBOROUGH, D. – KWONG, C. W. 2019. Pyrolysis temperature effects on biochar – Water interactions and application for improved water holding capacity in vineyard soils. In Soil Systems, vol. 3, 2019, no. 2, p. 27. ISSN 2571-8789.

RASTVOROVA, O. G. – ANDREEV, A. P. – GAGARINA, E. I. – KASATKINA, G. A. – FYEDOROVA, N. N. 1995. Chemical analysis of soils. St. Petersburg: St. Petersburg University Publishing, 1995, 264 p. (in Russian).

sciendo

DOI: 10.2478/ahr-2019-0011

Acta Horticulturae et Regiotecturae 2/2019 *Lucia Toková, Dušan Igaz, Elena Aydin*

Acta Horticulturae et Regiotecturae 2
Nitra, Slovaca Universitas Agriculturae Nitriae, 2019, pp. 61–64

MEASUREMENT OF VOLUMETRIC WATER CONTENT BY GRAVIMETRIC AND TIME DOMAIN REFLECTOMETRY METHODS AT FIELD EXPERIMENT WITH BIOCHAR AND N FERTILIZER

Lucia TOKOVÁ*, Dušan IGAZ, Elena AYDIN

Slovak University of Agriculture in Nitra, Slovak Republic

There are many methods used for soil water content measurement which we can divide into direct gravimetric methods from using soil samples or indirect methods that are based on the measurement of another soil property which is dependent on soil moisture. The paper presents the findings of volumetric water content measurements with gravimetric and time domain reflectometry (TDR) methods. We focused on four variants in the field experiment in Dolná Malanta (Slovakia): control variant (B0+N0), variant with biochar at dose 20 $t.ha^{-1}$ without N fertilizer (B20+N0), variant with biochar 20 $t.ha^{-1}$ and N fertilizer 160 $kg.ha^{-1}$ (B20+N160) and variant with biochar 20 $t.ha^{-1}$ and N fertilizer 240 $kg.ha^{-1}$ (B20+N240). TDR is nowadays a well-established dielectric technique to measure volumetric water content; however, its accuracy is influenced by high concentration of salts in soil. In this paper, we evaluated the effect of added N fertilizer on the measuring accuracy of HydroSense II device that is operating under the TDR principle.

Keywords: gravimetric method, TDR calibration, N fertilizer, soil salinization

Measurement of soil water content is fundamental to many investigations in agriculture, horticulture, ecology, forestry, hydrology, civil engineering, waste management and other environmental fields. Water present within soil pores is called soil water content which is accepted as reference to the water that may be evaporated from soil by heating from 100 up to 110 °C, but usually to 105 °C, until there is no further weight loss. This is the basis of the gravimetric method which is the oldest established and the only truly direct method of water content determination which requires samples for oven drying. It is the standard reference against which other techniques are normally calibrated. The other techniques rely on measurement of another soil property which is dependent on soil moisture (Smith and Mullins, 2001).

According to Smith and Mullins (2001), the development of dielectric methods since 1980 has introduced opportunities for rapid collection of soil water content data at short time intervals and permitted automation and logging of measurements. The ability to log soil water content automatically has opened ways of soil water monitoring and soil hydrological research that had previously been impossible. The most common dielectric method used is time domain reflectometry (TDR). TDR is nowadays a well-established technique to measure volumetric water content using the frequency in the range from 10 MH_z to 12 GH_z.

For saline soils, in certain cases the imaginary part of the dielectric constant can also affect the TDR reading. When the electrical conductivity (EC) of pore water is higher than 8–10 $dS.m^{-1}$, the TDR overestimates volumetric water content. There are conflicting results regarding the effect of the EC on volumetric water content. TDR values in some cases could be bias free, sometimes underestimated, sometimes overestimated, and sometimes both of them under- and overestimated relative to gravimetric method determination. The influence of high EC on TDR measurements seems to be soil specific (Nadler, Gamliel and Peretz, 1999; Bouksila et al., 2008). Also Wyseure, Mojid and Malik (1997) stated that electrical conductivity of a saline soil influences the measurement of the soil water content by TDR. Further, they stated that if the bulk electrical conductivity is kept less than 2 $dS.m^{-1}$, the overestimation stays within reasonable limits and can be disregarded. The study of Hook, Ferré and Livingston (2004) is focused on determination of the performance limits of TDR probes for measuring water content in high EC sands. Time domain measurement shows that there is an increase in the travel time of a pulse with increasing pore water salinity and that the variability of travel time measurements also increases with the pore water EC. According to Bonnell, Broughton and Enright (1991), the TDR technique can be used to ascertain absolute solution salinity levels, but only relative levels of bulk soil electrical conductivity are possible to be determined.

The main aim of the presented paper was to perform measurements of volumetric soil water content for four experimental variants (B0+N0, B20+N0, B20+N160 and B20+N240) in the field experiment at Dolná Malanta

Contact address: Ing. Lucia Toková, Slovak University of Agriculture in Nitra, Faculty of Horticulture and Landscape Engineering, Department of Biometeorology and Hydrology, Hospodárska 7, 949 01 Nitra, Slovakia, tel.: +421 37 641 52 52, e-mail: tokovalucia@gmail.com

(Slovakia). Soil water content was determined from the collected undisturbed soil samples by gravimetric method as well as by the TDR method. Another goal was to perform a calibration on a particular device we used for water content measurements in the field.

Material and methods

Field site

Several variants of the field experiment at the locality Dolná Malanta in Nitra region of Slovakia with different doses of biochar and N fertilisers to examine the effect of biochar application on greenhouse gas emissions (Horák et al., 2017), soil water regime (Igaz, Horák and Domanová, 2015) other soil properties (Igaz et al., 2018; Juriga et al., 2018) and crop yields (Kondrlová et al., 2017; Kondrlová, Horák and Igaz, 2018) were established in the experimental area in March 2014. Biochar for this field experiment was produced from the mixture of paper fibre and cereal husks by pyrolysis at 550 °C for 30 min and applied into the top layer of soil (0–10 cm). According to Igaz et al. (2018) the altitude of the site is 175 m, the soil is classified as Haplic Luvisol and the topsoil contains 249 g.kg^{-1} of clay, 599 g.kg^{-1} of silt and 152 g.kg^{-1} of sand, giving it a silt loam texture. The area of interest was used for agricultural production and research purposes and the whole site was sown by maize (*Zea mays* L.) during the sampling in 2017.

Soil sampling and subsequent analyses

We executed soil sampling on four variants in the experiment: control variant without biochar and N fertilizer (B0+N0), variant with biochar at dose 20 t.ha^{-1} without N fertilizer (B20+N0), variant with biochar at dose 20 t.ha^{-1} and N fertilizer at dose 160 kg.ha^{-1} (B20+N160) and variant with biochar at dose 20 t.ha^{-1} and N fertilizer at dose 240 kg.ha^{-1} (B20+N240). Undisturbed soil samples (100 cm^3) were taken from desired depths at 3 randomly selected locations at plots representing each of 4 variants for determination of selected soil characteristic – in our case it was volumetric water content (*VWC*). The soil samples were kept in airtight sealed containers to prevent losses of moisture prior measurement in laboratory. The soil samples were weighed and dried in an oven at 105 °C. After removing from oven and slow cooling to room temperature, the dry soil samples were weighed again. Soil sampling was conducted once per week during two month period (April and May 2017) and once a month during the rest of the vegetation period of maize (June to October 2017).

VWC (%) in the soil was calculated by a specific formula (Antal and Igaz, 2012):

$$VWC = \frac{V_w}{V_t} = \frac{(m_1 - m_2)\cdot \rho_w}{V_t} \cdot 100 \quad (1)$$

where:

V_w – the volume of soil water (cm^3)
V_t – the volume of soil sample (cm^3)
m_1 – the weight of wet soil (g)
m_2 – the weight of dry soil (g)
ρ_w – the soil water density (g.cm^{-3})

Equipment and instrumentation

At the same time, volumetric soil water content measurements were performed by HydroSense II probe (model CS659) (Campbell Scientific, Inc.®) using the TDR principle of measurement. This is an indirect method of *VWC* measurement based on the travel time of a high frequency electromagnetic pulse (MH_z, GH_z) through the soil. This travel time is used to calculate the dielectric constant of the material. The TDR probes are inserted directly into the soil for in situ measurement at the desired soil depths. The probe is an easy-to-use portable device for measuring *VWC* in agricultural soils. The calibration coefficients fixed in the HS2 sensor were determined in laboratory studies on typical soils. Its accuracy is ±3% *VWC* in typical soils with solution EC ≤6.5 dS.m^{-1}. When measuring atypical soils, user determined coefficients can often be applied. A soil specific calibration can be performed using an independent measure of water content such as gravimetric analysis (HS2, 2019).

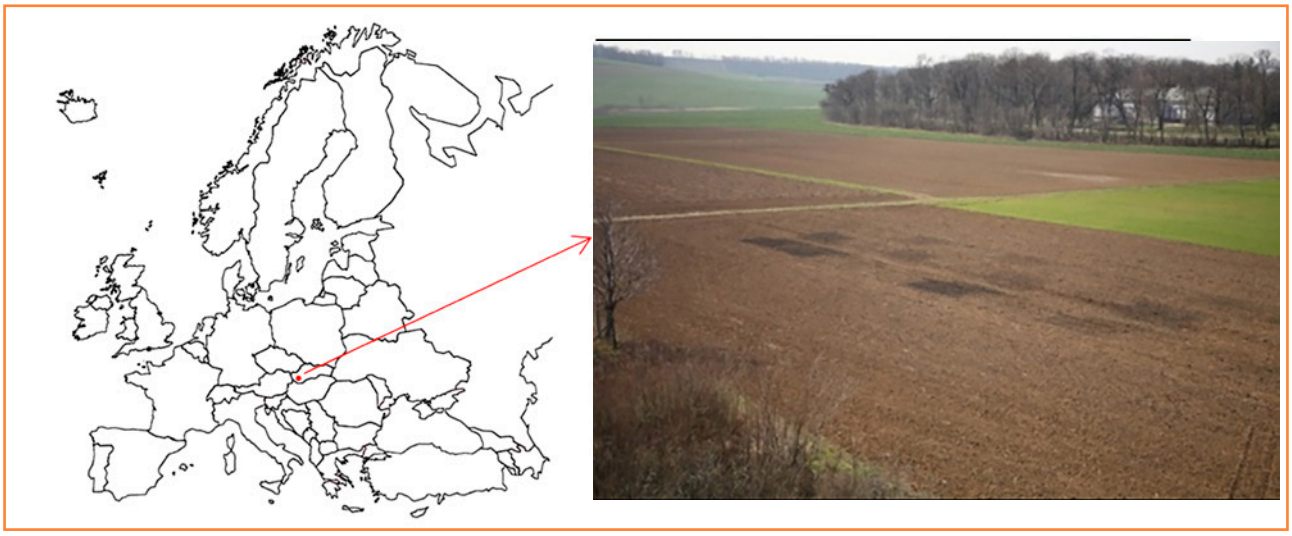

Figure 1 Field site location and photo of the experimental area
Photo: Tárník, 2014

Results and discussion

TDR calibration

Indirect methods usually require calibration for more accurate measurements in the particular investigated soil. The probe was calibrated using linear dependence relationship between standard gravimetric and TDR method. That means that there was a linear equation for a given dependence, and when calibrating the instrument, the values measured by the instrument were substituted as a parameter x in the equation $y = ax + b$. The graphical trend of the calibration equations for variants B0+N0, B20+N0, B20+N160 and B20+N240 is shown in Fig. 2.

Effect of N fertilizer on TDR measurement

The graphical course of soil water content measured by both methods (for the TDR method both before and after instrument calibration) during the whole growing season of the crop in 2017 can be observed in Fig. 3 (variant B0+N0), in Fig. 4 (B20+N0), in Fig. 5 for (B20+N160) and in Fig. 6 for (B20+N240). As it can be seen in Fig. 3 to Fig. 6, at the beginning of the growing season (April – June), the soil water content was higher (25–30% vol.). During this period, the soil moisture measured by both methods had the same course in all four experimental variants. The figures further show that during the dry summer period (June – Sept), the higher nitrogen load affected the accuracy of the instrument when compared to the standard gravimetric method. The instrument readings were much lower at the B20+N160 and B20+N240 variants. In the following period (Sept – Oct), the soil moisture increased due to the higher rainfall, and it again had approximately the same course for both methods.

Prior to the probe calibration, the measured volumetric water content differed in the range of 0 up to 5% when compared to the gravimetric method. This difference was modified after the specific calibration to range 0–2%. For non-fertilized treatments the observed differences in water content might have been caused by the TDR device measurement accuracy. However, the differences between the TDR and the gravimetric measurements were higher for fertilized treatments.

Depending on the soil characteristics at the specific site, the electrical conductivity values may be affected by the salt content in the soil, soil texture and soil moisture. One of the disadvantages of TDR devices is their inaccurate measurement in soils with higher salinity. We assume that N fertilization could increase the salt concentration in the soil and thus

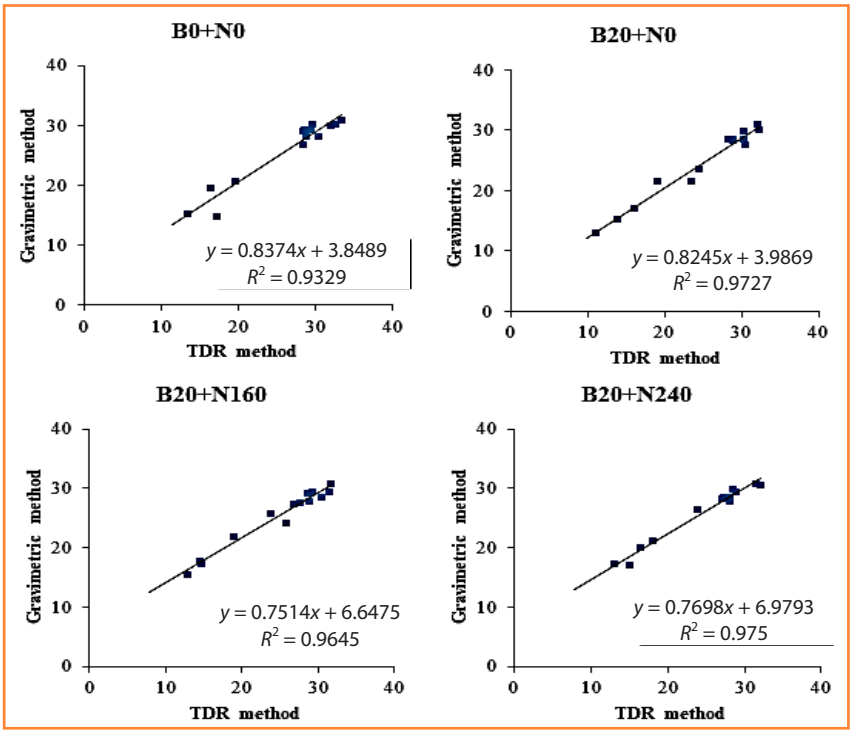

Figure 2 Graphical trend of calibration equations for treatments B0+N0, B20+N0, B20+N160 a B20+N240

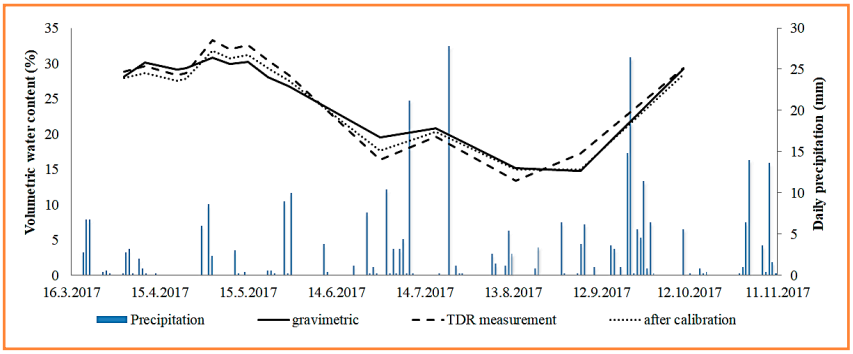

Figure 3 Graphical course of *VWC* for B0+N0

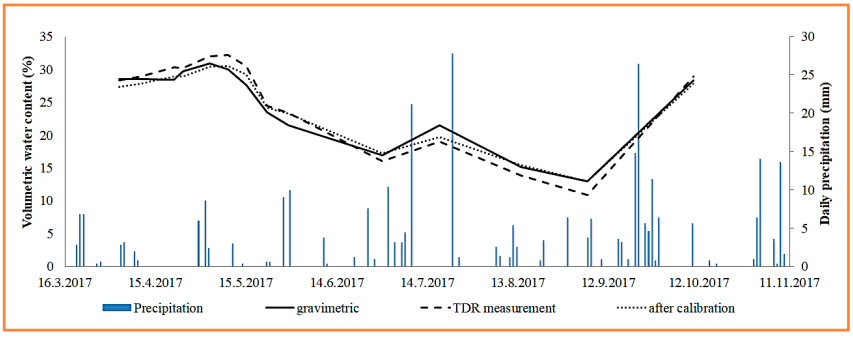

Figure 4 Graphical course of *VWC* for B20+N0

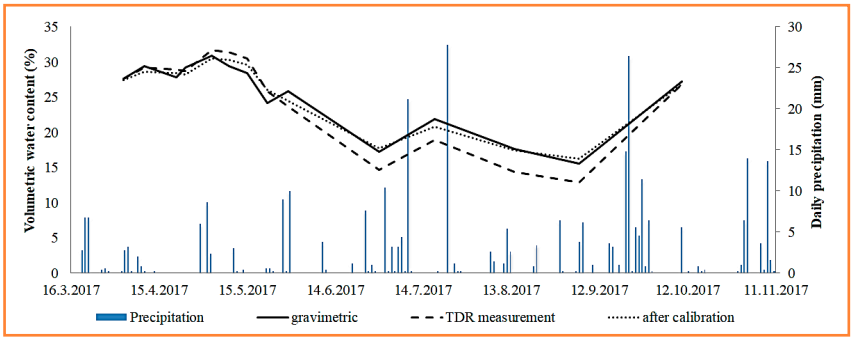

Figure 5 Graphical course of *VWC* for B20+N160

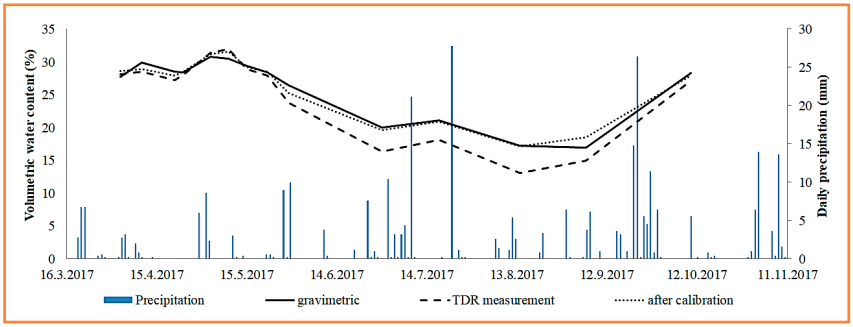

Figure 6 Graphical course of *VWC* for B20+N240

its electrical conductivity. Several authors, including Jingpei et al. (2015) have investigated the impact of N fertilizers on increasing soil salinity. In their particular study, nitrogen was applied at high doses of 600 and 1,200 kg.ha^{-1}. The authors state that salinity had increased significantly after N input. The increase in soil salinity was attributed to the nitrification of excess N fertilizer. Similarly, Bryla, Shireman and Machado (2010) pointed out that the application of granular N fertilizer may increase the electrical conductivity of the soil solution.

Conclusions

In this paper we focused on the measurement of soil volumetric water content by the gravimetric method and the TDR method in the field experiment in Dolná Malanta. Soil water content was measured in four experimental variants B0+N0, B20+N0, B20+N160 and B20+N240. We have found that in the variants with added nitrogen fertilizer (B20+N160 and B20+N240) the accuracy of measurement by the HydroSense II operating on the TDR method was lower when compared to the gravimetric method. According to Jingpei et al. (2015) and Bryla, Shireman and Machado (2010) N fertilization can increase soil salinity. We therefore assume that also in our case the measurement inaccuracy may be caused by increased salt concentration in the soil. To increase the measurement accuracy by the used device, we performed a specific calibration on a particular soil and thus adjusted the soil water content.

Acknowledgments

This study was financially supported by the projects KEGA 019SPU-4/2017, 026SPU-4/2017 and VEGA 1/0064/19.

References

ANTAL, J. – IGAZ, D. 2012. Aplikovaná agrohydrológia. Nitra : SPU, 2012. ISBN 978-80-552-0731-5.

BONNELL, R. B. – BROUGHTON, R. S. – ENRIGHT, P. 1991. The measurement of soil moisture and bulk soil salinity using time domain reflectometry. In Canadian Agricultural Engineering, vol. 33, 1991, no. 2, pp. 225–229.

BOUKSILA, F. – PERSSON, M. – BERNDTSSON, R. – BAHRI, A. 2008. Soil water content and salinity determination using different dielectric methods in saline gypsiferous soil (Détermination de la teneur en eau et de la salinité de sols salins gypseux à l'aide de différentes méthodes diélectriques). In Hydrological Journal, vol. 53, 2008, no. 1, pp. 253–265. Online: https://doi.org/10.1623/hysj.53.1.253

BRYLA, D. R. – SHIREMAN, A. D. – MACHADO, R. M. A. 2010 Effects of Method and Level of nitrogen Fertilizer Application on Soil pH, Electrical Conductivity, and Availability of Ammonium and Nitrate in Blueberry. In Acta horticulturae, 2010, (868). Online: DOI: 10.17660/ActaHortic.2010.868.8

HOOK, W. R. – FERRÉ, T. P. A. – LIVINGSTON, N.J. 2004. The Effects of Salinity on the Accuracy and Uncerainty of Water Content Measurement. In Soil Science Society of America Journal, vol. 68, 2004, pp. 47–56.

HORÁK, J. – KONDRLOVÁ, E. – IGAZ, D. – ŠIMANSKÝ, V. – FELBER, R. – LUKÁČ, M. – BALASHOV, E.V. – BUCHKINA, N.P. – RIŽIJA, E. – JANKOWSKI, M. 2017. Biochar and biochar with N-fertilizer affect soil N_2O emission in Haplic Luvisol. In Biologia, vol. 72, 2017, no. 9, pp. 995–1001. ISSN 0006-3088.

HS2. 2019. Product Manual: HS2 and HS2P (HydroSense II). © 2011–2019. Online: https://s.campbellsci.com/documents/us/manuals/hs2.pdf

IGAZ, D. – HORÁK, J. – DOMANOVÁ, J. 2015. The impact of biochar on the soil water characteristics In SGEM 2015.

IGAZ, D. – ŠIMANSKÝ, V. – HORÁK, J. – KONDRLOVÁ, E. – DOMANOVÁ, J. – RODNÝ, M. – BUCHKINA, N.P. 2018. Can a single dose of biochar affect selected soil physical and chemical characteristics? In Journal of hydrology and hydromechanics, vol. 66, 2018, no. 4, pp.421–428. ISSN 0042-790X.

JINGPEI, H. – JIACHUN, S. – LINGZAO, Z. – JIANMING, X. – LAOSHENG, W. 2015 Effects of nitrogen fertilization on the acidity and salinity of greenhouse soils. In Environmental Science and Pollution Research, vol. 22, 2015, no. 4, pp. 2976–2986. ISSN 0944-1344. Online: https://doi.org/10.1007/s11356-014-3542-z

JURIGA, M. – ŠIMANKSÝ, V. – HORÁK, J. – KONDRLOVÁ, E. – POLLÁKOVÁ, N. – BUCHKINA, N.P. – BALASHOV, E. 2018. The effect of different rates of biochar and biochar in combination with N fertilizer on the parameters of soil organic matter and soil structure. In Journal of Ecological Engineering, vol. 19, 2018, no. 6, pp. 153–161. ISSN 2081-139X.

KONDRLOVÁ, E. – HORÁK, J. – IGAZ, D. – DOBIÁŠOVÁ, D. 2017. The possibility of using digital images in assessment of plant canopy development and weed spread. In Acta Horticulturae et Regiotecturae, vol. 20, 2017, no. 2, pp. 35–39.

KONDRLOVÁ, E. – HORÁK, J. – IGAZ, D. 2018. Effect of biochar and nutrient amendment on vegetative growth of spring barley (*Hordeum vulgare* L. var. Malz). In Australian journal of crop science, vol. 12, 2018, no. 2, pp. 178–184. ISSN 1835-2693.

NADLER, A. – GAMLIEL, A. – PERETZ, I. 1999. Practical aspects of salinity effect on TDR-measured water content: a field study. In Soil Science Society of America Journal, vol. 63, 1999, no. 5, pp. 1070–1076.

SMITH, A.K. – MULLINS, E. CH. 2001. Soil and Environmental Analysis Physical Methods. New York : Marcel Dekker, Inc, 2001. ISBN 0-8247-0414-2.

WYSEURE, G. C. L. – MOJID, M. A. – MALIK, M. A. 1997. Measurement of volumetric water content by TDR in saline soils. In European Journal of Soil Science, vol. 48, 1997, pp. 347–354.

sciendo

DOI: 10.2478/ahr-2019-0012

Acta Horticulturae et Regiotecturae 2
Nitra, Slovaca Universitas Agriculturae Nitriae, 2019, pp. 65–70

EFFECTS OF BIOCHAR AND ITS REAPPLICATION ON SOIL PH AND SORPTION PROPERTIES OF SILT LOAM HAPLIC LUVISOL

Martin JURIGA*, Vladimír ŠIMANSKÝ

Slovak University of Agriculture in Nitra, Slovak Republic

In this paper we investigate the effects of biochar alone and its reapplication and combination with N-fertilizer (1) on the soil pH, and (2) sorption parameters. The soil samples were taken during growing period in 2018 from plots with different biochar (first application in 2014 – A, reapplication in 2018 – B) at application rates: 0 $t.ha^{-1}$ (B0 control), 10 $t.ha^{-1}$ (B10) and 20 $t.ha^{-1}$ (B20) and different nitrogen fertilization: N0 (no nitrogen) and N40 (40 $kg.ha^{-1}$). Our results showed that the first application of biochar at the rate of 20 $t.ha^{-1}$ (B20A) without N-fertilizer significantly increased the values of soil pH in H_2O, soil pH in KCl, the sum of base cations (SBC) and cation exchange capacity (CEC) compared to control (B0). Similar effects were observed also after reapplication of biochar (B10B). All investigated parameters in fertilized control treatment (B0N40) were worst and the first application, as well as the reapplication of biochar with N, caused significant increase of soil pH in H_2O, soil pH in KCl, SBC, CEC, BS and decrease of hydrolytic acidity.

Keywords: soil acidity, cation exchange capacity, base saturation, biochar, fertilization

Soil acidity presents a world-wide problem as it reduces the soil fertility. Acidification is a slow, continual and natural process that considerably affects the sustainability of agriculture (Rengel, 2002; Guo et al., 2010). Approximately 50% of world's arable land is considered acidic (Kochian et al., 2015). Acidic soil is unsuitable for most field crops with the exception of some. Soil pH value expresses the degree of acidity and alkalinity of soil. Soil sorption is arguably the most important physico-chemical process that ensures the retention of nutrients, heavy metals and other chemical substances in soil (Thompson et al., 2012). According to Essington (2004), the ability of soil to retain cations increases with increasing pH. This is supported by Zhang et al. (2015) who claim that pH value and soil organic carbon content (SOC) are the main factors influencing the content of basic cations exchange. In the acidic soils the total content of cations is considerably lower. In addition, cation exchange capacity (CEC) is dependent on soil organic matter content (SOM). In general, SOM has a high content of basic cations exchange due to the presence of functional groups on the surface area of its particles.

According to Dai et al. (2017), application of biochar, to raise soil pH, could present an acceptable solution to high soil acidity. There is a consensus that biochar application raises the pH in acidic soils (Juriga and Šimanský 2018; Šimanský et al., 2018). Adding biochar into the soil could prove to be a valuable instrument in the efforts to increase the soil fertility and its use is deemed an important to counter the risks of soil acidification (Dai et al., 2017). Biochar represents a solid carbon-based product, which is produced during the thermal decomposition of different organic materials, under conditions with limited access to oxygen (Lorenz and Lal, 2014). Biochar has specific properties which mainly depend on the type of material used for its production and producing conditions. Through its properties, biochar can influence various soil properties, such as: soil organic carbon content (Šimanský et al., 2018a; Juriga et al., 2018), aggregate stability (Šimanský et al., 2016), bulk density, soil pH, CEC, electric conductivity (Chintala et al., 2014), soil biota (Lehmann et al., 2011), etc.

There are several mechanisms that enable biochar to suppress the acidity of the soil and help to increase the soil pH (Dai et al., 2017). Biochar's specific properties reduce the soil acidity through its alkaline nature and high buffer capacity. The ability of biochar particles to absorb the H^+ ions, as well as decarboxylation processes, are probably the main factors in soil acidity neutralization (Wang, Li and Liang, 2013). The biochar particles in soil are subject to gradual oxidation which leads to the production of functional groups containing oxygen (Hansen et al., 2016). During pyrolysis, the cations such as: Ca, Mg, K and Si which are contained in the organic materials used in bio-fuel production, form carbonates or oxides (Zong et al., 2018). When we apply biochar to the acidic soil, these carbonates and oxides react with H^+ and Al^{+3} ions and thus increase the pH and decrease the soil's acidity (Novak et al., 2009).Yuan, Xu and Zhang (2011) have shown that functional groups such as COO– and O– can also react with H^+ and Al^{+3} ions in the soil and significantly contribute to the alkalinity of soil. The range of changes in pH and acidity depends on biochar properties. As stated by Fidel et al. (2017), biochar alkalinity strongly correlates with the content of basic cations in

Contact address: Ing. Martin Juriga, Slovak University of Agriculture in Nitra, Faculty of Agrobiology and Food Resources, Department of Soil Science, 949 76 Nitra, Tr. Andreja Hlinku 2, Slovak Republic, e-mail: xjuriga@uniag.sk

the soil. Ahmad et al. (2014) refers to surface absorption and electrostatic interactions as the main mechanisms in interaction between biochar particles and particles of organic matter. A large surface area, a high number of functional groups, a negative charge and also a porous structure have major functions in these processes (Dai et al., 2017; Yang, Ying and Kookana, 2009).

Based on the above context, we expect that application of biochar, biochar with N fertilizer and biochar reapplication could increase soil pH and improve soil sorptive properties in a silt loam Haplic Luvisol. Therefore, the aim of this study is to evaluate the effects of biochar, biochar with N fertilization and biochar reapplication on changes of soil pH and soil sorption parameters.

Material and methods

The study was conducted at the experimental station of Slovak University of Agriculture in Nitra (Dolná Malanta, 48° 10'00.0" N 18° 09'00.0 "E) during the growing period of spring barley in 2018. The station is situated approximately 4 km from Nitra in Žitava highlands, with an altitude of 175 m a. s. l. The soil is classified as silt loam Haplic Luvisol and on average it contained 9.13 $g.kg^{-1}$ of soil organic carbon, while the average soil pH was 5.71 (Šimanský et al., 2018a). The studied area has a planar character with a slight south western facing of the slope. Climate is warm and dry with an average annual air temperature of about 9.5 °C and average annual sum of precipitation 540 mm.

The experiment was established in 2014, before the sowing of spring barley. This is when biochar was applied for the first time at the rate of 10 and 20 $t.ha^{-1}$. From the beginning of the experiment until now, the following crops were grown on the field in the years 2014, 2015, 2016, 2017 and 2018, respectively: spring barley, corn, spring wheat, corn and spring barley. Before the sowing of spring barley, biochar was reapplied at the same rates in 2018. The overview of the treatments is shown in Table 1. Biochar used in this experiment was produced from grains husks and paper, at the temperature of 500 °C. Its basic composition and properties are given in Table 2. The nitrogen fertilizer – LAD 27 is used every year at different rates based on the crop's needs. N fertilizer was used at the rates of 40 $kg.N^{-1}.ha^{-1}$ in 2018.

Table 2 The basic chemical composition and properties of applied biochar

Total C	531 $g.kg^{-1}$
Total N	14 $g.kg^{-1}$
Ca	57 $g.kg^{-1}$
Mg	3.9 $g.kg^{-1}$
K	15 $g.kg^{-1}$
Na	0.7 $g.kg^{-1}$
Ash	383 $g.kg^{-1}$
pH in H_2O	8.8
Size of biochar	1–5 mm

The soil samples were collected at regular monthly intervals from all treatments during the growing season of spring barley in 2018 (from April to July). The sampling was carried out from the depth of 0–0.30 m. Subsequently, parts of plants were removed, and the samples were transported to the laboratory where they were dried. Finally, the following parameters in the soil samples were determined:

- soil pH in H_2O (ratio soil to distilled water, 1 : 2.5) and soil pH in 1 $mol.dm^{-3}$ KCl (ratio soil to KCl, 1 : 2.5) – potentiometrically (Fiala et al., 1999);
- hydrolytic acidity (H), the sum of basic cations (SBC) according to Kappen method (Fiala et al.,1999);
- cation exchange capacity (CEC) and base saturation (BS) according to equations 1 and 2:

$$CEC = H + SBC \quad (1)$$

$$BS = \frac{SBC}{CEC} \cdot 100 \quad (2)$$

Average values of soil pH and soil sorptive parameters by ANOVA single-factor analysis (Statgraphic Centurion XV Program I.) were determined. The LSD test with the level of significance P <0.05 was used to compare the effects of biochar, biochar with nitrogen fertilizer and biochar reapplication.

Table 1 The overview of evaluated treatments

B0	without biochar	control	without N fertilittzer
B10A	10 $t.ha^{-1}$of biochar	first biochar application (2014)	
B20A	20 $t.ha^{-1}$ of biochar		
B10B	10 $t.ha^{-1}$ of biochar	biochar reapplication (2018)	
B20B	20 $t.ha^{-1}$ of biochar		
B0N40	without biochar	N treatment	with N fertilizer
B10N40A	10 $t.ha^{-1}$ of biochar	first biochar application (2014)	
B20N40A	20 $t.ha^{-1}$ of biochar		
B10N40B	10 $t.ha^{-1}$ of biochar	biochar reapplication (2018)	
B20N40B	20 $t.ha^{-1}$ of biochar		

Results and discussion

The biochar application can be beneficial for soil pH enhancement (e. g. Chintala et al., 2013; Obia et al., 2015; Horák et al., 2017; Teutscherova et al., 2017; Šimanský et al., 2018) as confirmed by our data. As shown in Fig. 1, in the case of treatments with the first biochar application without a nitrogen fertilizer, the statistically significant effect on soil pH increase was recorded in B20A treatment. Consequently, the soil pH in H_2O significantly increased from 6.06 (B0) to 6.47 (B20A) and pH in KCl from 5.66 (B0) to 6.0 (B20A). However, the addition of 10 $t.ha^{-1}$ of biochar did not have significant influence on pH changes. Zong et al., (2018) also confirmed that higher rates of biochar are more beneficial, stating that the volume of biochar added to the soil is crucial when trying to affect the pH values and acidity of the soil. Biochar reapplication had a statistically significant effect on the pH values in treatments at both rates (B10B and B20B). The higher values in B20B treatment: 6.71 (pH in H_2O) and 6.23 (pH in KCl) than in B10B treatment: 6.47 (pH in H_2O) and 6.0 (pH in KCl) were measured. The same values – pH in H_2O (6.47) and pH in KCl (6.0) were found in B20A and B10B treatments. For example, Cornelissen et al. (2018) also observed a significant increase in pH soon after the application of biochar into the soil, while pH values gradually decreased due to the weakening of the biochar's liming effect in the following years. According to Cornelissen et al. (2018) this decrease could be caused by the gradual leaching of alkaline compounds from biochar. They consider effective to apply biochar to the soil every three years to maintain the neutralizing effect. Castaldi et al. (2011) stated that the ability of biochar to affect the soil pH decreased as soon as 14 months after the application. It was proven that different kinds of biochar affect the soil pH differently. This depends on the specific biochar properties, mainly on the used materials and production temperature (Keiluweit, Nico and Kleber, 2010; Ahmad et al., 2014; Masud, Li and Xu, 2014). Alkaline properties of biochar tend to increase with the pyrolysis temperature (Yuan, Xu and Zhang, 2011). In our case, the best results were recorded in the treatment with biochar reapplication at the rate of 20 $t.ha^{-1}$ which confirmed the data of above-mentioned authors (e.g. Castaldi et al., 2011; Cornelissen et al., 2018).

Since the biochar is alkaline, it might increase of soil pH, but this effect could be softened with adding

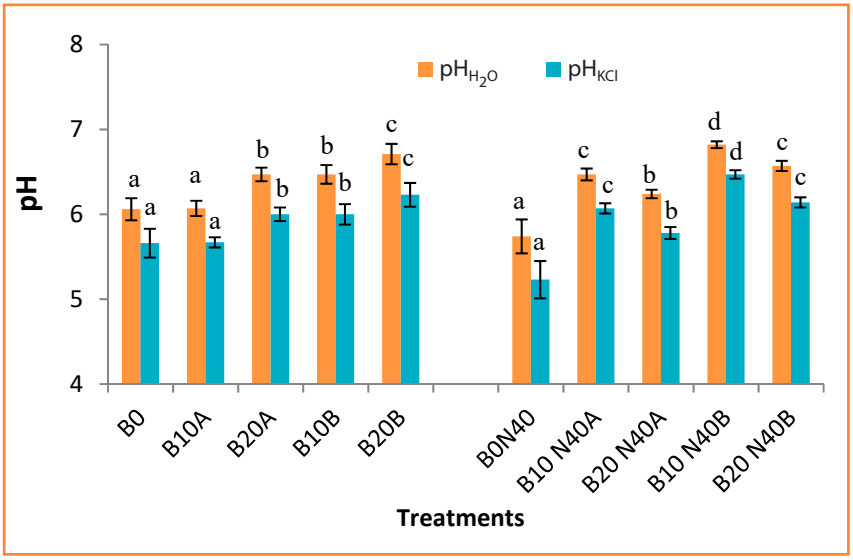

Figure 1 Statistical evaluation of soil pH
the individual letters (a, b, c, d) in columns (at the same colour) represent the statistical significance (P <0.05) of the application of biochar, biochar with N or biochar reapplication

Table 3 Statistical evaluation of soil sorption parameters

Treatments	H	SBC	CEC	BS
	mmol.kg^{-1}			%
B0	16.65±3.00^{bc}	137.28±8.29^{a}	153.93±6.45^{a}	89.14±2.24^{ab}
B10A	19.81±3.52^{c}	140.34±12.30^{ab}	160.15±10.40^{ab}	87.55±2.51^{a}
B20A	14.17±1.72^{b}	164.06±14.29^{b}	177.70±13.33^{b}	91.47±1.31^{bc}
B10B	15.20±3.01^{b}	163.80±8.97^{b}	179.25±6.29^{b}	91.99±1.92^{bc}
B20B	11.47±2.46^{a}	194.66±30.86^{c}	206.12±29.43^{c}	94.29±1.74^{c}
B0N40	27.53±1.11^{d}	117.90±10.67^{a}	145.43±10.58^{a}	80.99±1.60^{a}
B10 N40A	14.10±3.08^{b}	167.63±6.68^{b}	181.73±4.53^{bc}	92.22±1.80^{b}
B20 N40A	20.22±1.77^{c}	152.59±7.94^{b}	172.80±8.75^{b}	88.30±0.87^{b}
B10 N40B	6.29±2.89^{a}	226.28±6.03^{d}	232.57±7.67^{d}	97.32±1.19^{c}
B20 N40B	13.57±1.67^{b}	195.68±20.88^{c}	202.49±26.86^{c}	97.01±9.39^{c}

the individual letters (*a, b, c, d*) in lines represent the statistical significance (P <0.05) of the effect of the application of biochar, biochar with N or biochar reapplication, H – hydrolytic acidity, SBC – the sum of basic cations, CEC – cation exchange capacity, BS – base saturation

of nitrogen fertilization. Therefore, we evaluated also the changes in soil pH under treatments with N fertilization (Fig. 1). The lowest values of pH in H_2O and pH in KCl in treatments with N fertilization were measured in B0N40 treatment. However, when combined with biochar, the values increased significantly. Yu et al. (2017) compared the effects of N ammonium fertilizer alone at the rate of 30 $kg.N^{-1}.ha^{-1}$, but also the effect of its combination with 19.5 $t.ha^{-1}$ of biochar. After addition of N alone, the pH value was 5.3, while pH increased from 5.3 to 6.0 after the application of biochar with N. Long-term use of nitrogen fertilizers in the ammonium form can be the reason of soil acidification. This is initiated by the release of H^+ ions in the process of nitrification (Zhang, Zhang and Li, 2002). In our case, the effect was stronger after adding 10 $t.ha^{-1}$ rather than 20 $t.ha^{-1}$ (Fig. 1). The values of soil pH in H_2O in B10N40A, B20N40A, B10N40B and B20N40B treatments were higher than in B0N40 by 11.3%, 8.0%, 15.4% and by 12.6%, respectively. The values of soil pH in KCl in the same treatments were higher by 13.8%, 9.5%, 19.2% and 14.8%, respectively.

The average values of the sorption parameters in this study are shown in Table 3. We did not find any significant effects on hydrolytic acidity (H) in treatments with initial added biochar without N, however the values of sum of basic cations (SBC) and cation exchange capacity (CEC) in B20A treatment significantly increased by 16.3% and 13.4% compared to B0 treatment. On the other hand, B10A treatment showed no significant changes. In several studies (e.g. Wang, Li and Liang, 2013) the positive impact of biochar on the content of CEC has been demonstrated. The biochar effect increased along with its applied rate. The re-addition of biochar without N with the lower rate also significantly increased the SBC by 16.2% and CEC by 14.13% compared to B0 treatment (Table 3). Furthermore, the reapplication of biochar with higher rate suppressed H from 16.65 $mmol.kg^{-1}$ (B0) to 11.47 (B20B) $mmol.kg^{-1}$. The SBC value increased from 137.28 $mmol.kg^{-1}$ (B0) to 194.66 $mmol.kg^{-1}$ (B20B), CEC value from 153.93 $mmol.kg^{-1}$ (B0) to 206.12 $mmol.kg^{-1}$ (B20B) and the BS value from 89% (B0) to 94% (B20B). Better results were observed in B20B treatment than in B20A. After the biochar adding, it is subject to a whole range of biochemical reactions which can be reflected in a change in its properties over time (Liang et al., 2006). The study of Šimanský et al. (2018) also observed the gradual decline of biochar efficiency during the first three years in this experiment after its first application. The values of SBC, CEC and BS gradually decreased in almost all treatments. According to Ren, Yuan and Sun (2018), some biochar pores are blocked by fine soil particles. These gradually migrate from the outer to the inner portions of the pores. It may result in a reduction in surface area of biochar particles. As a result, it reflects on the suppression of its sorption capacity. In addition, the action of soil organisms can influence the structural properties of biochar, which is also shown to change its sorption capacity. At the same time, Ren, Yuan and Sun (2018) added that the effect of biochar increased in pollutant sorption in the first months after application. However, the biochar surface area gradually decreased over time, thereby decreasing its sorption capacity. It reached the control level within 2.5 years after adding biochar. A similar finding was also found by Martin et al. (2012). Our results showed that the greatest positive effects on the changes of sorption parameters were determined after the biochar reapplication at the rate of 20 $t.ha^{-1}$.

In the case of treatment with N fertilizer without biochar (B0N40), we found the highest value of H and the lowest values of SBC, CEC and BS. On the other hand, when the N fertilizer was used in combination with biochar, there was a significant decrease of H and the SBC, CEC and BS increased in of all four treatments (Table 3). Yu et al. (2017) stated that after the addition of N with biochar, the content of exchange cations was significantly higher than the addition of N fertilizer itself. Both rates of originally applied biochar: 10 $t.ha^{-1}$ and 20 $t.ha^{-1}$, respectively decreased H by 48.8% and 26.6%, increased SBC by 29.7% and 22.7%, CEC by 20%, and 15.8%, BS by 12.2% and 8.3% compared to B0N40 treatment. After the reapplication of biochar at both rates the H values dropped from 27.53 $mmol.kg^{-1}$ (B0N40) to 6.29 $mmol.kg^{-1}$ (B10B40B) and to 13.57 $mmol.kg^{-1}$ (B20N40B). The SBC values increased by 47.9% and 39.8%, CEC by 37.5% and 28.2%,BS by 16.8% and 16.5% compared to the B0N40 treatment. The most favourable effect of biochar in combination with N fertilizer was achieved in B10N40B treatment (H value – the lowest and opposite the highest values of SBC and CEC).

Conclusion

The results of our study showed the contrasting effects of the first application and the reapplication of pure biochar and biochar in combination with N fertilizer on improving of soil pH and soil sorption parameters.

In the case of the first biochar application without N, in B20A treatment we observed significant increase in pH in H_2O, pH in KCl, SBC and CEC by 6.3%, 5.7%, 16.3% and 13.4% compared to B0 treatment. The reapplication of lower biochar rate had a similar effect to the initial application of higher biochar rate. Additionally, the most beneficial effect in B20B treatment was achieved. We conclude that biochar reapplication at the higher rate had the most significant effect on increase of soil pH.

We found the higher values of pH in H_2O, pH in KCl, SBC, CEC, BS and lower value of H in B10N40A, B20N40A, B10N40B and B20N40B treatments compared to B0N40 treatment. In this case, the adding of fresh biochar was also more effective than the first application at the beginning of the experiment. The addition of 10 $t.ha^{-1}$ of fresh biochar had the most beneficial effect on soil pH and soil sorption parameters.

Based on the results of this study, we conclude that the addition of biochar into soil mainly at a higher rate or in combination with N every four years could be effective for increase of soil pH and improve soil sorption properties. In addition, we anticipate that shorter interval between biochar application could be even more advantageous.

Acknowledgements

This study was supported by Slovak Grand Agency VEGA (Project No. 1/0136/17).

References

AHMAD, M. – RAJAPAKSHA, A. U. – LIM, J. E. – ZHANG, M. – BOLAN, N. – MOHAN, D. – VITHANAGE, M. – LEE, S. S. – OK, Y. S. 2014. Biochar as a sorbent for contaminant management in soil and water: A review. In Chemosphere, vol. 99, 2014, pp. 19–33. DOI: 10.1016/j.chemosphere.2013.10.071

CASTALDI, S. – RIONDINO, M. – BARANTI, S. – ESPOSITO, F. R. – MARZAIOLI, R. – RUTIGLIANO, F. A. – VACCARI, F. R. – MIGIETTA, F. 2011. Impact of biochar application to a Mediterranean wheat crop on soil microbial acidity and greenhouse gas fluxes. In Chemosphere, vol. 85, 2011, pp. 1461–1471. DOI: 101.1016/j.chemosphere.011.08.031

CHINTALA, R. – MOLLINDE, J. – SCHUMACHER, T. E. – PAPIERNIK, S. K. – MALO, D. D. – KUMAR, S. – GULBRSDSON, D. W. 2013. Nitrate sorption and desorption in biochars from fast pyrolysis. In Microporous and Mesoporous Materials, vol. 179, 2013, pp. 250–257. DOI: 10.1016/j.micromeso.2013.05.023

CHINTALA, R. – SCHUMMACHER, T. E. – KUMAR, S. – MALO, D. D. – RICE, J. A. – BLEAKLEM, B. – CHILOM, G. – CLAY, D. E. – JULSOIN, J. L. – PAPIERNIK, S. K. – GU, Z. R. 2014. Molecular characterization of biochars and their influence on microbiological properties of soil. In Journal of Hazardous Materials, vol. 279, 2014, pp. 244–256. DOI: 10.1016/j.jhhazmat.2014.06.074

CORNELISSEN, G. – NURIDA, N. L. – HALE, S. E. – MARTINSEN, V. – SILVANI, L. – MULDER, J. 2018. Fading positive effect of biochar on crop yield and soil acidity during five growth seasons in an Indonesian Ultisol. In Science of The Total Environment, vol. 634, 2018, pp. 561–568. DOI: j.scietotenv.2018.03.380

DAI, Z. – ZHANG, X. – TANG, C. – MUHAMMAD, N. – WU, J. – BROOKES, P. C. – XU, J. 2017. Potential role of biochars in decreasing soil acidification. In Science of The Total Environmental, vol. 581–582, 2017, pp. 601–611. DOI: 10.1016/scietotenv.2016.12.169

ESSINGTON, M. E. 2004. Competetive sorption behavior of arsenic, sellenium, coper and lead by soil and biosolid nano and macro colloid particles. In Open Journal of Soil Science, vol. 4, 2004, pp. 293–304. DOI: 10.4236/ojss.2014.49031

FIALA, K. – KOBZA, J. – MATÚŠKOVÁ, Ľ. – BREČKOVÁ, V. – MAKOVNÍKOVÁ, J. – BARANČÍKOVÁ, G. – BÚRIK, V. – LITAVEC, T. – HOUŠKOVÁ, B. – CHROMANIČOVÁ, A. – VÁRADIOVÁ, D. – PECHOVÁ, B. 1999. Záväzné metódy rozborov pôd. Čiastkový monitorovací systém – PÔDA. 1. vyd. Bratislava : VUPOP, 1999, 142 s. ISBN 80-85361-55-8.

FIDEL, R. B. – LAIRD, D. A. – THOMPSON, M. L. – LAWRENKO, M. 2017. Characterization and quantification of biochar alkalinity. In Chemosphere, vol. 167, 2017, pp. 367–373. DOI: 10.1016/j.chemosphere.2016.09.151

GUO, J. H. – LIU, X. J. – ZHANG, Y. – SHEN, J. L. – HAN, W. X. – CHRISTIE, P. – GOULDING, K. W. T. – VITOSEK, P. M. 2010. Singificant acidification in major Chinese croplands. In College of Ressources and Evironmental Science, vol. 19, 2010, pp. 1008–1010. DOI: 10.1126/science.1182570

HANSEN, V. – STÓVER, D. M. – MUKHOLM, L. J. – PELTRE, C. – HAGGAARD-NIELSEN, H. – JENSEN, L. S. 2016. The effect of straw and wood gasification biochar on carbon sequestration, selected soil fertility indicators and functional groups in soil: An incubation study. In Geoderma, vol. 269, 2016, pp. 99–107. DOI: j.geoderma.2016.01.033

HORÁK, J. – KONDRLOVÁ, E. – IGAZ, D. – ŠIMANSKÝ, V. – FELBER, R. – LUKAC, M. – BALASHOV, E. V. – BUCHKINA, N. P. – RIZHIYA, E. Y. – JANKOWSKI, M. 2017. Biochar and biocharwith N fertilizeraffectsoil N_2O emission in HaplicLuvisol. In Biologia, vol. 72, 2017, pp. 995–1001. DOI: 10.1515/biolog-2017-0109

JURIGA, M. – ŠIMANSKÝ, V. – HORÁK, J. – KONDRLOVÁ, E. – IGAZ, D. – POLLÁKOVÁ, N. – BUCHKINA, N. P. – BALASHOV, E. 2018. The effect of different rates of biochar and biochar in combination with N fertilizer on the parameters of soil organic matter and soil structure. In Journal of Ecological Engineering, vol. 19, 2018, pp. 153–161. DOI: 10.129/22998993/92894

JURIGA, M. – ŠIMANSKÝ, V. 2018. Effect of biochar on soil structure-review. In Acta fytotechnica et zootechnica, vol. 19, 2018, pp. 11–19. DOI: 10.15414/afz.2018.21.01.11-19

KEILUWEIT, M. – NICO, P. S. – KLEBER, M. 2010. Dynamic molecular structure of plant biomaso-derived black carbon (biochar). In Environmental Science and Technol., vol. 44, 2010, pp. 1247–1253. DOI: 10.1021/es9031419

KOCHIAN, L. V. – PIÑEREROS, M. A. – LIU, J. – MAGALHAES, I. V. 2015. Plant adaptation to acid soils: The molecular basis of crop aluminium resistance. In Annual Review of Plant Biology, vol. 66, 2015, pp. 571–598. DOI: 10.1146/annurev-arplant-043014

LEHMANN, J. – RILLING, M. C. – THIES, J. – MASIELLO, C. A. – HOCKADAY, W. C. – CROWLEY, D. 2011. Biochar affect on soil biota – A review. In Soil Biology and Biochemistry, vol. 43, 2011, pp. 1812–1836. DOI: 10.1016/j.soilbio.2011.04.022

LIANG, B. – LEHMANN, J. – SOLOMON, D. – KINYANG, J. – GROSSMAN, J. – O'NEILL, B. – SKIEMSTAD, J. O. – LUZAO, T. J. – PETERSEN, J. – NEVES, E. G. 2006. Black carbon increases cation exchange capacity in soil. In Soil Sciency Society of American Journal, vol. 70, 2006, pp. 35–44.

LORENZ, K. – LAL, R. 2014. Biochar application to soil for climate change mitigation by soil organic carbon sequestration. In Journal of Plant Nutrition and Soil Science, vol. 177, 2014, pp. 651–670. DOI: 10.1002/jpnl.201400058

MARTIN, S. M. – KOOKANA, R. S. – ZWEITEN, L. V. – KRULL, E. 2012. Marked changes in herbicide sorption desorption upon ageing of biochars in soils. In Journal of Hazardous Materials, vol. 231–232, 2012, pp. 70–78. DOI: 10.1016/j.jhazmat.2012.06.040

MASUD, M. M. – LI, J. Y. – XU, R. K. 2014. Use of alkaline slag and crop residue biochars to promote base saturation and reduce acidity of an acidic Ultisoil. In Pedosphere, vol. 21, 2014, pp. 791–798. DOI: 10.1016/S1002-0160(14)60066-7

NOVAK, J. M. – LIMA, I. – XING, B. – GSKIN, J. W. – STEINER, CH. – DAS, K. C. – AHMEDNA, M. – REHRAH, D. – WATTS, D. W. – BUSSCHER, W. J. – SCHOMBERG, H. 2009. Characterization of designer biochar produced at different temperatures and their effect on a Loamy sand. In Annals of Environmental Science, vol. 3, 2009, pp. 195–206. ISSN 1939-2621.

OBIA, A. – CORNELISSEN, G. – MOLDE, J. – DÖRSH, P. 2015. Effect of soil pH increase by biochar on NO, H_2O and N_2 production during denitrification in acid soils. In Research Article, vol. 10, 2015. DOI: 10.1371/journal.pone.01387

REN, X. YUAN, X. – SUN, W. 2018. Dynamic changes in atrazine and phenauthrene sorption behaviors during the aging of biochar in soils. In Environmental Science and Pollution Research, vol. 25, 2018, pp. 81–90. DOI: 10.1007/s11356

RENGEL, Z. 2002. Handbook of planth growth, pH as the master variable. New York : Marcel Dekter, 2002, 446 p. ISBN 9780824707613

ŠIMANSKÝ, V. – HORÁK, J. – IGAZ, D. – BALASHOV, E. – JONCZAK, J. 2018. Biochar and biochar with N fertilizer as a potential tool for improving soil sorption of nutrients. In Journal of Soils and Sediments, vol. 18, 2018, pp. 1432–1440. DOI: 10.1007/s11368-017-1886-y

ŠIMANSKÝ, V. – HORÁK, J. – IGAZ, D. – JONCZAK, J. – MARKIEWICZ, M. – FELBER, R. – RIZHIYA, E. Y. – LUKAC, M. 2016. How dose of biochar and biochar with nitrogen can improve the parameters of soil organic matter and soil structure? In Biologia, vol. 71, 2016, no. 9, pp. 989–995. DOI: 10.1515/biolog-2016-0122

ŠIMANSKÝ, V. – IGAZ, D. – HORÁK, J. – ŠURDA, P. – KOLENČÍK, M. – BUCHKINA, N. P. – UZAROWICZ, Ł. – JURIGA, M. – ŠRANK, D. – PAUKOVÁ, Ž. 2018a. Response of soil organic carbon and water-stable aggregates to different biochar treatments including nitrogen fertilizer. In Journal Hydrology and Hydromechanics, vol. 66, 2018, pp. 429–436. DOI: 10.2478/john-2018-0033

TEUTSCHEROVA, N. – VAZGUEZ, E. – SANTANA, D. – NAVAS, M. – MASAGUER, M. B. 2017. In fluence of pruning waste compost maturity and biochars on carbon dynamics in acid soil: Incubation study. In European Journal of Soil Biology, vol. 78, 2017, pp. 66–74. DOI: 10.1016/j.ejsobi.2016.12.001

THOMPSON, R. C. – BAKIR, A. – STEVEN, J. – RICHARD, C. 2012. Competetive ofpersistant organic pollutants into microplastic in the marine environment. In Marine Pollution Bulletin, vol. 64, 2012, pp. 2782–2789. DOI: 10.1016/j.marpollbul.2012.09.010

WANG, B. – LI, C. – LIANG, H. 2013. Bioleaching of heavy metal from woody biochar aging Acidithio bacillusferrooxidans and activation for adsorption. In Bioresource Technology, vol. 146, 2013, pp. 803–806. DOI: 10.1016/j.biotech.2013.08.020

YANG, X. – YING, G. G. – KOOKANA, R. S. 2009. Reduced plant uptake of pesticides with biochar additions to soil. In Chemosphere, vol. 76, 2009, pp. 665–667. DOI: 10.1016/j.chemosphere.2009.04.001

YU, L. – LU, X. – YU, M. – XU, J. 2017. Combined application of biochar and nitrogen fertilizer benefits nitrogen retention in the rhizosphere of soybean by increasing microbial biomass but not altering microbial community structure. In Science of the Total Environment, vol. 187, 2017, pp. 640–641. DOI: 10.1016/j.scitoenv.2018.06.018

YUAN, J. H. – XU, R. K. – ZHANG, H. 2011. The forms of alkalis in the biochars produced from crop residues at different temperatures. In Bioresource Technology, vol. 102, 2011, pp. 3488–3497. DOI: j.biotech.2010.11.018

ZHANG, S. – ZHANG, B. – LI, X. 2002. Evolution of soil fertility and fertilizer benefits under different soil types and cropping systems. In Plant Nutrition Fertilization Science, vol. 8, 2002, pp. 9–15.

ZHANG, Y. – YANG, S. – FU, M. M. – CAI, J. P. – ZHANG, Y. Y. – WANG, R. Z. – XU, Z. W. – BAI, Y. T. – JIANG, Y. 2015. Sheep manure application increases soil exchangeable base cations in a semi-arid steppe of Inner Mongolia. In Journal of Arid Land, vol. 7, 2015, pp. 361–369. DOI: 10.1007/s40333015-0004-5

ZONG, Y. – WANG, Y. – SHENG, Y. – WU, C. – LU, S. 2018. Ameliorating soil acidity and physical properties of two contrasting texture Ultisols with wastewater sludge biochar. In Environmental Science and Pollutant Research, vol. 25, 2018, pp. 25726–25733. DOI: 10.1007/s11356-017-9509-0

sciendo

DOI: 10.2478/ahr-2019-0013

Acta Horticulturae et Regiotecturae 2/2019 *Ronald Pöppl, Elena Aydin*

Acta Horticulturae et Regiotecturae 2
Nitra, Slovaca Universitas Agriculturae Nitriae, 2019, pp. 71–74

IDENTIFICATION OF STUDY SITES FOR PLACEMENT OF SEDIMENT TRAPS IN VEGETATED BUFFER STRIPS

Ronald PÖPPL[1], Elena AYDIN[2]*

[1]University of Vienna, Austria
[2]Slovak University of Agriculture in Nitra, Slovak Republic

The aim of this contribution was to outline the decision procedure for selecting potential sites suitable for installing sediment traps in vegetation buffer strips in the Fugnitz catchment, Austria. The selection procedure consisted of GIS data processing where the contributing areas of specific sites were specified according to the selected criteria (i.e. slope above 2°, vegetation strip in between agriculturally used land and river network, contributing area of at least 300 m^2). Available landuse maps were updated with formerly not-digitized structures potentially influencing connectivity (e.g. ephemeral streams and road ditches) which were mapped in the field. From 31 pre-defined sites 15 were selected, taking into account as additional selection criteria the slope angle, soil erodibility and size of the contributing area. Two sites were selected for further investigations – i.e. installation of the sediment traps in vegetation filter strips collecting event-based sediment yields from adjacent arable fields. We conclude that GIS analysis has shown to be useful for the first step-delineation of potential sites of interest on the catchment scale. However, field-based surveys have been shown to be inevitable to obtain on-site information on vegetation characteristics and fine-scale topographic and management information.

Keywords: water erosion, sediment delivery, connectivity, buffer strips

The process of water erosion not only causes soil loss and changes in soil properties on-site, but is followed by various off-site effects (Antal et al., 2014). According to Boardman et al. (2019), off-site impacts of the soil erosion are often of greater social and economic concern in Western Europe than on-site impacts. They fall into two related categories: muddy flooding of properties and ecological impacts on watercourses because of excessive sedimentation and associated pollutants. Scientists have tried to understand, describe and quantify surface runoff and sediment fluxes at multiple scales for many years. In the past two decades, a new concept called connectivity has been used by Earth Scientists as a means to describe and quantify the influences on the fluxes of water and sediment on different scales: aggregate, pedon, location on the slope, slope, watershed, and basin (Keesstra et al., 2018). When considering the hydro-geomorphic processes in catchment systems, according to the connectivity approach, three types of linkages can be differentiated (Fryirs et al., 2007):

a) Longitudinal (upstream – downstream and tributary-main stem relationships), which drive the transfer of flow and sediment through the catchment.
b) Lateral (channel – floodplain and slope-channel relationships), which manage the supply of materials to the channels.
c) Vertical (surface-subsurface) interactions of water, sediment and nutrients.

Although several authors have pointed out that the spatial distribution of vegetation along slopes has a significant impact on the reduction of surface runoff and sediment entrainment under various environmental conditions (Li et al., 2009, Pugh, 2014), relatively little information is available on the effect of spatial and species composition of vegetation buffer strips on lateral connectivity, especially when considering long-term monitoring (Yuan et al., 2009; Keesstra et al., 2012; Poeppl et al., 2012).

Various techniques are used worldwide to assess the instant or long-term intensity of water erosion processes in the field, such as surface runoff trapping, volumetric analyses of erosion and rainfall simulations (e.g. Antal et al., 2014; Toy, Foster and Renard, 2012). Mainly because of time, labour and cost requirements, laboratory and field experiments on hillslope scale predominate over comprehensive studies of the causes and effects of water erosion on the catchment scale (Maetens et al., 2012). On the one hand, field measurements are very important as they provide information for model calibration. On the other hand, GIS-based assessment of erosion risk allows capturing the spatial variability of erosion factors on the catchment scale (Mitasova et al., 2013; Šinka and Kaletová, 2013). Due to hydro-geomorphic complexity inherent in catchment systems (Bracken et al., 2015; Poeppl, Keesstra and Maroulis, 2017), upscaling of plot-scale observations often does not result in accurate watershed-scale estimates of runoff and erosion (Sadeghi et al., 2013).

Contact address: Ing. Elena Aydin, PhD., Department of Biometeorology and Hydrology, Slovak University of Agriculture, Hospodárska 7, 949 76 Nitra, Slovakia, +421 37641 52 52, e-mail: elena.aydin@uniag.sk

Considering the special geomorphologic situation of Austria, of which more than 60% is the Alpine territory with high relief energies, erosion and erosion control have been a major issue for a long time. Land management is certainly one of the key factors for on-site erosion risk. With the participation of Austria in the European Union, the first concerted efforts to reduce the soil erosion by water at the national scale were initiated by the Austrian Programme for a Sustainable Agriculture that was launched in 1995 (Strauss and Klaghofer, 2006). It offered environmental contracts to farmers who were willing to implement specific protection measures, such as erosion control on vineyards, orchards and farmland. Besides the given subsidy, some farmers found it difficult to follow these incentives due to various reasons, such as inadequate machinery, additional planning, work and organization.

The loess soils of the Federal State of Lower Austria are especially prone to the soil erosion by water. The situation becomes even more problematic when protected areas are affected by high input rates of (nutrient- and pollutant-laden) sediment input, as in the case of the Thayatal National Park.

The aim of this contribution is to outline the decision procedure for selecting potential sites suitable for the assessment of sediment trap efficiencies of vegetation buffer strips in the Fugnitz River catchment.

Material and methods

Study area

The Fugnitz River catchment (size ~138 km^2) is located in Lower Austria near the Czech Republic border (Figure 1). About 34% of the catchment area is covered by forests, 5% is taken by built up area, while 60% is agricultural land. After high precipitation events, the Fugnitz River is very often carrying (nutrient- and pollutant-laden) sediments, mainly originating from extensively used agricultural areas, further entering the Thaya River in the Thayatal National Park (Figure 2).

Selection of study sites using GIS

Since our aim was to study the sediment trap efficiency of vegetation filter strips, the selection of study sites was limited to strips of vegetation located adjacent to intensively cultivated agricultural land. Potential study sites were pre-selected via visual interpretation of recent orthophotos (source: the Federal State of Lower Austria). Thereafter, for each of the selected vegetation strips contributing areas with a minimum size of 300 m^2 were calculated in ArcGIS v. 10.2 using a DEM with a resolution of 1 m by 1 m (source: the Federal State of Lower Austria). This area threshold was chosen to avoid locations with very small contributing area where no surface runoff was observed in the field. Therein, we adopted the approach by Fryirs et al. (Fryirs et al., 2007; Poeppl et al., 2012), i.e. taking into account only areas with slope angles above 2°, reflecting energy conditions capable of entraining and transporting sediment along hillslopes. 15 were selected from 31 pre-defined sites, taking into account slope angle, soil erodibility expressed as K-factor according to Strauss (2007) and size of the contributing area as additional selection criteria.

Figure 1 Location of the Fugnitz River catchment in Austria
Source: Poeppl et al., 2013

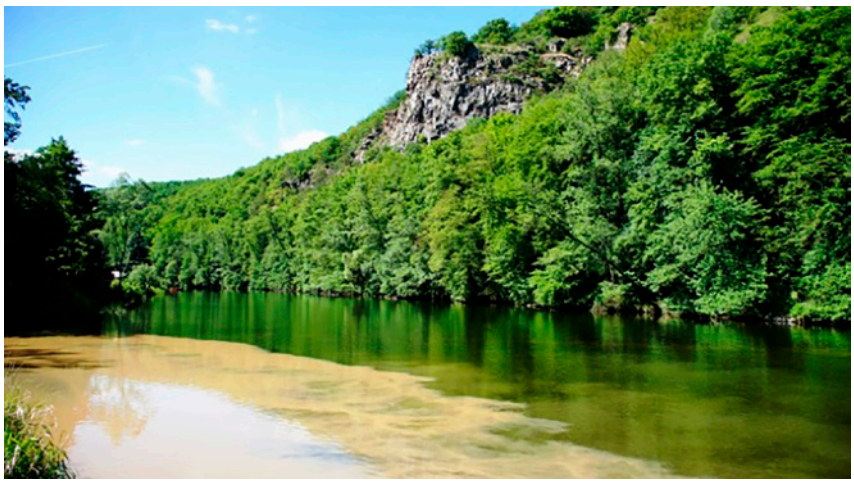

Figure 2 Visual difference in water quality at the confluence of the Fugnitz and Thaya Rivers caused by high sediment loads in the Fugnitz River
Photo: Aydin, 2017

Field survey

The conditions of 15 sites were investigated in the field during the field campaign in summer 2017. Crucial information on vegetation buffer strips and adjacent arable fields, such as crop type, vegetation buffer structure, observed water erosion processes, accessibility and features not shown on land use map or ortophotos were recorded in the field. After the field visit, the original land use map of the pre-selected sites was updated with formerly non-digitized structures potentially influencing connectivity (e.g. ephemeral streams and road ditches) (Figure 3).

Results and discussion

According to the landuse analysis, the vegetation strips in the Fugnitz catchment were generally located along waterways. About 32% of the vegetation strips have been dominated by grasses and herbs, occasionally accompanied by scattered trees or shrubs. They were selected as priority areas because of their common proximity to agricultural land (Figure 4). The example showing the selected vegetation strip including calculated contributing areas is shown in Figure 3.

Two sites (i.e. "Felling" and "Heufurth"), meeting our selection criteria as described above, were selected for further investigations – i.e. installation of sediment traps in vegetation filter strips collecting event-based sediment yields from adjacent arable fields. A 2.5 m belt of predominantly grassy vegetation with minor seasonal occurrence of various herbaceous species has been located on a small slope between arable land and a functional road ditch draining the surface runoff to the river network at the "Felling" site (Figure 5a). The arable field has been linked to a 2.5 m belt of grasses and herbs (especially *Urtica dioica* L.) forming a first line of riparian vegetation at the "Heufurth" site (Figure 5b). To further assess the sediment trap efficiency of vegetated filter strips, constructed sediment traps (60 × 40 × 30 cm) were placed and secured with 10 cm long nails 2 m from the upper border of the strip. Moreover, the sites have been equipped with rain gauges and soil moisture measurement devices.

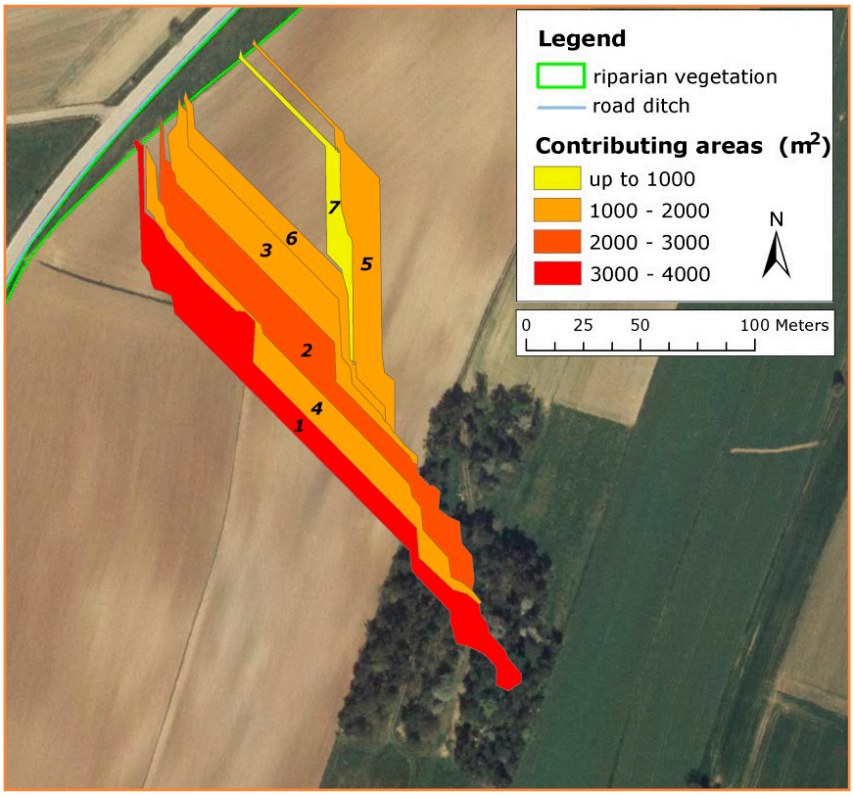

Figure 3 The selected vegetation strip including calculated contributing areas along a road ditch
Source of the ortophoto: The Federal State of Lower Austria, 2017

Figure 4 Exceeding of sediment trap capacity of local grass filter strip after rainfall event
Photo: Aydin, 2017

Conclusion

In our contribution, we have tried to outline the procedure of the selection of suitable study sites for further investigations on the effects of vegetation strips on lateral sediment connectivity. GIS analysis has shown to be useful for the first step-delineation of potential sites of interest on the catchment scale. However, field-based mapping has been shown to be inevitable to obtain on-site information on vegetation characteristics, fine-scale topographic and management information.

Figure 5 Experimental setting for event-based sediment yield and vegetation buffering efficiency measurements, strip in a) "Felling" and b) "Heufurth"
Photo: Aydin, 2017

Acknowledgement

This work was supported by the Slovak Research and Development Agency under the contract No. SK-AT-2017-0008, Cultural and Educational Grant Agency under the contract No. 026SPU-4/2017 and grant of Action Austria-Slovakia.

References

ANTAL, J. – BÁREK, V. – ČIMO, J. – HALAJ, P. – HALÁSZOVÁ, K. – HORÁK, J. – IGAZ, D. – JURÍK, Ľ. – MUCHOVÁ, Z. – NOVOTNÁ, B. – ŠINKA, K. 2014. Hydrológia poľnohospodárskej krajiny. Nitra : SPU, 2014, 371 s. ISBN 978-80-552-1257-9 (in Slovak).

BOARDMAN, J. – VANDAELE, K. – EVANS, R. – FOSTER, J. D. L. 2019. Off-site impacts of soil erosion and runoff: Why connectivity is more important than erosion rates. In Soil Use and Management, vol. 35, 2019, no. 2, pp. 245–256. DOI: 10.1111/sum.12496.

BRACKEN, L. J. – TURNBULL, L. – WAINWRIGHT, J. – BOGAART, P. 2015. Sediment connectivity: a framework for understanding sediment transfer at multiple scales. In Earth Surf. Process. Landforms, vol. 40, 2015, no. 2, pp. 177–188. DOI: 10.1002/esp.3635.

FRYIRS, K. – BRIERLEY, G. J. – PRESTON N. J. – SPENCER, R. 2007. Catchment-scale (dis)connectivity in sediment flux in the upper Hunter catchment, New South Wales, Australia. In Geomorphology, vol. 84, 2007, pp. 297–316. DOI: 10.1016/j.geomorph.2006.01.044.

KEESSTRA, S. – NUNES, J. – SACO, P. – PARSONS, T. – POEPPL, R. – MASSELINK, R. – CERDÀ, A. 2018. The way forward: can connectivity be useful to design better measuring and modelling schemes for water and sediment dynamics? In Science of The Total Environment, vol. 664, 2018, pp.1557–1572. DOI: 10.1016/j.scitotenv.2018.06.342.

KEESSTRA, S.D. – KONDRLOVA, E. – CZAJKA, A. – SEEGER, M. – MAROULIS, J. 2012. Assessing riparian zone impacts on water and sediment movement: a new approach. In Netherlands Journal of Geosciences, vol. 91, 2012, no. 1/2, pp. 245–255. ISSN 0016-7746.

LI, M. – YAO, W. Y. – DING, W. F. –YANG, J. – CHEN, J. 2009. Effect of grass coverage on sediment yield in the hillslope-gully side erosion system. In J. Geogr. Sci., vol. 19, 2009, no. 3, pp. 321–330. DOI:10.1007/s11442-009-0321-8.

MAETENS, W. – VANMAERCKE, M. – POESEN, J. – JANKAUSKAS, B. – JANKAUSKIENE, G. – IONITA, I. 2012. Effects of land use on annual runoff and soil loss in Europe and the Mediterranean: a meta-analysis of plot data. In Progress in Physical Geography, vol. 36, 2012, no. 5, úp. 597–651. DOI:10.1177/0309133312451303.

MITASOVA H. – BARTON M. – ULLAH I. – HOFIERKA J. – HARMON R. S. 2013. GIS-based soil erosion modeling. In Treatise on geomorphology (ed. SHRODER, J. F.), vol. 3, 2013, pp. 228–258.

POEPPL, R.– KEILER, M. – VON ELVERFELD, K. – ZWEIMUELLER, I. – GLADE, T. 2012. The influence of riparian vegetation cover on diffuse lateral sediment connectivity and biogeomorphic processes in a medium-sized agricultural catchment, Austria. In Geografiska Annaler: Series A, Physical Geography, vol. 94, 2012, no. 4, pp. 511–529. DOI:10.1111/j.1468-0459.2012.00476.x.

POEPPL, R. E. – KEESSTRA, S. D. – KEILER, M. – COULTHARD, T. – GLADE, T. 2013. Impact of dams, dam removal and dam-related river engineering structures on sediment connectivity and channel morphology of the Fugnitz and the Kaja Rivers. In 5th Symposium for Research in Protected Areas, 10 to 12 June 2013, Mittersill, pp. 607–613. [online], [cit. 2019-06-01] Available online at: <https://www.zobodat.at/pdf/NP-Hohe-Tauern-Conference_5_0607-0613.pdf>

POEPPL, R. E. – KEESSTRA, S. D. – MAROULIS, J. 2017. A conceptual connectivity framework for understanding geomorphic change in human-impacted fluvial systems. In Geomorphology, vol. 277, 2017, pp. 237–250. DOI: 10.1016/j.geomorph.2016.07.033.

PUGH, D. 2014. The need for stream buffers. NEFA background paper. [online], [cit. 2019-06-26] Available online at: <https://d3n8a8pro7vhmx.cloudfront.net/ncec/pages/66/attachments/original/1422848063/NEFA_The_Need_for_Stream_Buffers.pdf?1422848063The%20Need%20for%20Stream%20Buffers>

SADEGHI, S.H. R. – BASHARI SEGHALEH, M. – RANGAVAR, A. S. 2013. Plot sizes dependency of runoff and sediment yield estimates from a small watershed. In Catena, vol. 102, 2013, pp. 55–61. DOI: 10.1016/j.catena.2011.01.003.

STRAUSS, P. 2007. Flächenhafter Bodenabtrag durch Wasser (Areal soil loss by water). Kapitel 8.4. In Bundesministerium für Land- und Forstwirtschaft, Umwelt und Wasserwirtschaft (Hrsg.): Hydrologischer Atlas Österreich, Wien, Österreich, 2007.

STRAUSS, P. – KLAGHOFER, E. 2006. Austria. In Soil erosion in Europe (eds. BOARDMAN, J. – POESEN, J.), pp. 205–212. Chichester : John Wiley & Sons Inc., 2006, 855 p. ISBN 13 978 0-470-85910-0.

ŠINKA, K. – KALETOVÁ, T. 2013. Determining the characteristics of direct runoff from real rain using GIS environment. In Acta horticulturae et regiotecturae, vol. 16, 2013, no. 2, pp. 48–52. DOI:10.2478/ahr-2013-0012.

TOY, J. T. – FOSTER, R. G. – RENARD, G. K. 2002. Soil erosion: processes, prediction, measurement, and control. New York : John Wiley & Sons Inc., 2002, 338 p. ISBN 0-471-38369-4.

YUAN, Y. – BINGNER R. L. – LOCKE, M. A. 2009. A review of effectiveness of vegetative buffers on sediment trapping in agricultural areas. In Ecohydrol., vol. 2, 2009, pp. 321–336. DOI: 10.1002/eco.82.

sciendo

DOI: 10.2478/ahr-2019-0014

Acta Horticulturae et Regiotecturae 2/2019 *Janarul Shaikh et al.*

Acta Horticulturae et Regiotecturae 2
Nitra, Slovaca Universitas Agriculturae Nitriae, 2019, pp. 75–79

IMPACT ASSESSMENT OF VEGETATION GROWTH ON SOIL EROSION OF A LANDFILL COVER SURFACE

Janarul SHAIKH[1]*, Sudheer Kumar YAMSANI[2], Manash Jyoti BORA[3], Sreedeep SEKHARAN[3], Ravi Ranjan RAKESH[4], Atharva MUNGALE[5], Sanandam BORDOLOI[3]

[1]C. V. Raman College of Engineering, Bidyanagar, Mahura, Janla, Bhubaneswar, Odisha, India
[2]Vaagdevi College of Engineering, Warangal, Telangana, India
[3]Indian Institute of Technology Guwahati, Kamrup, Assam, India
[4]Bhabha Atomic Research Centre, Mumbai, Maharashtra, India
[5]Veermata Jijabai Technological Institute, Mumbai, Maharashtra, India

Soil erosion is a very common phenomenon encountered at many sloped earthen geotechnical structures. For instance, the surface soil of an inclined landfill cover system undergoes the erosion due to various adverse atmospheric variants. This is one of the major causes for performance failure in the cover system. However, previous researchers have rarely conducted the study for field assessment of soil erosion in high rainfall tropical regions such as northeast India. The literature advocates the utilization of vegetation for erosion management. This study investigated the impact of vegetation growth on soil erosion of a cover surface layer under both natural and controlled artificial rainfall. The soil erosion was monitored by collecting the soil loss due to rainfall. Vegetation growth was evaluated based on photographic image analyses. The study clearly indicates that the vegetation growth can contribute to reduction of soil erosion from the landfill cover surface.

Keywords: vegetation growth, water infiltration, soil erosion, landfill cover, artificial rainfall

Growing demand for energy and improved infrastructure have led to increase in high contaminant wastes that need sustainable isolation systems for their safe containment in an engineered landfill (Kumar et al., 2008; EEA, 2013). Multi-layered composite cover system is usually constructed over a landfill after its full capacity to secure the global ecosystem from the underlying wastes (Morris and Barlaz, 2011; Yamsani, Sreedeep and Rakesh, 2016). The landfill cover structure experiences various types of adverse phenomena due to different weather variants. Rainfall induced soil erosion of cover surface layer is one such phenomenon which causes deterioration in performance efficiency of landfill cover systems (Vereecken, Kollet and Simmer, 2010). Failure investigations of several existing waste containment facilities have identified the erosion to be the main cause for degradation of structural stability and performance (Huvaj-sarihan and Stark, 2008). Erosion of surface soils is affected by multiple factors namely soil water content, soil density, vegetation growth, anticipated rainfall, wind direction, soil type, slope length and gradient, etc. (Prosdocimi, Cerda and Tarolli, 2016; Nearing et al., 2017; Sachs and Sarah, 2017). There are different erosion management practices such as the use of geotextile (Luo et al., 2013), berm construction, mulching (Wang et al., 2015), vegetation growth (Butt, Waoas and Mahmood, 2010). The literature strongly recommends the use of vegetation for controlling soil erosion from sloped earthen structures such as landfill cover systems. However, the field investigation of soil erosion from surface layer of any landfill cover system constructed in a high rainfall tropical region such as northeast India has not been carried out previously.

The aim of the study is to evaluate the impact of vegetation growth on soil erosion of a landfill cover surface under the natural and controlled artificial rainfall. The soil erosion has been measured weekly by determining the mass of soil loss due to precipitation. The study utilized the photographic image analyses of vegetated surface to identify the role of vegetation growth to affect the soil erosion from the landfill cover surface. The hypothesis of the present study is to explore the survival period of the landfill cover system due to the positive effect of vegetation growth on the surface layer to prevent its soil erosion.

Material and methods

Construction of experimental cover setup

A pilot experimental field cover system was constructed at 5% slope near geotechnical laboratory at the Indian Institute of Technology Guwahati, India (26.18° N, 91.40°E). The experimental cover setup consisted of a fixed masonry construction to accommodate pilot cover system, a rainfall simulation system and a collection chamber of accumulated soil loss. The schematic outline and the pictorial view of the

Contact address: Janarul Shaikh, Assistant Professor, C.V. Raman College of Engineering, Department of Civil Engineering, Bidyanagar, Mahura, Janla, Bhubaneswar 752 054, Orissa, India, phone: +91-96 78 02 72 98, e-mail: janarul@gmail.com

experimental setup are shown in Fig. 1. The construction of experimental set-up was done according to standard practices. The leakage through the lateral walls or base was restricted by using impermeable masonry finishing. Medium plastic red soil (RS) was used to construct top surface layer of the field cover setup. RS was collected locally from the hilly area of Guwahati city. It is a medium plastic silty soil and qualifies for the requirement of surface soil layer in the cover system (USEPA, 1989; Landreth et al., 1991). The basic physical, geotechnical and chemical properties of the soil materials were investigated using standard laboratory procedures reported in the relevant code of Indian standard (IS) or international American society of testing and materials (ASTM) and presented in Table 1.

Rainfall simulator

The rainfall simulator was made of four "Full Cone square spray – 1/2HH-40WSQ" nozzles from Spraying Systems Co. fitted to a 12 mm diameter pipe at a height of 2 m from ground surface. An interferential, single jet, super dry straight reading type, hermetically sealed water meter confirming to ISO-4064, controlled the inlet pressure for rain simulator. The rainfall simulator was calibrated for intensity versus inlet pressure before starting the experimentation of the field setup. The spatial uniformity was established in terms of the coefficient of uniformity (CuC) presented in the equation 1 (Christiansen, 1941). Table 2 summarized the rainfall calibration results, which indicate that the simulated rainfall intensity and raindrop size increased with increase in the inlet pressure. The uniformity was satisfactorily recorded in between 80 to 90%. The raindrop size was evaluated using the flour pellet method defined by Kincaid et al. (1996).

$$CuC = \left(1 - \frac{\sum_1^N \left|X_i - \bar{X}\right|}{N\bar{X}}\right) 100 \qquad (1)$$

where:

CuC – the coefficient of uniformity (%)
X_i – is the rainfall at any measurement location (mm)
X – the mean rainfall amount (mm)
N – the number of locations chosen for measuring rainfall

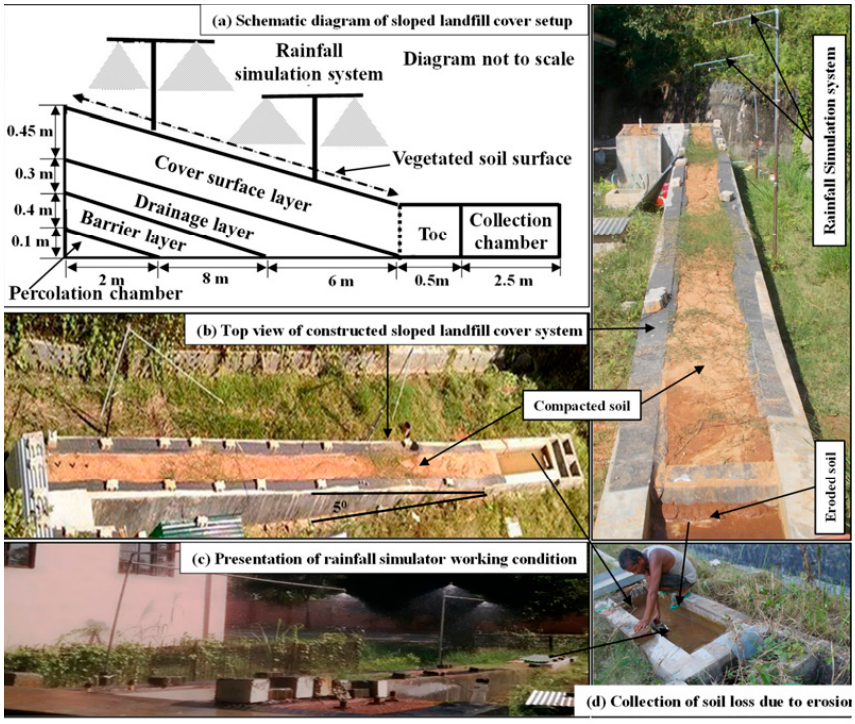

Figure 1 Schematic diagram of test cover setup and pictorial view after its construction

Table 1 Basic characteristics of soil material used in the study

Properties	Red soil (RS)
General	
Specific gravity, G	2.65
Hygroscopic water content (%)	5
Saturated hydraulic conductivity ($m.s^{-1}$)	2.9E-8
Specific surface area ($m^2.g^{-1}$)	55
Linear shrinkage (%)	2
Free swell index (%)	10
Particle size distribution	
% of gravel (>4.75 mm)	0
% of coarse sand (2.00–4.75 mm)	17
% of medium sand (0.425–2.00 mm)	16
% of fine sand (0.075–0.425 mm)	16
% of silt (0.002–0.075 mm)	19
% of clay (<0.002 mm)	32
Atterberg's limits	
Liquid limit (%)	42
Plastic limit (%)	22
Shrinkage limit (%)	21
Plasticity index (%)	20
USCS classification	ML
Standard compaction	
Optimum moisture content, OMC (%)	20
Maximum dry density, MDD ($g.cm^{-3}$)	1.73

Table 2 Characteristics of simulated rainfall events

Nozzle type	Orifice diameter (mm)	Pressure (kPa)	Flow meter (l.min^{-1})	Rain drop size (mm)	Rainfall intensity (mm.hr^{-1})	Coefficient of uniformity (CuC) (%)
Full Cone square spray – 1/2HH-40WSQ	6.4 mm (maximum free passage 3.2 mm)	70	15.2	2.1 ±0.1	60 ±5	87.3
		90	17.8	2.4 ±0.1	80 ±5	81.4
		120	19.7	2.9 ±0.2	100 ±5	89.7

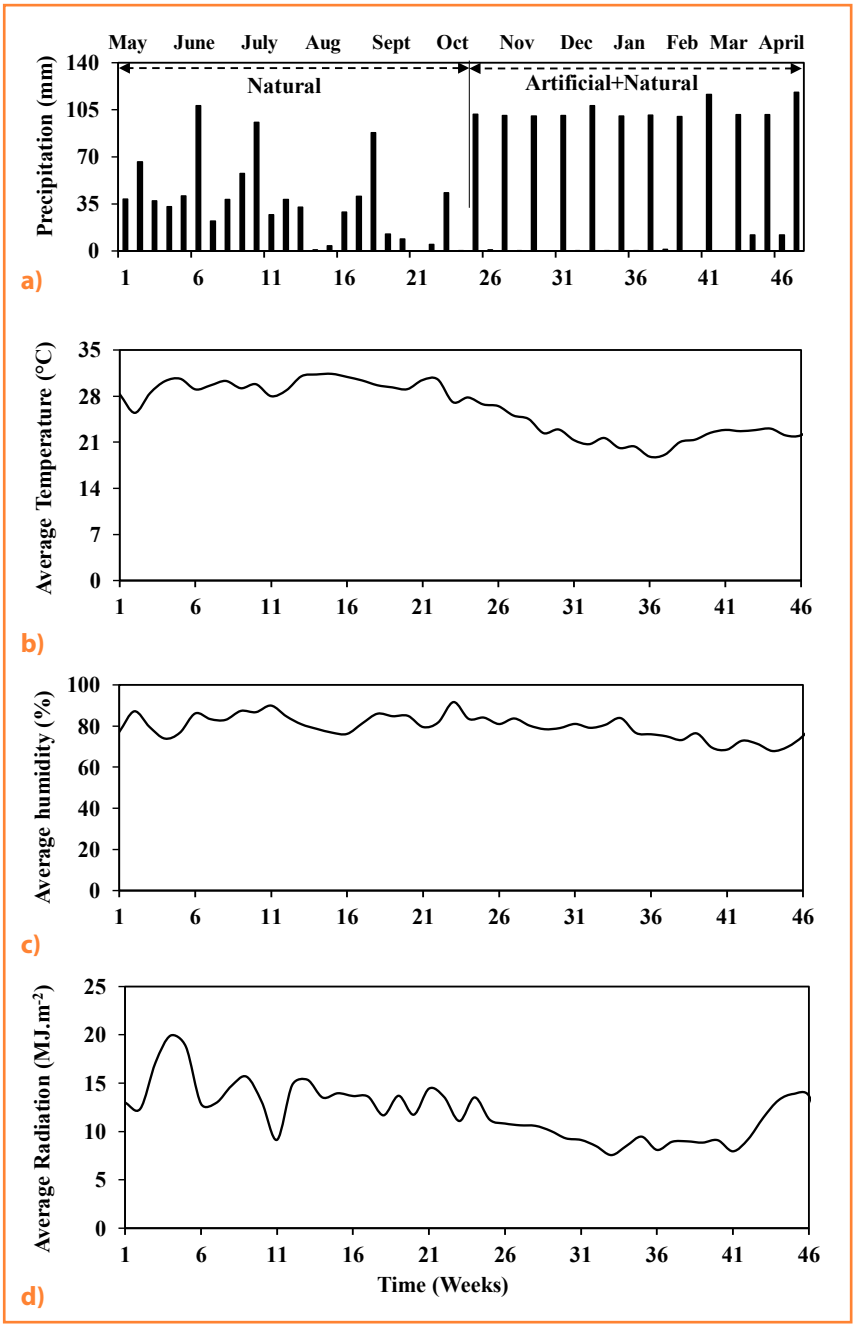

Figure 2 Various weather parameters during the monitoring period of the field cover setup

Testing program and methods

The sloped soil surface was initially exposed to natural weather variations for a period of six months (May – October, 2016) during the monsoon period. The climatic variations in northeast India are of mixed type that includes heavy rainfalls and high temperatures, causing cyclic wetting and drying. The natural weather variations during the study period were monitored using microclimate weather station (Decagon devices Inc., 2015) installed near the experimental site. Fig. 2 presents various weather parameters. For systematic investigation, after completion of monsoon, rainfall events of about 100 ±5 mm.hr^{-1} were simulated on the cover surface for the duration of an hour biweekly as a basis in this study. Eleven rainfall events were simulated in the period starting from November 2016 to April 2017. Fig. 2 (a) shows the summary of rainfall events which includes both natural and simulated rainfall. The soil loss, percentage of vegetated area, eroded soil profile and weather parameters were monitored during the entire experimental period. The eroded soil mass settled under rainwater was collected from all four chambers provided at the toe region of the sloped cover setup and the soil loss was evaluated based on the collected soil mass. 98% of the soil is recovered from the 2.5 m collection chamber present immediate to the pilot cover slope. The amount of soil erosion is expressed in terms of rate of soil loss (kg.m^{-2}.s^{-1}) by considering the total sloped surface area and the time of rainfall simulation.

The images of the nine sections were captured using an advanced photographic camera (NIKON D5200, Exposure time 1:4000 s, FL-26 mm, Aperture 4.2, ISO 1000) on weekly basis. The images were analysed using Matlab image processing tool to evaluate the percentage of vegetated area based on the colour index. Fig. 3 demonstrates the schematic process of calculating vegetation index using the image analysis. The average of readings from 9 sections was reported as the percentage vegetation for the given week. The depth of soil surface was also measured at 5 points on three horizontal axes (width-wise) in all these

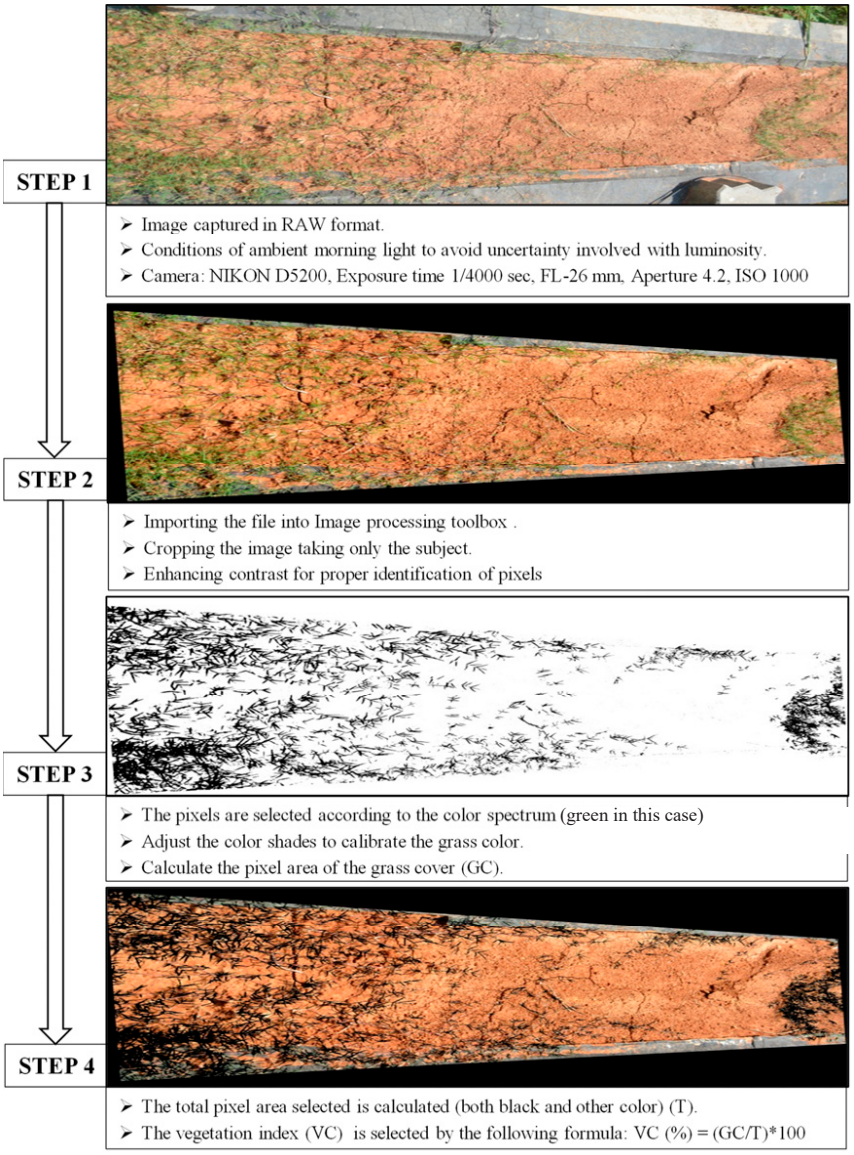

Figure 3 Schematic process of calculating vegetation index using image analysis

nine sections. A 3 dimensional spatial plot of observed data was reported to describe the changes in soil profile of the sloped surface.

Results and discussion

Vegetation growth

Fig. 4 (a) depicts the variation in green vegetation growth on the surface layer of field cover setup. The figure showed that the percentage of vegetated area consistently increased during the monitoring period except in the months of January and February of winter season. This may be due to the drop in its photosynthetic action in winter season (Jiang et al., 2017), resulting in dry grass over the cover surface. The drop in solar radiation during the winter (as observed in Fig. 2 (d)) strongly supports this phenomenon. Further, the increment rate of vegetation growth is observed to be relatively less in initial 24 weeks than that noted afterwards. This can be attributed to higher temperature and rainfall (simulated events of 100 mm per 2 weeks) after first 24 weeks. Similar observations are reported by Propastin, Kappas, and Muratova (2008). However, the method of evaluating the vegetated area using image analysis has some limitations which were reported in the literature (Kondrlova et al. 2017).

Erosion rate

Fig. 4 (b) details weekly variation of soil erosion from the surface layer of the experimental cover setup subjected to both natural and artificial rainfall. The Fig. 4 (b) clearly indicates that the erosion rate was mostly affected by the duration and intensity of rainfall events. Particularly, the soil erosion rate rose during the initial stage when the simulated rainfall of high intensity was applied. However, the effect of surface dryness was also noted during the summer season. For instance, the soil erosion in 16th week was observed to be higher than in 17th week, even though 16th week received similar amount of rainfall as 17th week. This indicates the probability of higher erosion when the soil surface was dry. The surface dryness can be ascertained from the temperature recordings depicted in Fig. 2 (b).

Vegetation effect on soil erosion

Fig. 4 (a) and (b) show that the soil erosion rate was found to be higher if the natural rainfall was higher during the initial days of field monitoring when the vegetation growth was absent on the surface layer. However, the erosion rate was seen to be comparatively higher during simulated artificial rainfall events. This may be due to its higher intensity and bigger size of artificial raindrops causing higher impacting force to erode the soil particles from the cover surface. The soil erosion rate induced by the artificial rainfall diminished over the time as the vegetation growth gradually covered larger area on the soil surface. The drop in vegetation growth and evapotranspiration rate in the month of January and February slightly affected the soil erosion induced by the artificial rainfall. The erosion rate was significantly reduced due to further growth of vegetation after these two months.

Conclusion

This article deals with the impact assessment of vegetation growth on the soil erosion of surface layer of a pilot cover system subjected to natural and simulated rainfall for a period of one year. The study indicates progressive increase of vegetated area on the surface soil of the field setup along the time. The months of January and February showed the drop in vegetation

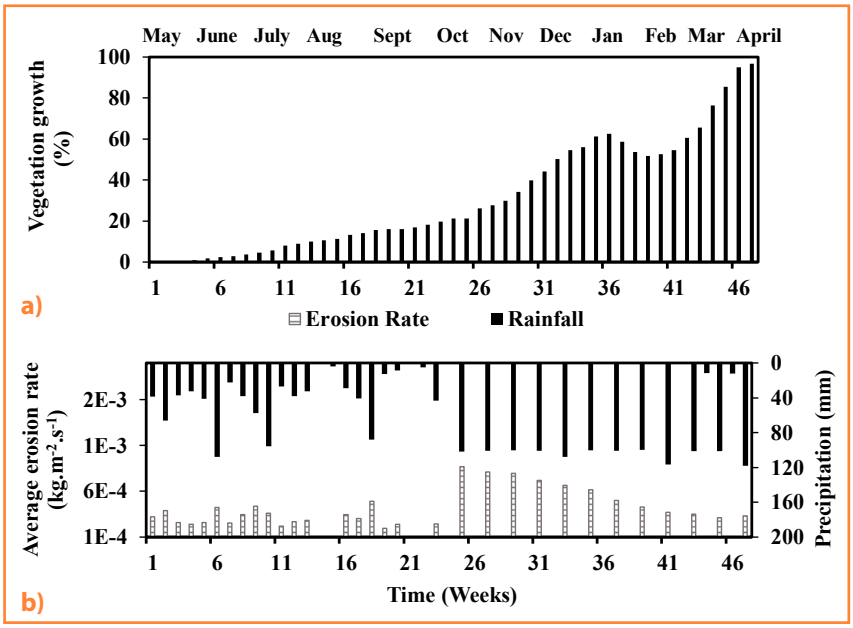

Figure 4 Temporal variation in (a) percentage of vegetated area and (b) average soil erosion rate on the cover surface layer subjected to natural and artificial rainfall events

growth due to lesser solar radiation causing inefficient photosynthetic activity during the winter season. The study also demonstrated that the cover surface encountered significant soil erosion due to heavy and prolonged rainfall events. Furthermore, the study indicates the considerable effects of the vegetation growth on the soil erosion from sloped cover surface. Soil erosion rate of any sloped earthen surface can be minimized by increasing the percentage of vegetated area.

Acknowledgment

Authors would like thankfully acknowledge board of research in nuclear sciences (BRNS), Department of Atomic Energy (DAE), India for the financial support provided for the work reported in this paper vide project no. 2013/36/06-BRNS.

References

ATUCHA, A. – MERWIN, I.A. – BROWN, M.G. – GARDIAZABAL, F. – MENA, F. – ADRIAZOLA, C. 2013. Soil erosion, runoff and nutrient losses in an avocado (*Persea americana* Mill) hillside orchard under different groundcover management systems. In Plant and Soil, 2013, 368, pp. 393–406.

BUTT, M.J. – WAQAS, A. – MAHMOOD, R. 2010. The Combined Effect of Vegetation and Soil Erosion in the Water Resource Management. In Water Resources Management, 2010, 24, pp. 3701–3714.

CHRISTIANSEN, J.E. 1941. The uniformity of application of water by sprinkler systems. In Agricultural Engineering, vol. 22, 1941, no. 3, pp. 89–92.

DECAGON DEVICES Inc. 2015. Microclimate monitoring system for measuring various weather parameters, Operator's User Manual, Decagon Devices Inc., Pullman, WA, United States of America (USA).

EEA. 2013. Managing municipal solid waste – a review of achievements in 32 European counties. Publications Office of the European Union, Report No. 2, 2013, pp. 1–40.

HUVAJ-SARIHAN, N. – STARK, T.D. 2008. Back-Analyses of Landfill Slope Failures. In 6th International Conference on Case Histories in Geotechnical Engineering. Arlington, VA. 2008, pp. 1–7.

JIANG, L. – JIAPAER, G. – BAO, A. – GUO, H. – NDAYISABA, F. 2017. Science of the Total Environment Vegetation dynamics and responses to climate change and human activities in Central Asia. In Science of the Total Environment, 2017, 599–600, pp. 967–980.

KINCAID, D.C. 1996. Spray drop kinetic energy from irrigation sprinklers. In Transactions of the ASAE, vol. 39, 1996, no. 3, pp. 847–853.

KONDRLOVÁ, E. – HORÁK, J. – IGAZ, D. – DOBIAŠOVÁ, D. 2017. The possibility of using digital images in assessment of plant canopy development and weed spread. In Acta Horticulturae et Regiotecturae, vol. 20, 2017, no. 2, pp. 35–39.

KUMAR, S. – MUKHERJEE, S. – CHAKRABARTI, T. – DEVOTTA, S. 2008. Hazardous waste management system in India: An overview. In Critical Reviews in Environmental Science and Technology, vol. 38, 2008, no. 1, pp. 43–71.

LANDRETH, R.E. – DANIEL, D.E. – KOERNER, R.M. – SCHROEDER, P.R. – RICHARDSON, G.N. 1991. Design and construction of RCRA-CERCLA final covers. In Seminar Publication. Washington DC, 1991.

LUO, H. – ZHAO, T. – DONG, M. – GAO, J. – PENG, X. – GUO, Y. – WANG, Z. – Liang, C. 2013. Field studies on the effects of three geotextiles on runoff and erosion of road slope in Beijing, China. In Catena, 2013, 109, pp. 150–156.

MORRIS, J.W.F. – BARLAZ, M.A. 2011. A performance-based system for the long-term management of municipal waste landfills. In Waste Management, vol. 31, 2011, no. 4, pp. 649–662.

NEARING, M.A. – YIN, S. – BORRELLI, P. – POLYAKOV, V.O. 2017. Catena Rainfall erosivity: An historical review. In Catena, 2017, 157, pp. 357–362.

PROPASTIN, P.A. – KAPPAS, M. – MURATOVA, N.R. 2008. Inter-Annual Changes in Vegetation Activities and Their Relationship to Temperature and Precipitation in Central Asia from 1982 to 2003. vol. 12, 2008, no. 2, pp. 75–87.

PROSDOCIMI, M. – CERDÀ, A. – TAROLLI, P. 2016. Catena Soil water erosion on Mediterranean vineyards: A review. In Catena, 2016, 141, pp. 1–21.

SACHS, E. – SARAH, P. 2017. Catena Combined effect of rain temperature and antecedent soil moisture on runoff and erosion on Loess. In Catena, 2017, 158, pp. 213–218.

USEPA. 1989. Requirements for hazardous waste landfill design, construction, and closure. In Seminar publication. United States Environmental Protection Agency, Cincinnati, Report No. 625/4-89/022, 1989, pp. 1-127.

VEREECKEN, H. – KOLLET, S. – SIMMER, C. 2010. Patterns in Soil – Vegetation – Atmosphere Systems: Monitoring, Modelling, and Data Assimilation. In Vadose Zone Journal, vol. 9, 2010, no. 4, pp. 821–827.

WANG, Q. – SONG, X. – LI, F. – HU, G. – LIU, Q. – ZHANG, E. – WANG, H. – DAVIES, R. 2015. Optimum ridge – furrow ratio and suitable ridge-mulching material for Alfalfa production in rainwater harvesting in semi-arid regions of China. In Field Crops Research, 2015, 180, pp. 186–196.

YAMSANI, S.K. – SREEDEEP, S. – RAKESH, R.R. 2016. Frictional and Interface Frictional Characteristics of Multi-Layer Cover System Materials and Its Impact on Overall Stability. In International Journal of Geosynthetics and Ground Engineering, vol. 2, 2016, no. 3, pp. 1–9.

sciendo

DOI: 10.2478/ahr-2019-0015

Acta Horticulturae et Regiotecturae 2
Nitra, Slovaca Universitas Agriculturae Nitriae, 2019, pp. 80–83

MOVEMENT OF THE SUSPENDED FLOW IN THE OPEN IRRIGATION CHANNELS

Aybek ARIFJANOV[1]*, Alisher FATXULLOEV[1], Tatiana KALETOVÁ[2]

[1]Tashkent Institute of Irrigation and Agricultural Mechanization Engineers, Uzbekistan
[2]Slovak University of Agriculture in Nitra, Slovak Republic

The article deals with the issues of turbulent movement of a suspended flow in open channels. Differential equations of a suspended flow were used with considering the interaction of the fluid and solid particles. The solution of equations for steady flow was obtained by a numerical method. Field data measured in irrigation channels in Tashkent and Parkent were used to estimate the velocity distribution over the depth of the stream. Developed method for calculating the formation of velocity field in statically and dynamically stable channels considered the turbulent characteristics and the presence of suspended sediments in the stream. The possibilities of practical application of the above-mentioned differential equations to the solution of the problem of a suspended solids flow's forming a velocity field were discussed. The developed analytical formulas make it possible to determine the value of flow parameters. The result is a new generalization of the mathematical model of the velocity field formation regularity at different flow saturations with a suspension. On its basis, the method is developed for calculating the parameters of the weighing process and transport of suspended particles in open channels.

Keywords: suspended solid flow, open channel, sediment, modelling

Flow turbulence affects the flow and channel cross section processes, determines the internal mechanism of the channel process, and forms the velocity structure of the suspended (two-phase) flow. What is the most important factor in assessing the stability condition of the channel? The importance and complexity of the turbulent motion of a suspended solid flow led to the development and improvement of various models of turbulent flow (Fidman, 1991; Frankl, 1953; Velikanov, 1955; Mikhailova, 1966).

There are numerous studies in open channels in this direction (e.g. Depeweg, 2002; Pal and Ghoshal, 2017; Lee et al., 2015). The most important kinematic and dynamic flow parameters, such as flow and channel interaction, velocity distribution and flow turbulence are studied. The result of the first approximation of mentioned parameters has been studied only, but the accuracy of predicting the formation of a stable channel section, considering transportation and sediment deposition, as a rule, remains low (Das, 2008; Karaushev, 1977). Therefore, many of the problems associated with the theory of interaction between the flow and the channel bed, as well as the formation of a stable cross section in the deformed channel, considering the turbulent structure of the suspended solid flow, are not studied thoroughly.

The difficulty and limitations in the practical implementation of existing models consist in the closure of the equations of motion system, as well as in considering that suspended particles affects the structure of the turbulent flow. In view of this, the streams with a low concentration of small particles are considered in some theories, which implies neglecting the effect of suspended sediment particles on the flow structure and the interaction of particles during their possible collisions. In this case, the averaged velocities of both phases are assumed to be the same, and when describing the velocity distribution profile, they use known dependencies derived for a single-phase flow in the beds, which significantly limits the scope of the solutions obtained.

Material and methods

In recent years, the theory of interpenetrating and interacting media, each phase of which is given by its equation (Rossinsky and Debolsky, 1960), has become applied widely in solving practical problems. In this theory, each medium is considered continuous; its movement is considered as a movement in a porous medium formed by the other phases. The system of equations developed according to this theory is closed, which makes it possible to theoretically investigate the phenomena occurring in a suspended turbulent flow.

When considering the movement of each phase separately, external forces are distributed to each phase. In addition, there is a force of interaction between the phases which, when considering a mixture in the flow, is an internal force. It follows that the forces acting on each phase consist of surface, mass and interaction forces. In this connection, the equations of motion for the *i*-th phase in differential form can be written as:

Contact address: prof. Aybek Arifjanov, Tashkent Institute of Irrigation and Agricultural Mechanization Engineers, Hydraulic Department, 39 KoriNiyoziy,100 000 Tashkent, Uzbekistan; e-mail: obi-life@mail.ru

$$\rho_1 \frac{d\bar{U}_i}{dt} = \text{div}\,\bar{P}_i + \bar{\Pi}_i + \rho_i \bar{F}_i \quad (1)$$

where:

$P_{ij} = -f_i\,\text{grad}P + \frac{\partial \tau_{ij}}{\partial x_{ij}}$ – the stress tensor acting on the *i*-th phase

τ_{ij} – internal stresses

f_i – volume content of the *i*-th phase ($i = 1, 2$)

The interaction force depending on the difference of the velocities of each phase is considered in the form:

$$\Pi_i = \left(K\bar{U} - \overline{U_s}\right) \quad (2)$$

Substituting the value of the parameters, equation (1) can be written in the form:

$$\rho_i = \frac{d\bar{u}_l}{dt} = -f_k\,\text{grad}P + \frac{d\tau_{kj}}{K\left(\bar{U} - \overline{U_s}\right) + \rho_i F_i dx_j} + \quad (3)$$

where:

$\bar{U}, \overline{U_s}$ – the velocity vectors of the carrier fluid and solid particles, respectively

K – coefficient of interaction between phases (carrier fluid and solid particles)

f_i – mass forces, in this case, mainly the components of gravity are considered

The main and defining characteristics of the turbulent flow structure are turbulent shear stresses. Turbulent shear stresses are determined according to the model developed in (Borovkov, 1989):

$$\tau_{ijl} = f_i \mu_i \left(-\frac{2}{3}\text{div}\overline{V_k} + 2\frac{\partial v_{kj}}{\partial x_j}\right) - \int LV_i d_n \quad (4)$$

with $j = l (\bar{n} = 1,2,3)$

$$\tau_{ijl} = f_i \mu_i \left(\frac{\partial v_{kl}}{\partial x_j} + \frac{\partial v_{kj}}{\partial x_j}\right)$$

with $j \neq l$

Then equation (3) considering (4) in projections on the coordinate axes ($j = x, y, z$; $l = x, y, z$) for the first phase of the suspended solid flow can be written as:

$$\begin{aligned}
\rho_1 \frac{du_1}{dt} &= \frac{\partial}{\partial x}\left(2f_1\mu_1\frac{\partial u_1}{\partial x}\right) + \frac{\partial}{\partial y}\left(f_1\mu_1\left(\frac{\partial u_1}{\partial y} + \frac{\partial v_1}{\partial x}\right)\right) + \frac{\partial}{\partial z}\left(f_1\mu_1\left(\frac{\partial u_1}{\partial z} + \frac{\partial w_1}{\partial x}\right)\right) \\
&\quad - Lu_1 + K(u_1 - u_2) + \rho_1 F_x \\
\rho_1 \frac{dv_1}{dt} &= \frac{\partial}{\partial y}\left(2f_1\mu_1\frac{\partial v}{\partial y}\right) + \frac{\partial}{\partial x}\left(f_1\mu_1\left(\frac{\partial u_1}{\partial x} + \frac{\partial v_1}{\partial y}\right)\right) + \frac{\partial}{\partial z}\left(f_1\mu_1\left(\frac{\partial v_1}{\partial z} + \frac{\partial w_1}{\partial y}\right)\right) \\
&\quad - Lv_1 + K(v_1 - v_2) + \rho_1 F_y \\
\rho_1 \frac{dw_1}{dt} &= \frac{\partial}{\partial z}\left(2f_1\mu_1\frac{\partial w}{\partial z}\right) + \frac{\partial}{\partial x}\left(f_1\mu_1\left(\frac{\partial w_1}{\partial x} + \frac{\partial u_1}{\partial z}\right)\right) + \frac{\partial}{\partial y}\left(f_1\mu_1\left(\frac{\partial v_1}{\partial z} + \frac{\partial w_1}{\partial y}\right)\right) \\
&\quad - Lw_1 + K(w_1 - w_2) + \rho_1 F_z
\end{aligned} \quad (5)$$

Respectively, for the second phase can be written as:

$$\begin{aligned}
\rho_2 \frac{du_2}{dt} &= \frac{\partial}{\partial x}\left(2f_2\mu_2\frac{\partial u_2}{\partial x}\right) + \frac{\partial}{\partial y}\left(f_2\mu_2\left(\frac{\partial u_2}{\partial y} + \frac{\partial v_2}{\partial x}\right)\right) + \frac{\partial}{\partial z}\left(f_2\mu_2\left(\frac{\partial u_2}{\partial z} + \frac{\partial w_2}{\partial x}\right)\right) \\
&\quad - Lu_2 + K(u_1 - u_2) + \rho_2 F_x \\
\rho_2 \frac{dv_2}{dt} &= \frac{\partial}{\partial y}\left(2f_2\mu_2\frac{\partial v}{\partial y}\right) + \frac{\partial}{\partial x}\left(f_2\mu_2\left(\frac{\partial u_2}{\partial x} + \frac{\partial v_2}{\partial y}\right)\right) + \frac{\partial}{\partial z}\left(f_2\mu_2\left(\frac{\partial v_2}{\partial z} + \frac{\partial w_2}{\partial y}\right)\right) \\
&\quad - Lv_2 + K(v_1 - v_2) + \rho_2 F_y \\
\rho_2 \frac{dw_2}{dt} &= \frac{\partial}{\partial z}\left(2f_2\mu_2\frac{\partial w_2}{\partial z}\right) + \frac{\partial}{\partial x}\left(f_2\mu_2\left(\frac{\partial w_2}{\partial x} + \frac{\partial u_2}{\partial z}\right)\right) + \frac{\partial}{\partial y}\left(f_2\mu_2\left(\frac{\partial v_2}{\partial z} + \frac{\partial w_2}{\partial y}\right)\right) \\
&\quad - Lw_2 + K(w_1 - w_2) + \rho_2 F_z
\end{aligned} \quad (6)$$

where:

u, v, w – components of velocity in projections on the coordinate axes

The field data were obtained in two irrigation channels in Tashkent and Parkent, northeastern part of Uzbekistan (Fig. 1). The channels are situated in Syr-Darya River basin. The channels are modified with concrete (n = 0.0225), slope 0.14‰.

Figure 1 Map of Uzbekistan and location of field measurements
Source: https://upload.wikimedia.org/wikipedia/commons/7/7e/Uzbekistan-CIA_WFB_Map.png, modified by authors

Results and discussion

A feature of the proposed system of differential equations is that the right side of the equations imply two additional terms (*L*, *Ls*), which characterize the turbulence of the channel flow-weighted. Solving a system of equations requires a search for flow parameters (*L*, *Ls*) characterizing the turbulence of a suspended solid flow, which is determined based on the developments given in Volgin (2009), Latipov and Umarov (1969), Latipov and Arifjanov (1994), Arifjanov and Fatkhullaev (2014).

To solve practical problems of the channel flow, it is necessary to develop a method for calculating the distribution of the averaging velocity of the suspended flow, which is used in wide variation ranges of the flow motion parameters conditions of the transported fluid and solid particles.

To develop a method for calculating the averaged velocity distribution over the depth of the suspended solid flow in the open channels, the system of differential equations (5 and 6) in the case of steady $\left(\frac{\partial u}{\partial t}=0\right)$, one-dimensional $\left(\frac{\partial u}{\partial x}=\frac{\partial u}{\partial z}=0\right)$ and uniform flow (assuming $f = s$ is the concentration of the second phase in the stream), the system of equations (5 and 6) is written in the form:

a) for carrier fluid:

$$\frac{\partial}{\partial y}\left[(1-s)\mu\frac{\partial u}{\partial y}\right]+K(u_s-u)-(1-s)Lu=-(1-s)\rho gi \qquad (7a)$$

b) for suspended solids flow:

$$\frac{\partial}{\partial y}\left[s\mu\frac{\partial u_s}{\partial y}\right]+K(u-u_s)-sL_su_s=-s\rho_T gi \qquad (7b)$$

where:

ρ, ρ_T – density of the transported fluid and solid particles
i – the slope of the water surface

The system of differential equations (7a and 7b) is solved numerically using the finite difference method (Arifjanov and Fatkhulloev, 2017). The field data obtained on Tashkent and Parkent channels, as well as data from other researchers were used to verify the reliability of the proposed dependencies on the calculation of the averaged velocity distribution over the depth of the flow for the existing computing methods comparative analysis. The comparison and comparative analysis with the results of field data and dependencies described in detail and given in Belolipetsky and Genova (2004), Borovkov et al. (2012), Debolsky et al. (1994), Ibad-Zade (1983), Iovchu (2006) and Zidshlag (2008) were done.

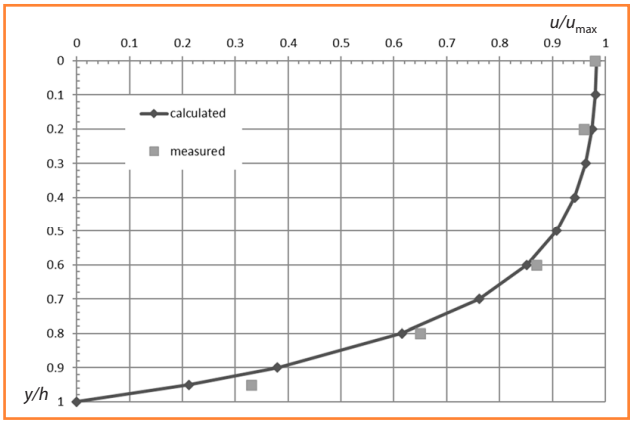

Figure 2 Comparison of calculated and measured data on the Tashkent channel

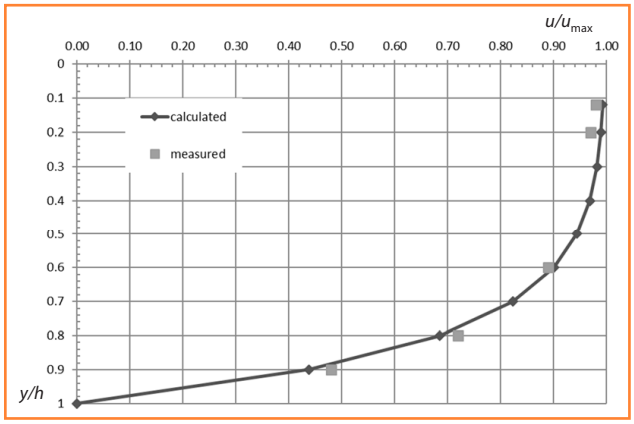

Figure 3 Comparison of calculated and measured data on the Parkent channel

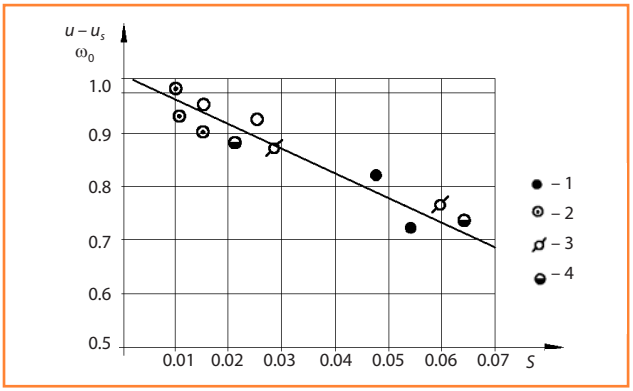

Figure 4 The dependence of the relative difference in the fluid velocity and particles on the concentration of suspension according to Grishanin (1992)

The results of field studies were used to assess the formation of the velocity field according to equations (7a and 7b). Those results of calculations present that the value of the relative velocity is the difference in the velocities of the transported fluid and the solid particle varies in depth with the flow (Fig. 2 and Fig. 3). This is obvious, since when the suspension flow moves in open channels, the concentration distribution of suspended particles through the flow depth is exponential. Therefore, the concentration of suspended particles increases with increasing depth. It is necessary to consider the fractional composition, which has a perceptible influence on the distribution of the relative velocity through the flow depth (Fig. 4).

Calculations show that the value of the relative longitudinal velocity is equal to the hydraulic extent only when are corrected for constraint.

The dependence of the relative velocity on the saturation of the flow with a suspension is given in Fig. 4. The experimental data are given in this work. Particles increase with the concentration of sediment; the velocity of a solid particle lags far behind the flow, as can be seen in the Fig. 4. Note that the resulting relationship for determining the relative velocity takes place for a certain range of the size of solid sediment particles, which the flow can transport in a suspended state.

Conclusion

Based on the analysis and generalization, available theoretical and experimental studies in the field of dynamics of flows in channels improved mathematical model that describes the steady flow in open channels, considering the saturation of the flow sediment. As a result, it is possible to interconnect the formation of the channel and flow parameters in statically and dynamically stable sections of the channels.

The method for calculating the formation of the velocity field in statically and dynamically stable channels has been developed, considering turbulent characteristics and the presence of suspended sediments in the stream. The possibility of using the proposed methods for practical calculations is substantiated by data from the field studies on Tashkent and Parkent channels. The developed analytical formulas make it possible to determine the value of flow parameters. Whereby, comparison of the results provides satisfactory convergence of measured and calculated data.

References

ARIFJANOV, A.M. – FATKHULLAEV, A.M. 2014. Dynamics of a suspended flow in the channels. Tashkent : Fan, 2014, 180 p.

ARIFJANOV, A.M. – FATKHULLOEV, A.M. 2017. The program for calculation of dynamic parameters of a turbulent weighing flow. Copyright certificate for computer No. DGU 04730. Intellectual Property Agency of the Republic of Uzbekistan. Tashkent, 2017.

BELOLIPETSKY, V.M. – GENOVA, S.N. 2004. Computational algorithm for determining the dynamics of suspended sediment and bottom sediment in the river bed. In Computation. technology, vol. 9, 2004, no. 2, pp. 9–25.

BOROVKOV, V.S. – BAIKOV, V.N. – PISAREV, D.V. – VOLYNOV M.A. 2012. Local similarity of the flow and velocity distribution in turbulent flows. In Engineering – Construction Journal, 2012, no. 6, pp. 12–19.

BOROVKOV, V.S. Channel processes and dynamics of river flows in urban areas. L: Gidrometeoizdat, 1989, 286 p.

DAS, A. 2008. Chance constrained design of trapezoidal channels. In Journal of Water Resources Planning and Management, vol. 134, 2008, pp. 310–313.

DEBOLSKY, V.K. et al. 1994. Dynamics of channel flows and lithodynamics in the coastal zone of the sea. Moscow : Nauka, 1994, 301 p.

DEPEWEG, H. 2002. Sediment transport applications in irrigation canals. In Irrigation and Drainage, vol. 51, 2002, pp. 167–179. doi: 10.1002/ird.49

FIDMAN, B.A. 1991. Turbulence of water flows. Leningrad : Hydrometeoizdat, 1991, 240 p.

FRANKL, F.I. 1953. On the theory of suspended sediment movement. Report. In USSR Academy of Sciences, vol. 92, 1953, no. 2, pp. 247–250.

GRISHANIN, K.V. 1992. Hydraulic resistance of natural channels. St. Petersburg: Gidromnteoizdat, 1992, 133 p.

IBAD-ZADE, Y.A. 1983. Transportation of water in open channels. Moscow : Stroyizdat, 1983, 555 p.

IOVCHU, Y.I. 2006. Model studies of rough channels of canals. Ways to improve the efficiency of irrigated agriculture: Sat. Art. FGNU "RosNIIPM"; by ed. VN Shchedrina – Novocherkassk : Helikon LLC, vol. 36, 2006, pp. 145–150.

KARAUSHEV, A.V. 1977. Theory and methods of calculation of river sediments. Leningrad : Gidrometeoizdat, 1977, 270 p.

LATIPOV, K.Sh. – ARIFJANOV, A.M. 1994. Issues of motion of a suspended flow in open channels. Tashkent : Publisher "Mekhnat", 1994, 110 p.

LATIPOV, K.Sh. – UMAROV, A.I. 1969. On the coefficient of interaction of multiphase media. In Questions of Mechanics, 1969, no. 7, pp. 57–60.

LEE, C-H. – HUANG, Z. – CHIEW, Y.-M. 2015. A multi-scale turbulent dispersion model for dilute flows with suspended sediment. In Advances in Water Resources, vol. 79, 2015, pp. 18–34. https://doi.org/10.1016/j.advwatres.2015.02.002

MIKHAILOVA, N. A. 1966. Transfer of solid particles by turbulent water flows. Hydrometeorological publishing house, 1966.

PAL, D. – GHOSHAL, K. 2017. Hydrodynamic interaction in suspended sediment distribution of open channel turbulent flow. In Applied Mathematical Modelling, vol. 49, 2017, pp. 630–646. doi: 10.1016/j.apm.2017.02.045

ROSSINSKY, K.I. – DEBOLSKY, V.K. 1960. River sediments. Moscow : Science, 1960, 215 p.

VELIKANOV, M.A. 1955. Dynamics of channel flows. Moscow : Gostekhizdat, 1955, 323 p.

VOLGIN, V.G. 2009. The influence of the length of the implementation of the velocity pulsations on the accuracy of the calculation of turbulent shear stresses. Moscow. In Vestnik MGSU, 2009, no. 9, pp. 93–99.

ZIDSHLAG, S. 2008. Modern method of measuring the flow rate used in the measurement of water consumption by the standard method. In Journal of Meteorology and Hydrology, 2008, no. 10, pp. 100–104.

sciendo

DOI: 10.2478/ahr-2019-0016

Acta Horticulturae et Regiotecturae 2
Nitra, Slovaca Universitas Agriculturae Nitriae, 2019, pp. 84–87

SENSITIVITY ANALYSIS OF INPUT DATA IN SURFACE WATER QUALITY MODELS

Martin MANINA*, Peter HALAJ

Slovak University of Agriculture in Nitra, Slovak Republic

The article is focused on analysis of input data impact on outputs of water quality models. The authors examined the impact of roughness coefficient, both boundary and initial conditions setup on changes of outputs generated by HEC-RAS model. Simulation results have shown a various response rate of input data on simulated results. The strong impact shows roughness coefficient setup that through the value of longitudinal dispersion coefficient affects pollution transport process. Changes in boundary conditions have had less influence on outputs. Relatively strong impact shows the setup of initial state of pollution concentration along the reach mainly for the case of low gradient rivers.

Keywords: sensitivity analysis, water quality modelling, open channel, HEC-RAS

With the development of economies and the improvement of living standards, our environment, especially natural water is constantly being polluted. In recent years, water pollution and water shortages in climate change conditions are two of the most serious and widespread environmental problems. Therefore, study of the analysis and management of the water quality of rivers recharged with reclaimed water has high theoretical and practical significance (Sokáč and Velísková, 2015). Mathematical models are used for approximation of various complex processes and phenomena (Ivan and Macura, 2014). The water quality modeling has the goal to provide as exactly as possible description of transport processes related to water quality changes. The determination of model parameters belongs among the most significant factors that affect the model results. The sensitivity analysis of these parameters is the crucial task in process of model validation (Hamby, 1994) and also provides support tools for decision making process in planning extent of field measurements necessary for modelling of transport processes in rivers and helps us to decide where we should focus data collection activities. The objectives of the sensitivity analysis are usually as follows: defining the model and its independent and dependent variables, identification of inputs which most influence the variability of outputs, determination of additional research of parameters for improving the knowledge base, reduction of the output uncertainty, determination of parameters which are most highly correlated with the output and in process of model use what consequence results from changing a given input parameter (Hamby, 1994). We may use several ways for conducting of sensitivity analyses. However, we may expect that for the same tasks we do not achieve identical results. We may distinguish quantitative and qualitative methods (Cariboni et al., 2007). There exist two basic approaches for sensitivity analysis (SA) – local SA and global SA. The local SA examines the local response of the outputs by varying input parameters one at a time, holding other parameters to a central value; and the global SA examines the global response averaged over the variation of all the parameters of model output by exploring a finite region (Xu et al., 2004).

Material and methods

For generating of simulated data sets for sensitivity analysis a model HEC-RAS has been used. It represents traditional numerical hydraulic model used to solve various river engineering tasks (USACE HEC, 2010). The water quality module that is a part of the HEC-RAS model, uses the QUICKEST-ULTIMATE explicit numerical scheme described by (Leonard, 1991), which solves the one-dimensional advection-dispersion equation (ADE) (Zhang and Johnson, 2014). The model includes transport and reactions that affect water quality variables that are either dissolved or in particulate form in the water column. For relatively simple transport scenarios, the ADE can be represented in the one-dimensional form (1):

$$\frac{\partial}{\partial t}(VC) = -\frac{\partial}{\partial x}(QC)\Delta x + \frac{\partial}{\partial x}\left[AD_x \frac{\partial C}{\partial x}\right]\Delta x + S_L + S_B + S_K \quad (1)$$

where:

V – volume of the water quality cell (m^3)
C – concentration of a constituent ($g.m^{-3}$)
Q – inflow ($m^3.s^{-1}$)
x – distance along channel (m)
D_x – water quality cell length (m)
A – cross-sectional flow area (m^2)
t – time (s)
D_x – dispersion coefficient ($m^2.s^{-1}$)

Contact address: Ing. Martin Manina, Slovak University of Agriculture in Nitra, Faculty of Horticulture and Landscape Engineering, Department of Water Resources and Evironmental Engineering, Hospodárska 7, 949 76 Nitra, Slovak Republic, +421 37 641 52 39, e-mail: martinmanina@yahoo.com

S_L – source/sink term representing direct and diffuse loading rate (g.m^{-3}.s^{-1})
S_B – source/sink term representing boundary loading rate, including upstream, downstream, and benthic (g.m^{-3}.s^{-1})
S_K – source/sink term representing biogeochemical reaction rate (g.m^{-3}.s^{-1})

For sensitivity analysis we used "Measure of Local Sensitivity" approach that is, conceptually, the simplest method for sensitivity analysis which repeatedly varies one parameter at a time while holding the others (Hamby, 1994). A sensitivity ranking can be obtained quickly by increasing each parameter by a given percentage while leaving all others constant and quantifying the change in model outputs. The sensitivity assessment is based on a comparative analysis of model outputs reflecting the changes of parameters which describe model structure changes. Input parameters are represented by bed roughness coefficient, friction slope at both downstream and upstream boundaries, bed slope homogeneity and outputs are represented by maximal concentration of pollution course along the canal and travel time of pollution peak. Finally, the results were evaluated with sensitivity characteristic defined as an absolute value of ratio percentage of output change to percentage of input change.

Case study characteristics

The simulation analysis has been carried out for reference channel prototype represented by prismatic channel with bed slope S_o = 0.001, bed width w = 1.00 m, bank slope V : H = 1 : 1, channel depth d = 1.00 m, Manning´s roughness coefficient n = 0.030 and channel length L = 1,000 m. The distance of cross sections Δx = 50 m and water quality cell lengths Δx_q = 50 m.

Model inputs and loading scenarios

The analysis has been conducted for one loading scenario with initial conditions C_o = 0 mg.l^{-1} for the whole length of the canal. At the upstream boundary condition the instantaneous mass injection of 50,000 g NaCl was simulated. We simulated steady flow conditions with a constant discharge Q = 0.500 m^3.s^{-1}. Both the upstream and the downstream boundary conditions have been defined as a normal depth described by friction slope S_f = 0.001 as a reference condition. Dispersion coefficients D_x were computed by the model on the basis of hydraulic variables at each face according to Fischer equation (Fischer, 1979) (2). This approach avoids potential model instability (USACE HEC, 2010):

$$D_x = 0.011 \frac{u^2 W^2}{y u^*} \quad (2)$$

where:
u – face velocity (m.s^{-1})
W – average channel width (m)
y – depth of water in channel (m)
u^* – shear velocity (m.s^{-1})

The shear velocity is:

$$u^* = \sqrt{g d S_f} \quad (3)$$

where:
g – gravitational constant (9.81 m. s^{-2})
d – average channel depth (m)
S_L – friction slope (unitless)

Input parameter setup

The sensitivity analysis is based on input parameters changes and quantifying the change in model outputs. The comparison assumes that input parameter value ranges model structure are realistic and based on knowledge published in literature.

Results and discussion

The sensitivity analysis is based on a comparison of model outputs reflecting the changes of input parameters which are represented by channel roughness coefficient, and friction slope at both downstream and upstream boundaries. The outputs are represented by maximal concentration of pollution course in water quality cell (WQC) between river stations along the channel and travel time of pollution peak to given distance from injection point. Reference roughness state is defined with Manning's roughness coefficient n = 0.030.

Run 1
Input data – channel roughness with reference state n = 0.030
Model output – maximal concentration of pollution in particular WQC

The model output response in the first run was represented by dataset of maximal pollution concentration calculated for center of WQC. The input parameters changes are presented in Table 1. The obtained results are demonstrated in Table 2. Value ΔI (%) is percentage of input parameter change (roughness) and ΔO_m (%) is mean output change for all particular WQC.

Table 1 Channel roughness coefficients n and corresponding longitudinal dispersion coefficient D_x calculated by model and their changes to reference values (for n = 0.030)

n	**0.020**	**0.030**	**0.040**	**0.060**	**0.080**	**0.100**
Δn	-33%	0%	33%	100%	167%	233%
D_x (m^2.s^{-1})	0.98	0.52	0.33	0.18	0.11	0.07
ΔD_x	-88%	0%	37%	65%	79%	87%

Table 2 Pollution concentration peak changes caused by channel roughness changes

Roughness		Centre of WQC distance from injection point (meters)											
		50	150	250	350	450	550	650	750	850	950	1,000	
n	±Δ*n*	$C_{max\ changes}$ (%)											
0.020	-33%	25	37	36	36	36	35	36	35	34	36	36	1.04
0.030	0%	0	0	0	0	0	0	0	0	0	0	0	0
0.040	33%	-16	-21	-19	-19	-20	-20	-19	-20	-20	-12	-14	0.50
0.060	100%	-35	-42	-41	-41	-41	-40	-41	-41	-41	-41	-41	0.40
0.080	167%	-47	-53	-60	-59	-59	-59	-59	-59	-58	-68	-68	0.35
0.100	233%	-54	-60	-60	-60	-60	-60	-60	-60	-60	-60	-60	0.25

Table 3 Travel time changes of pollution peak to a particular WQC caused by channel roughness change

Roughness		Centre of WQC distance from injection point (m)											
		0	150	250	350	450	550	650	750	850	950	1,000	
n	Δ*n*	travel time changes (%)											
0.020	-33%	0	0	-17	-30	-23	-25	-32	-27	-28	-30	-27	0.65
0.030	0%	0	0	0	0	0	0	0	0	0	0	0	0
0.040	33%	0	33	33	20	23	25	21	23	24	17	30	0.68
0.060	100%	0	67	67	60	62	63	68	68	68	17	30	0.52
0.080	167%	0	100	150	120	131	131	137	136	132	67	67	0.64
0.100	233%	0	133	150	130	131	138	142	136	140	143	157	0.55

Run 2

Input data – channel roughness/reference state $n = 0.030$

Model output – travel time changes of pollution peak in particular WQC

The model output response in the second run was represented by dataset of pollution peak travel time calculated to center of particular WQC. The obtained results are presented in Table 3.

The presented analyses show that model outputs reflecting the roughness change in the same order of magnitude as maximal pollution concentration and travel time of pollution concentration peak. There exist uniform changes of pollution peak concentration along the whole experimental reach where most sensitive were roughness decreasing ($n = 0.020$) and also increasing ($n = 0.040$) close to reference value ($n = 0.020$). A sensitivity characteristic was -1.04 for $n = 0.020$ and -0.50 for $n = 0.040$. Travel time outputs show higher uniformity and sensitivity characteristics reached values from 0.52 to 0.68. We may see different shape of concentration profiles presented in Fig. 1 and 2, where channel with higher values of the Manning´s coefficient has typical course with prolonged falling limb of maximal concentration connectors.

Run 3

Input data – friction slope at boundaries/reference state $S_f = 0.001$

Model output – change of pollution peak concentrations and travel time to particular WQC

The model output response in the third run was represented by data set of pollution peak changes caused by friction slope changes at upstream (US) and downstream (DS) boundaries (Table 4). The setup of friction slope S_f is

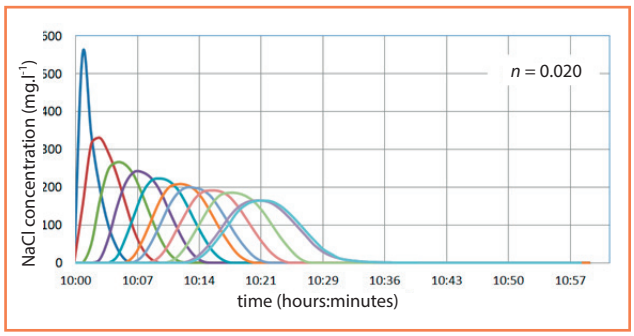

Figure 1 Concentration profiles for particular WQCs for $n = 0.020$ (from 50 to 950 m from injection point)

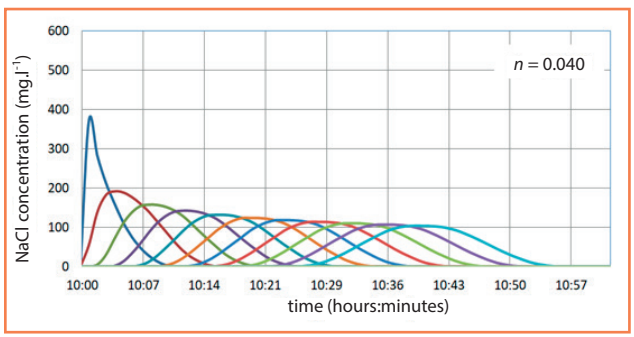

Figure 2 Concentration profiles for particular WQCs for $n = 0.040$ (from 50 to 950 m from injection point)

Table 4 Pollution concentration peak changes caused by friction slope changes at US and DS boundaries

Friction slope		Centre of WQC distance from injection point (m)				
		50	150	550	1,000	
S_f	Δt_f	$C_{max\ changes}$ (%)				
0.00025	-75%	0%	0%	-4%	-23%	0.31
0.00050	-50%	0%	0%	-1%	-12%	0.24
0.00100	0%	0%	0%	0%	0%	0.00
0.00200	100%	0%	0%	0%	0%	0.00
0.01000	900%	0%	0%	0%	4%	0.00

Table 5 Travel time changes of pollution peak caused by friction slope changes at US and DS boundaries (boundary conditions = normal depth)

Friction slope		WQC distance from injection point (m)				
		50	150	550	1,000	
S_f	$\pm\Delta_f$	travel time changes (%)				
0.00025	-75%	0%	0%	0%	13%	0.18
0.00050	-50%	0%	0%	0%	7%	0.13
0.00100	0%	0%	0%	0%	0%	0.00
0.00200	100%	0%	0%	0%	0%	0.00
0.01000	900%	0%	0%	0%	0%	0.00

necessary to setup boundary conditions defined as a normal depth. Roughness coefficient equals $n = 0.030$.

An effect of friction slope changes on outputs has not major influence (table 4 and 5). The S_f changes have been more reflected at reaches next to downstream boundary for lower values of friction slope ($S_f = 0.00025$ and 0.0005). It is due to forming of backwater curve that decreases the value of longitudinal dispersion coefficient. The higher values of n have not been projected to outputs value increases. The sensitivity characteristics reached values from 0.00 to 0.31 for pollution concentration peak changes and from 0.00 to 0.18 for travel time changes of pollution peak.

Conclusion

The sensitivity analysis represents a tool for the assessment of the input parameters with respect to their impact on model outputs. We can identify which parameters are important in the prediction of transport processes modelling. Sensitivity analysis helps us to decide where we should focus data collection activities. Our analyses have shown that most of the input parameters changes appear in the same order of magnitude as a response of outputs. The attention should be paid to exact determination of roughness coefficient where small differences from exact value sensitively affect the outputs. The results have also shown that accurate setup of boundary conditions is important for the case that normal depth is selected as a boundary condition and we have to determine the friction slope on basis of preliminary computations.

Acknowledgement

This work has been supported by the Research Support Scheme of the Slovak Research and Development Agency by projects APVV-16-0278 and APVV No. 0274-10.

References

CARIBONI, J. – GATELLI, D. – LISKA, R. – SATELLI, A. 2007. The role of sensitivity analysis in ecological modelling. In Ecological Modelling, 2007, 203, pp. 167–182.

FISHER, H.B. – LIST, E.J. – KOH, R.C.Y. – IMBERGER, J. – BROOKS, N.H. 1979. Mixing in inland and coastal waters. New York : Academic, 1979, pp. 104–138.

HAMBY, D.M. 2014. A review of techniques for parameter sensitivity analysis of environmental models. In Environmental Monitoring and Assessment, 2014, 32, pp. 135–154.

IVAN, P. – MACURA, V. 2014. Assessment of the quality of an aquatic habitat for Schneider in Nitrica river. In International Multidisciplinary Scientific GeoConference Surveying Geology and Mining Ecology Management, SGEM, vol. 1, 2014, no. 3, pp. 97–103.

LEONARD, B.P. 1991. The ULTIMATE conservative difference scheme applied to unsteady one-dimensional advection Computer Methods in Applied Mechanics and Engineering. 88, 1991, pp. 17–74.

SOKÁČ, M. – VELÍSKOVÁ, Y. 2015. Dispersion coefficient sensitivity analysis on simulation results: A case study Grote Laak River. In International Multidisciplinary Scientific GeoConference Surveying Geology and Mining Ecology Management, SGEM, vol. 1, 2015, no. 3, pp. 213–220.

USACE HEC. HEC-RAS River Analysis System User's Manual Version 4.1. 2010, 766 p.

ZHANG, Z. – JOHNSON, B. E. 2014. Application and Evaluation of the HEC-RAS-Nutrient Simulation Module. NSM I, EMRRP-SR-47, U.S. Vicksburg : Army Engineer Research and Development Center, 2014, 19 p.

XU, C. – HU, Y. – CHANG, Y. – JIANG, Y. – LI, X. – BU, R. – HE, H. 2004. Sensitivity analysis in ecological modeling Ying Yong Sheng Tai Xue Bao. vol. 15, 2004, no. 6, pp. 1056–1062.

DOI: 10.2478/ahr-2019-0017

Acta Horticulturae et Regiotecturae 2
Nitra, Slovaca Universitas Agriculturae Nitriae, 2019, pp. 88–92

SOLUTION OF THE FOREST ROAD NETWORK OPTIMIZATION IN THE TRANSFORMATION TO A SELECTIVE SILVICULTURE METHOD

Jaromír SKOUPIL[1]*, Petr PELIKÁN[1], Jiří KADLEC[2]

[1]Mendel University in Brno, Czech Republic
[2]SZIF RO Olomouc, Státní zemědělský intervenční fond, Regionální odbor Olomouc, Czech Republic

The paper is focused on the forest road access in the area of supposed specific method of forest management. The studied forest area of 81 hectares (ha) is intended for transformation by selective silviculture method demanding dense forest road network. The parameters of the current road network were analysed by Beneš method based on quantifying the general geometric and configuration criteria of the road network. The new road distribution was designed with respect to the results of the terrain slope and runoff concentration analyses to reduce the negative impacts of the roads on the surrounding environment. The new road layout resulted to the decrement of all types of skidding distances. The real skidding distance Ds decreased by 51% to the value of 72 m. In addition, the road network efficiency was increased by 14%.

Keywords: road network efficiency, runoff concentration, slope analysis, timber skidding

The road network is an integral part of forest management and an important tool for forestry. Other forest management technologies depend on the road network. The forest road network should be designed to allow to choose the most optimal timber harvesting and concentration technology in the given conditions, meeting the requirements for high productivity, low cost and environment-friendly.

Accessing the forest during the transition to a selective silviculture method has certain specifics. The selective forest is created as a result of the application of the so-called selective forest management method. To put it simply, instead of the usual harvesting of trees of a certain age, the trees of the target thickness are regularly harvested, while at the same time aiming for the highest age and spatial diversity of such a forest achieved by "cultivation selection". Selective forests often originated from so-called "farmer forests" or municipal forests where the selection of timber needed for running the farm or community was used (Ammon, 2009). The contrast of thickness classes in the selected and clearcut forest is typical. While in the passive forest the thickness of the trees depicts a Gaussian curve, a typical declining curve (hyperbola) showing a decrease in abundance towards higher thickness classes is typical for the forest (most trees are in lower thickness classes and their number rapidly decreases towards the target thickness). The forest stand stock is evenly distributed over the entire forest area in a mixed group structure. An important feature is the sustained vertical canopy of trees (Ammon, 2009). The structure of the forest is similar to some temperate wildwood. In order to be able to manage a forest (tree felling and timberskidding), a sufficiently dense transport network is required to facilitate any tree to be cut down and transported. We distinguish two economic ways in a selective forest: individually selective and group selective. In the case of the individually selected management method, the individual "mature" trees are harvested according to the target thickness and thus the auspicious individuals are eased on the lower floors from the subjection of other trees. Trees are removed if it is economically favourable or phytopathologically necessary. Dead, diseased or withered trees are also removed. This method is convenient for shady (fir, beech) or shade-tolerant (spruce) woods (Polanský, 1966). Small-scale cultivation and felling operations take place in small-scale groups, which are convenient for sunny tolerant species. Due to age and spatial diversity, the selective forest is able to withstand harmful influences such as wind, snow or pests. Durability, safety and fluency (yield equilibrium) are secured on a much smaller area than other forest types (an area of 10 ha or less is stated).

It also allows small scale owners to receive regular yields without having to wait for rotation period. This way of management perfectly uses the soil and air space. Several tree layers attract and use an incident light better. Clearing is not necessary and the forest performs its non-production functions better and more permanently. Usually no artificial afforestation is needed (natural reproduction occurs spontaneously) (Polanský, 1966).

The selective forest management is demanding in terms of expertise and time of the forest manager. Timber harvesting and skidding is technologically more difficult, less centralized (scattered over a larger area), and therefore, may be more expensive. It requires perfect accessibility; therefore a dense transport network is a condition for successful management. The optimal skidding traces

Contact address: Ing. Jaromír Skoupil, Ph.D., Mendel University in Brno, Faculty of Horticulture, Department of Horticultural Machinery, Valtická 337, 691 44 Lednice

spacing in the selection forest is equal to the twofold height of the tree from the group of target thicknesses. Depending on the tree species and habitat, the spacing is about 50 m. Directional felling is directed from the stand to the skidding trace to minimize damage of the surrounding trees in the stand. It is very important that the used forwarder is able to harmlessly move along the skidding trace, so it is advisable to design its width of 3.5–4 m. It is also very important to consider slope conditions in the design of the road network to avoid excessive damage of the soil surface and subsequent erosion. Due to the character of the selective management and the individual selection, the predominant technology will be the use of a chainsaw and a tractor with a winch, or a forwarder with a winch for skidding the timber assortment from the stand to the trace and then skidding to the loading bay. The use of harvesters in timber extraction cannot be used because of the high extraction costs caused by scattered cutting and the different masses of timber on the harvested area.

The calculations of the road network parameters and related engineering tasks can be very time consuming, hence the geographical information systems are often used (Lotfalian, Zadeh and Hosseini, 2011). In recent years, LiDAR technology has also undergone great advances and shows applicability to forest management, becoming the source of high precision geometric data (Novo et al., 2019).

The aim of this work is to optimize the design process of forest road network. The use of geographic information systems make it possible to find suitable terrain with low water runoff concentration to minimize negative impacts in the construction of forest roads, such as erosion.

Material and methods

Study area

In order to evaluate the condition of the forest road network and to propose its optimization with the aim of transformation to a selective silvicultural management method, a site located in the cadastral area of Nový Hrozenkov (Vsetín District), which is a part of the protected landscape area Beskydy (Fig. 1), was selected. It is a forest area of 81 ha, managed by the Augustinian Abbey Forests. The boundary of the territory is formed by a reinforced haul road 1 L class in the north; the ridge is the southern border, which is also the state border with Slovakia. It is a difficult accessible locality due to the broken terrain ranging from 600 to 870 m above sea level. The average slope of the terrain is 33.8%. There are only unpaved forest roads and skidding traces inside the territory.

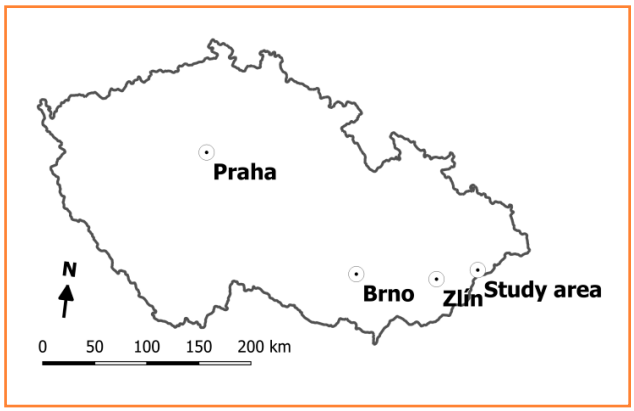

Figure 1 Localization of the study area

Road network evaluation

Road network was evaluated by means of Beneš methodology presented in 1986. The method was developed for forest haul road network assessment. The practical application consists of the road network distribution optimization within the various morphologic areas (flatlands, uplands and mountains). The methodology is based on quantifying the general geometric and configuration criteria of the road network.

The road density is often considered as the main criterion of the access. The density H (m·ha^{-1}) is given by equation

$$H = \frac{D}{S} \quad (1)$$

where:
D – the total road network length (m)
S – the accessed area (ha)

As the parameter does not provide any information on the road network distribution, the additional parameters are implemented (Hrůza, Pelikán and Hemr, 2019). The method deals with various types of distances representing the traces of timber transport from the point of harvesting to the haul road. The points of harvesting represent the centroids of squares orderly located in the grid within the accessed area. The original method assumes the particular square area of 10 ha. The 1 ha grid was used with regard to the special purpose of the method and total small study area.

The theoretic skidding distance D_t (m) is an average skidding distance due to the optimal distribution of roads in the accessed area and it depends on the road density H:

$$D_t = \frac{10{,}000}{4H} \quad (2)$$

The geometric distance D_g (m) represents the direct distance from point of harvesting to the haul road (Beneš, 1986). The average value of D_g depends on the road distribution and generally is higher than the theoretic skidding distance:

$$\overline{D_g} = \frac{D_{g1} + D_{g2} + \ldots D_{gn}}{n} \quad (3)$$

The real skidding distance D_s (m) was considered as the distance from point of harvesting measured along the fall line until crosses the trace of timber skidding, haul road or study area boundary:

$$\overline{D_s} = \frac{D_{s1} + D_{s2} + \ldots D_{sn}}{n} \quad (4)$$

In some cases, the correction factor of mean skidding distance is calculated from the division of real mean skidding

distance by theoretical mean skidding distance (Lotfalian, Zadeh and Hosseini, 2011). We would rather focus on the road network efficiency in the study. The efficiency of the road network U (%) is finally calculated from the theoretic and average geometric distance:

$$U = \frac{D_t}{D_g} \cdot 100 \quad (5)$$

An important aspect is perfect knowledge of terrain configuration (Beneš, 1973). The analysis of road network parameters was performed in the open source geographic information system QGIS Desktop. The regular grid of points of harvesting and line shapefile of road network were used as the main input data. In addition, the data of the 5th generation digital terrain model of the Czech Republic (DMR 5G) in the text format were used for the digital elevation model creation (DEM). The geometric skidding distances from grid points to roads were performed by vector analysis tool Distance to nearest hub.

The analysis of skidding distances required the application of the set of tools. The data of DMR 5G were interpolated into the DEM with sink removal, flow direction, slope and flow accumulation analysis. The vector road network and points of harvesting grid were converted into the raster. The raster road network was burned into the DEM as a barrier; hence the Flow path length tool was performed to calculate real skidding distances. The other supporting calculations were processed in the MS Excel spreadsheet.

Road network design

To design routes of the forest road network three degrees of the ground slope were determined. Specification of the extent of slope intervals for particular degrees is based on the terrain classification prepared by Lesprojekt (1980). The classification is commonly used in forest practice and serves also for the so-called technological typification (Simanov, Macků and Popelka, 1993).

Degrees (Deg.) of the ground slope:

- Deg. 1 – slope 0–25%, areas of small slope, suitable for building the forest road network.
- Deg. 2 – slope 26–40%, areas of medium slope, less suitable for building the forest road network.
- Deg. 3 – slope >40%, areas of high slope, unsuitable for building the forest road network.

The forest road network significantly influences the circulation of water in the area. It results in the increase of surface water runoff from the area and a related increase of soil erosion. A surface runoff concentration can be used as a further criterion for optimizing the forest transport network to reduce the negative effects on water outflow (Krešl, 1990). The study area was divided into three zones of runoff concentration. The threshold values are considered as the delimiting values of the particular modeled microcatchment areas in their outlet nodes.

Degrees (Deg.) from the aspect of runoff concentration:

- Deg. 1 – areas with low concentration of runoff, suitable for building the road network (microcatchment area <50 m^2)
- Deg. 2 – areas with medium concentration of runoff, less suitable for building the forest road network (microcatchment area 50–150 m^2)
- Deg. 3 – areas with high concentration of runoff, unsuitable for building the forest road network (microcatchment area >150 m^2)

Results and discussion

Actual road network parameters

The actual total length of unbound roads is 6,090 m within the study area. The road network density reaches 75.2 m·ha^{-1} and average geometric distance D_g is 53 m. However, the average real skidding distance D_s is 147 m, the value can be considered too high for purposes of transformation to selective forest management. The theoretic distance D_t is 33 m and the road network efficiency is U = 63%. The results of the analysis show that the road layout is unbalanced because of too high average real skidding distance due to the quite low efficiency.

Road network optimization

In order to design the optimal road network layout, slope and runoff concentrations were performed. The raster outputs were reclassified in order with above-mentioned classification scale (degrees of suitability) as discussed in Skoupil (2006). The rasters were combined with the use of map algebra (summation of map layers) to the resulting map with delimitation of the three zones from the point of view of the design and building forest roads (Table 1, Fig. 2):

1 – areas suitable for building the forest road network
2 – areas less suitable for building the forest road network
3 – areas unsuitable for building the forest road network

Table 1 Area delimitation according to suitability for planning and building forest roads

		Surface runoff concentration		
		Deg. 1 low	**Deg. 2 medium**	**Deg. 3 high**
Ground slope	**Deg. 1 low (0–25%)**	1 (1 + 1 = 2)	1 (1 + 2 = 3)	2 (1 + 3 = 4)
	Deg. 2 medium (26–40%)	1 (2 + 1 = 3)	2 (2 + 2 = 4)	3 (2 + 3 = 5)
	Deg. 3 high (>40%)	2 (3 + 1 = 4)	3 (3 + 2 = 5)	3 (3 + 3 = 6)

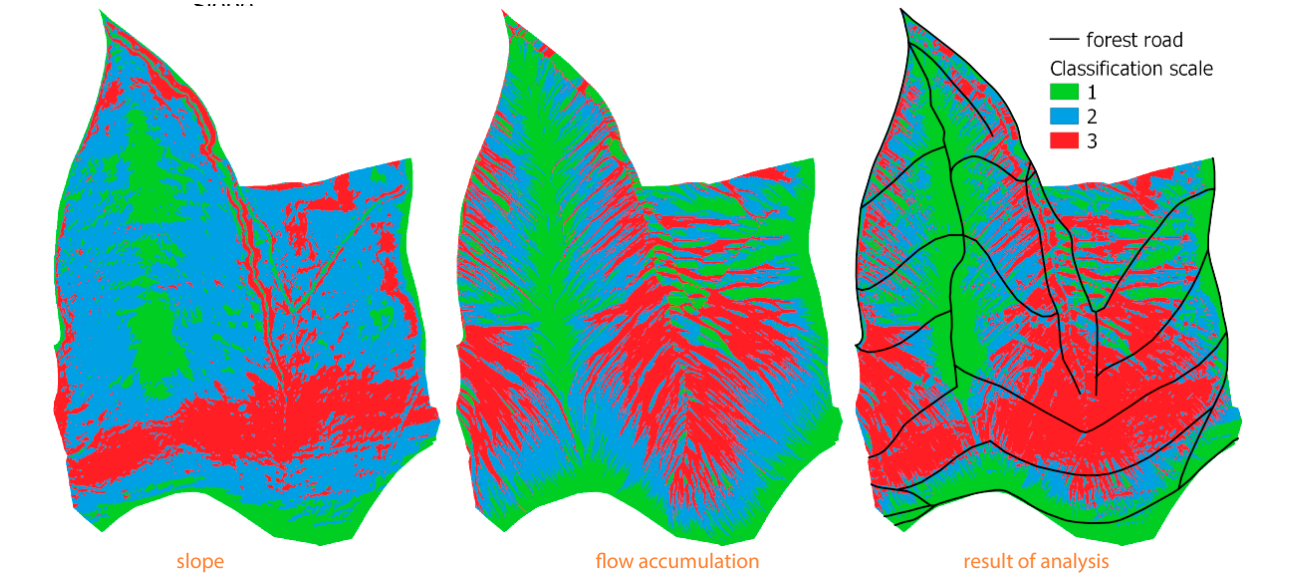

Figure 2 Slope and runoff concentration analyses with the forest road network design

A new proposal for the optimization of the forest road network was accomplished on the basis of the analysis and delimitation of the study area into zones according to suitability for the design and construction of roads. The creation of the new proposal was driven by the desire to place the road network predominantly in the zones 1 and 2. The other goal of road network optimization was to decrease the average real skidding distance and to increase the efficiency *U* concurrently. The network was extended by 3.235 m of new roads situated with respect to the terrain configuration and erosion prevention. The new roads almost follow the contours, however they are designed in optimal longitudinal slope for well structure drainage (Fig. 3). The designed solution supposed the elimination of 299 m of roads traced out inappropriately and the recultivation of the affected forest land.

The actual and designed forest road network parameters are summarized in Table2. The new road layout caused the decrease of all types of skidding distances. The real skidding distance Ds decreased by 51% to the value of 72 m. In addition, the road network efficiency increased by 14%.

Lotfalian, Zadeh and Hosseini (2011) investigated the skidding and theoretic distances in Chafrood forest using the same methodology developed by Beneš, however they focused on the estimation correction factor of mean skidding distance. The parameters of the designed optimal

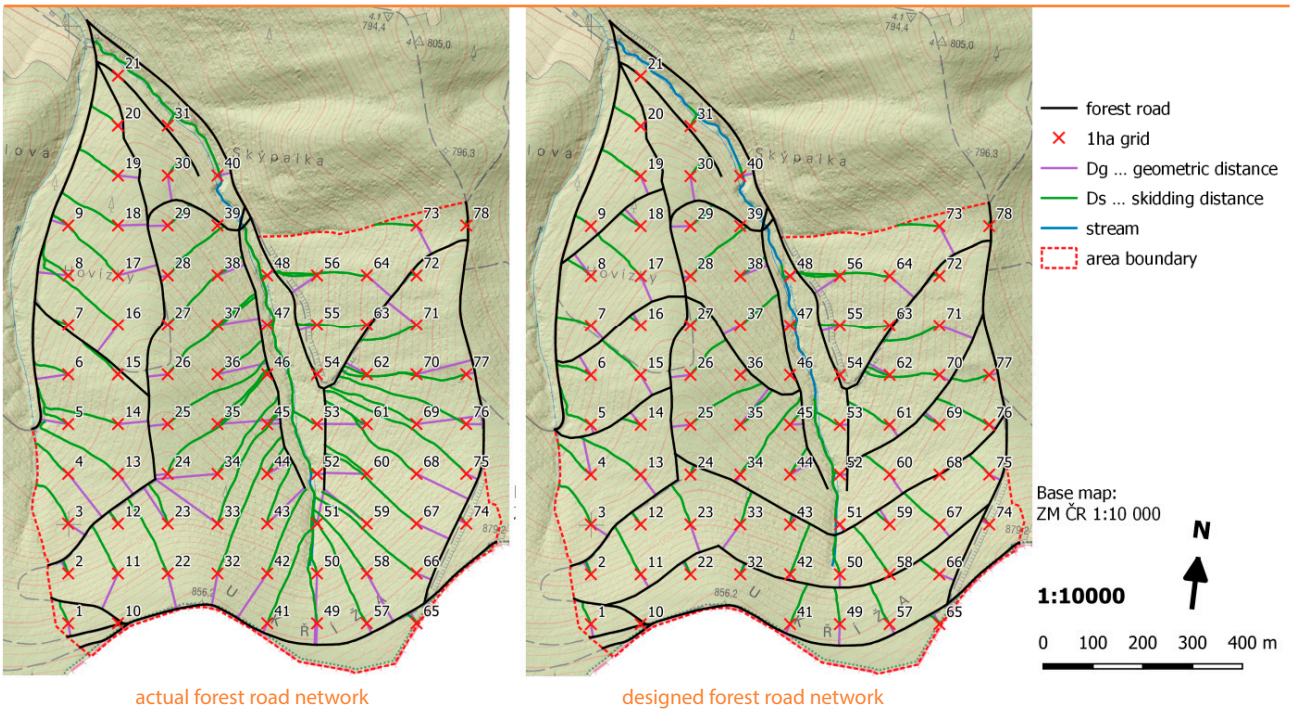

Figure 3 The actual and designed forest road network

Table 2 Road network parameters

	D (m)	H (m·ha^{-1})	D_sØ (m)	D_gØ (m)	D_t (m)	U (%)
Actual	6,090	75	147	53	33	63
Design	9,026	111	72	31	22	72
Difference	+ 48.0%	+ 48.0%	- 51.0%	- 41.5%	- 33.0%	+ 14.0%

forest road network in the Beskydy Mountains reach slightly different parameters due to the special demands on the forest management, but reaching high value of the road network efficiency of 72%.

Conclusion

The benefit of the forest road network optimization using slope analysis and runoff concentration is to reduce the negative impacts of the roads on the surrounding environment. A significant reduction in skidding distances was achieved by supplementing the road network in the area of interest, which will allow a successive transformation to a selective forest management.

References

AMMON, W. 2009. Výběrný princip v lesním hospodářství. 1. vyd., Zlín : Lesnická práce s.r.o., 2009, 157 s. ISBN 978-80-87154-25-0.

BENEŠ, J. 1973. Vliv tvaru terénu na dopravní zpřístupnění lesa. In Lesnictví, roč. 19, 1973, č. 6, s. 479 – 492.

BENEŠ, J. 1986. The preconditions of opening up of the forests. Folia Universitatis Agriculturae. Brno : VŠZ, 1986.

HRŮZA, P. – PELIKÁN, P. – HEMR, O. 2019. Comparison of the current solution of the single trail Moravský kras centre with a selected centre abroad. In Public recreation and landscape protection – with sense hand in hand...: Conference proceeding, 1st ed., Brno : MZLU, 2019, pp. 62–66. ISBN 978-80-7509-659-3.

KREŠL, J. 1990. Kriteria řešení lesní dopravní sítě z hlediska vodohospodářských požadavků. Závěrečná zpráva SVE VI-6-7/04-02, Brno : VŠZ, 1990, 37 s.

LOTFALIAN, M. – ZADEH, E. H. – HOSSEINI, S. A. 2011. Calculating the correction factor of skidding distance based on forest road network. In Journal of forest science, vol. 57, 2011, no. 11, pp. 467–471

NOVO, A. et al. 2019. Automatic detection of forest-road distances to improve clearing operations in road management. International Archives of the Photogrammetry, 2019. Remote Sensing and Spatial Information Sciences – ISPRS Archives, vol. XLII-2/W13, pp. 1083–1088.

POLANSKÝ, B. 1966. Pěstění lesů. 1. vyd. Praha : SZN, 1966, 514 s.

SIMANOV, V. – MACKŮ, J. – POPELKA, J. 1993. Nový návrh terénní klasifikace a technologické typizace. In Lesnictví, roč. 39, 1993, č. 10, s. 422–428.

SKOUPIL, J. 2006. Optimalizace tvorby a rekonstrukce lesní dopravní sítě z hlediska integrovaných funkcí lesa. Disertační práce : Ústav tvorby a ochrany krajiny LDF MZLU, Brno, 2006, 100 s.

sciendo

DOI: 10.2478/ahr-2019-0018

Acta Horticulturae et Regiotecturae 2/2019 *Jasna Grabić et al.*

Acta Horticulturae et Regiotecturae 2
Nitra, Slovaca Universitas Agriculturae Nitriae, 2019, pp. 93–96

IRON AND MANGANESE IN WELL WATER: POTENTIAL RISK FOR IRRIGATION SYSTEMS

Jasna GRABIĆ*, Milica VRANEŠEVIĆ, Radoš ZEMUNAC, Senka BUBULJ, Atila BEZDAN, Milica ILIĆ

University of Novi Sad, Serbia

In the light of climate changes and in order to achieve stable crop production, irrigation represents an inevitable measure. Apart from water quantity, water quality represents a matter of concern. The paper elaborates on the presence of iron and manganese, as the main factors of causing the clogging of irrigation systems. The examined well water samples were taken mainly from Serbia. Photometric methods were applied for determining iron and manganese, and sensors for pH and conductivity. The obtained values were later subjected to a classification for irrigation water and the well water samples were classified according to the given thresholds. Precise location and presentation of the obtained results were done using the Geographic information system. The research has shown that from the analysed well water, only in 6 samples iron concentrations were increased up to a level classified as "extreme restrictions," 4 samples as "warning," while 31 samples of water were "adequate for irrigation." Concerning manganese, in only one sample water was classified as "extreme restrictions," in 14 as "warning" and in 26 as "adequate for irrigation." pH and conductivity did not coincide with elevated concentrations of iron and manganese, but in the cases of exceeding thresholds, special attention should also be paid to these parameters.

Keywords: water quality, groundwater, irrigation, iron, manganese

Climate changes are manifested as more frequent extreme events, as heatwaves and phenomena of long-lasting drought periods, but also as extreme precipitation events (IPCC, 2014). All these events pose challenges for achieving stable and sustainable crop production. Increased water shortages, particularly in the spring and summer months, increase the water requirement for irrigation (Levidow et al., 2014). In Europe, the most negative effects for the continental climate were found in the Pannonian zone, which includes Hungary, Serbia, Bulgaria, and Romania. This region will suffer from increased incidents of heatwaves and droughts (Olesen et al., 2011).

In order to mitigate or even overcome water deficiency, irrigation has to be introduced. It is well known that agriculture accounts for 70% of global freshwater withdrawals. Presently irrigated agricultural production is estimated to account for 20% of the arable land and this share is expected to be increased to 47% by 2030, and irrigated food production will be increased by more than 50 percent by 2050 (FAO, 2017). These facts point to the significance of irrigation as an agro-technical measure. Apart from water quantity, the quality of water for irrigation is also very important. Water used for irrigation must have certain physical, chemical and mechanical properties, otherwise, it can cause damage to irrigated crops and human and animal health (Kaletova and Jurik, 2018) and soil. Despite the fact that intensive crop production assumes irrigation as an indispensable measure, it often faces many challenges. The overall problem of irrigation may be categorized in several aspects:

1. available water quality and quantity;
2. influence on cultivated plants;
3. influence of irrigation practices on soil conservation;
4. preservation of irrigation equipment during exploitation.

In order to perform successful irrigation practices, it is necessary to satisfy all the mentioned aspects. In this context, application of water quality classifications for irrigation plays an important role. According to Bortolini, Maucieri and Borin (2018), apart from agronomical and health and hygiene indicators, management quality indicators are also important assuming: parameters causing a negative effect on irrigation systems, where especially clogging needs to be resolved. Fe and Mn are considered to be essential elements/micronutrients for plants (Dalcorso et al., 2014; Rout and Sahoo, 2015), but their higher concentration above the allowed can be reflected through the negative effects on the soil, cultivated plants and clogging of irrigation equipment (Xiufu and Zinati, 2005), as well as aesthetic nuisance forming rusty deposits on the surrounding objects and plants.

In the province of Vojvodina, the water quality of surface water bodies in most cases is good and adequate for irrigation (Vranešević, Ilić and Bezdan, 2018; Ilić et al., 2019), except for some reaches of the Hydro System Danube-Tisa-Danube (Grabić et al., 2016). However, many farmers from the region, because of practical reasons, use groundwater. In such water, there could be a problem of increased salinity and the presence of Fe and Mn, which is not only the

Contact address: Jasna Grabić, Ph.D., University of Novi Sad, Faculty of Agriculture, Department of Water Management; Trg. D. Obradovića 8, 21000 Novi Sad, Serbia, phone +381 21 485 34 12; e-mail: jasna.grabic@polj.uns.ac.rs

problem for the region, but rather the general characteristic of groundwaters of the Pannonian Basin (Rowland et al., 2010).

In this study, the main focus was on determining the presence of Fe and Mn in groundwater used for irrigation and their spatial presentation using GIS tools. Furthermore, using current classification for irrigation, the intention has also been to assess potential risks for irrigational systems. Besides, values of pH and electrical conductivity (EC) were determined, as the most common and the most general parameters for irrigation water.

Material and methods

Study area and well water sampling

The study presents results of testing of 41 water samples of well water. The water was sampled in the territory of Serbia, mainly in the territory of the Autonomous Province of Vojvodina (northern part of Serbia), while several water samples are from countries from the region: Bosnia and Herzegovina, Montenegro and Slovakia. The scattered geographical position of samples was due to the intentions of individuals to invest or to enlarge irrigation systems, or as a control since the problems of water quality have been previously reported. The water samples were collected by the personal departure to the field, or with the help of associates (students, acquaintances, agricultural companies, etc.). The underground water was pumped out directly from wells, completely filling 1.5 l clean plastic bottles. The bottles were sealed and transported to the laboratory, where the samples were stored in the refrigerator below 8 °C prior to analysis. For each sample, the location of the well, from where the water was taken, was recorded. On the basis of the coordinates provided, maps with locations of sampled water were later produced.

Methods for water quality analyses

In each water sample there were detected the following parameters using appropriate equipment: pH – sensory method: pH meter, produced by TESTO Germany, measuring range 0–14; EC – sensory method: EC meter, produced by EuTech, the Netherlands, measuring range 0–199.9 $mS.cm^{-1}$; Fe and Mn – photometric methods: multiparameter photometer (produced by LOVIBOND, Germany, with detection limits of 0.02 mg $Fe.l^{-1}$ and 0.01 mg $Mn.l^{-1}$.

Water quality standards

There is no clearly defined categorization (classification) of the usability of water for irrigation in the legislation of the Republic of Serbia. In order to classify water samples into appropriate classes for irrigation, thresholds proposed by the Bortolini, Maucieri and Borin (2018) were used. Threshold values for examined irrigation water quality parameters, elaborated in this study, are given in Table 1, as well as some usual ranges for irrigation water proposed by FAO (Ayers and Wescot, 1985).

GIS mapping and software

Production of maps, containing locations of well water samples, was done using GIS tools. For this purpose, Quantum GIS software (version 2.16) was used. This is free software, which is used for editing, analysing and presenting geospatial data. Quantum GIS is a multiplatform application that runs on different operating systems, such as Mac OS, Linux, Microsoft Windows, and Android. Maps were generated using the World Geodetic System (WGS84). Besides the locations of the wells from which samples were taken, there are also stored values of examined water quality parameters in attribute tables. This enabled later production of maps for each water quality parameter, with the respect to water quality thresholds according to the chosen classification.

Results and discussion

The results of well water analysis are presented in Fig. 1–4, where different colours indicate water quality classes according to Bortolini, Maucieri and Borin (2018). Research results showed that Fe concentrations were in the range of less than 0.02 to 12.7 mg $Fe.l^{-1}$. The highest concentration of 12.7 mg $Fe.l^{-1}$ was measured in the sample collected from the well of the Faculty of Agriculture, the University of Novi Sad, Serbia (FAUNS, SRB), followed by Nitra (Slovakia) and KK Granicar (SRB) with values 8.59 and 8.3 mg $Fe.l^{-1}$, respectively.

Concerning minimal values, 7 samples had concentration below the detection limit (i.e. 0.02 mg $Fe.l^{-1}$). If mentioned extreme values are excluded, the average for other samples was 0.48 mg $Fe.l^{-1}$. Mn concentrations were in the range of 0.01 mg.l^{-1} to 4.1 mg.l^{-1}. The highest concentration of Mn was in the sample collected in Nitra (Slovakia) of 4.1 mg $Mn.l^{-1}$, followed by 0.75 (KK_Granicar, SRB) and 0.69 (Futog, SRB) and 0.67 mg $Mn.l^{-1}$ (FAUNS, SRB).

Table 1 Threshold values for irrigation water quality

Parameters	Units	The usual values in irrigation water	Adequate for irrigation	Warning	Extreme restrictions
		Ayers and Wescot, 1985	Bortolini, Maucieri and Borin, 2018		
pH		6.5-8.4	6.00–8.00	5.00–5.99	<5.00
EC	$mS.cm^{-1}$	0–3,000	<700	700–6,500	>6,500
Fe	$mg.l^{-1}$	max 5	<0.50	0.05–1.50	>1.50
Mn	$mg.l^{-1}$	max 0.2	<0.10	0.10–1.50	>1.50

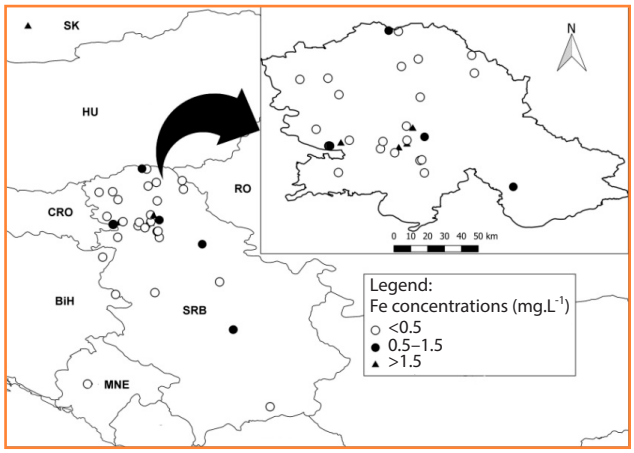

Figure 1 Locations of well water samples, Fe concentrations

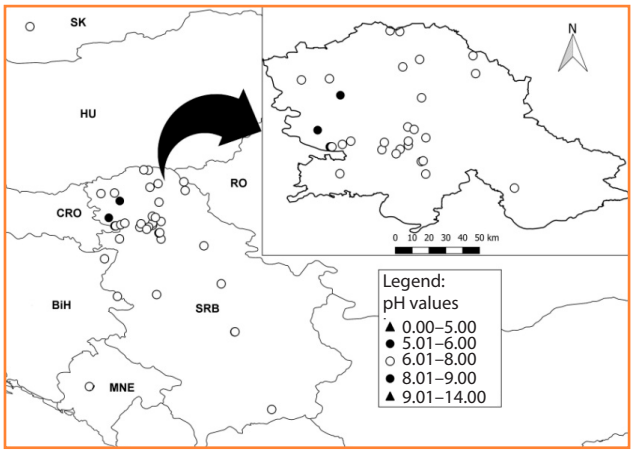

Figure 3 Locations of well water samples, pH value

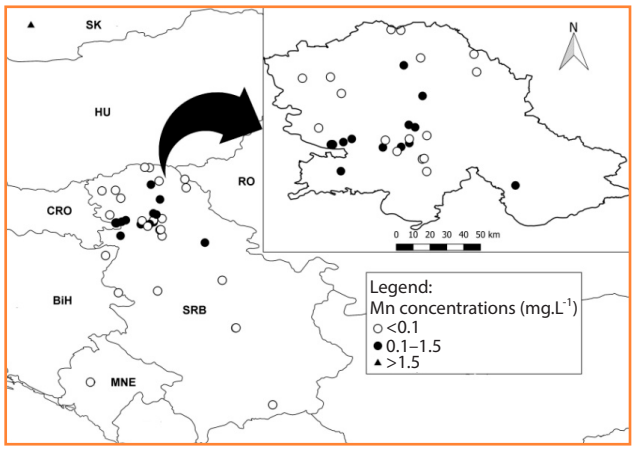

Figure 2 Locations of well water samples, Mn concentrations

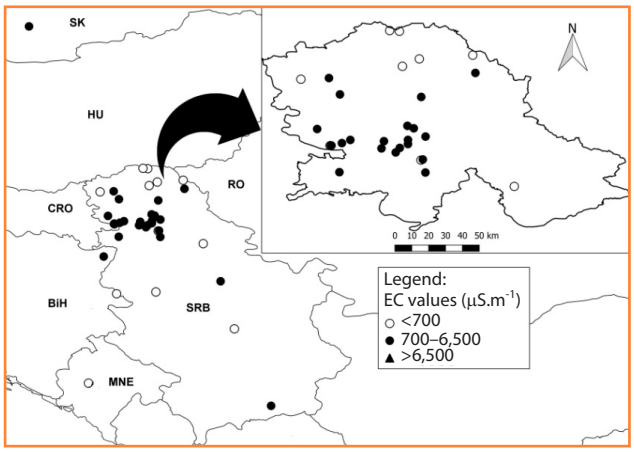

Figure 4 Locations of well water samples, EC value

The values of pH reaction were generally ranging within the posed thresholds. The highest concentration was detected in the sample from Bač (SRB) of 8.10 and Romania (SRB) of 8.06, while the lowest value was 6.51, measured in well water from Kać (SRB). Values of EC were in the range of 438 (Palić, SRB) to 3,120 mS.cm^{-1} (Romania, SRB).

The obtained results of measured parameters are in compliance with the findings obtained from the official network of wells for systematic control of groundwater in Serbia (RHMSS, 2010–2017) and results on the evaluation of groundwaters quality within 3 Vojvodinian regions. Moreover, the problem of elevated concentrations of Fe and Mn has also been discussed by Varsányi and Kovács (2006) and Rowland et al. (2010) and for the Pannonian Basin, as well as by Barloková and Ilavský (2018) for groundwaters in Slovakia.

The acidity and alkalinity indicator, pH value, rarely poses a problem in itself. Water used for irrigation should have a pH ranging from 6.5 to 8.4, and if the pH is outside of these values, this may cause a nutritional imbalance or may contain a toxic ion, or even can lead to degradation of soil and irrigational equipment (Ayers and Wescot, 1985). Increasing the concentration of dissolved salts in the soil elevates the osmotic pressure of the soil solution and in such conditions, plants cannot adapt easily. Therefore, as the salt concentration (expressed as EC) in soil increases, water becomes less accessible to plants, even if the soil contains significant amounts of water and looks moist. In general, Fe is not toxic to plants in aerated soils but can contribute to soil acidification and loss of availability of essential phosphorus and molybdenum. If irrigation by sprinklers is applied it may lead to Fe deposits on plants, equipment, and buildings. Concerning Mn, it is toxic to a number of crops at a few-tenth to a few mg.l^{-1}, but usually only in acid soils (Ayers and Wescot, 1985).

In situations where high Fe and Mn concentrations are found in irrigation water, some of the possibilities for their removal from the water should be considered. Therefore, in these cases, it is necessary to consider the following options:

1. possibilities for their removal from the well water;
2. to apply an adequate type of irrigation (e.g. not to use sprinkler irrigation);
3. to take care of sensitive crops.

However, if drip irrigation is practiced, there is a need for obligatory upgrading irrigation systems with appropriate filters. This research showed that Fe and Mn are present in a number of the well water samples. According to some estimates in Vojvodina Province, there is 950,200 ha of potential areas for irrigation (Potkonjak, Zoranović and Mačkić, 2010), and therefore examining water quality for irrigation must be an obligatory measure, in order to avoid

losses of crop yields and the risk of malfunctioning of irrigational systems.

Conclusion

The research has shown that from the analysed well water, only in 6 samples Fe concentrations were increased up to a level classified as "extreme restrictions," 4 samples as "warning," while in 31 samples water was "adequate for irrigation". Concerning, Mn in only one sample, water was classified as "extreme restrictions," in 14 as "warning" and in 26 as "adequate for irrigation." The results of this research indicate that even the occurrence of higher concentrations of Fe and Mn is not frequent within the examined region; regular practice of assessing water quality for irrigation may prevent undesired effects on irrigation equipment, toxicity to plants and degradation of soil.

References

AYERS, R.S. – WESTCOT, D.W. 1985. Water Quality for Agriculture. FAO Irrigation and Drainage Paper 29 Rev. 1st, Rome : FAO. Available at: www.fao.org/3/T0234E/T0234E00.htm

BARLOKOVÁ, D. – ILAVSKÝ, J. 2018. Groundwater: An Important Resource of Drinking Water in Slovakia. In: Negm, A. – Zeleňáková, M. (eds). Water Resources in Slovakia: Part I. The Handbook of Environmental Chemistry, Springer, Cham. vol. 69, 2018.

BLUEWATERS. 2005. Project 353 Draft report: Sustainable solutions to improve quality of drinking water affected by high arsenic contents in 3 Vojvodinian regions. 2005, Book II: Groundwater sources Stadt Wien MA 31 – Water Management. Available at: http://www.ekourbapv.vojvodina.gov.rs/wp-content/uploads/2018/09/book2hydrogeology.pdf

BORTOLINI, L. – MAUCIERI, C. – BORIN, M. 2018. A Tool for the Evaluation of Irrigation Water Quality in the Arid and Semi-Arid Regions. In Agronomy, vol. 8, 2018, no. 23, pp. 1–15. https://www.mdpi.com/2073-4395/8/2/23

DALCORSO, G. – MANARA, A. – PIASENTIN, S. – FURINI A. 2014. Nutrient metal elements in plants. In Metallomics: Integrated biometal science, vol. 6, 2014, no. 10. doi:10.1039/c4mt00173g

FAO. 2017. Water for Sustainable Food and Agriculture. A report produced for the G20 Presidency of Germany, Rome. ISBN 978-92-5-109977-3.

GRABIĆ, J. – BENKA, P. – BEZDAN, A. – JOSIMOV-DUNĐERSKI, J. – SALVAI A. 2016. Water quality management for preserving fish populations within Hydro-system Danube-Tisa-Danube, Serbia. In Carpathian journal of earth and environmental sciences. vol. 11, 2016, pp. 235–243. www.ubm.ro/sites/CJEES/viewTopic.php?topicId=613

ILIĆ, M. – VRANEŠEVIĆ, M. – BEZDAN, A. – BLAGOJEVIĆ, B. 2019. Classification of Water Quality of Banat Watercourses in Serbia for the Needs of Irrigation. In Journal of Environmental Geography, vol. 12, 2019, no. 1–2, pp. 51–57. doi.org/10.2478/jengeo-2019-0006

IPCC. 2014. Climate change 2014: Synthesis report. Contribution of working groups I, II and III to the 5th Assessment Report of the Intergovernmental Panel on Climate Change. Core Writing Team, R. K. Pachauri and L. A. Meyer, edsitors. Geneva (Switzerland): IPCC; p. 151. doi:10013/epic.45156.d001

KALETOVA, T. – JURIK, L. 2018. Quality of Water Required for Irrigation. In book: The Handbook of Environmental Chemistry Water Resources in Slovakia: Part I Assessment and Development. 1st ed., Berlin, Heidelberg : Springer. doi: 10.1007/698_2017_214

LEVIDOW, L. – ZACCARIA, D. – MAIA, R. – VIVAS, E. – TODOROVIC, M. – SCARDIGNO, A. 2014. Improving water-efficient irrigation: Prospects and difficulties of innovative practices. In Agricultural Water Management, vol. 146, 2014, pp. 84–94. ISSN 0378-3774. doi.org/10.1016/j.agwat.2014.07.012

OLESEN, J.E. – TRNKA, M. – KERSEBAUM, K.C. – SKJELVÅG, A.O. – SEGUIN, B. – PELTONEN-SAINIO, P. – ROSSI, P. – KOZYRA, – MICALE J.F. 2011. Impacts and adaptation of European crop production systems to climate change. In European Journal of Agronomy, vol. 34, 2011, no. 2, pp. 96–112. ISSN 1161-0301. doi.org/10.1016/j.eja.2010.11.003

POTKONJAK, S. – ZORANOVIĆ, T. – MAČKIĆ, K. 2010. The irrigation influence on agricultural intensification in Serbia. In Economics of agriculture, International scientific meeting: Multifunctional agriculture and rural development (V) – regional specifities, Banja Vrujci, Serbia, 2nd–3rd, December 2010, special issue. Available at: www.ea.bg.ac.rs/index.php/EA/article/view/1000

REPUBLIC HYDROMETEOROLOGICAL SERVICE OF SERBIA – RHMSS. 2010-2017. Hydological yearbooks, Part III: Water Qaulity.

ROUT, R.G. – SAHOO S. 2015. Role of iron in plant growth and metabolism. In Reviews in Agricultural Science, vol. 3, 2015, pp. 1–24. doi:10.7831/ras.3.1

ROWLAND, H.A.L. – OMOREGIE, E. – MILLOT, R. – JIMENEZ, C. – MERTENS, J. – BACIU, C. – HUG, S.J. – BERG, M. 2010. Geochemistry and arsenic behaviour in groundwater resources of the Pannonian Basin (Hungary and Romania). In Applied Geochemistry, 2010. doi:10.1016/j.apgeochem.2010.10.006

VARSÁNYI, I. – KOVÁCS, L.Ó. 2006. Arsenic, iron and organic matter in sediments and groundwater in the Pannonian Basin, Hungary. In Applied Geochemistry, 2006, no. 21, pp. 49–963.

VRANEŠEVIĆ, M. – ILIĆ, M. – BEZDAN, A. 2018. Irrigation water quality of the Tamiš River. In Annals of Agronomy, vol. 42, 2018, no. 1, pp. 17–25. Available at: http://polj.uns.ac.rs/sr/node/1423

XIUFU, S. – ZINATI, G. 2005. Management of Iron in Irrigation Water. Rutgers University, New Jersey Agricultural Experiment Station: New Brunswick, New Jersey. Fact Sheet FS516. Available at: https://njaes.rutgers.edu/fs516/

sciendo

DOI: 10.2478/ahr-2019-0019

Acta Horticulturae et Regiotecturae 2/2019 *Öner Çetın, Erhan Akalp*

Acta Horticulturae et Regiotecturae 2
Nitra, Slovaca Universitas Agriculturae Nitriae, 2019, pp. 97–102

EFFICIENT USE OF WATER AND FERTILIZERS IN IRRIGATED AGRICULTURE: DRIP IRRIGATION AND FERTIGATION

Öner ÇETİN*, Erhan AKALP

Dicle University, Diyarbakır, Turkey

Increasing food demand and decreasing water resources have composed a kind of pressure to find new technologies for efficient use of water and fertilizers in agriculture. Drip irrigation can be able to save irrigation water from 30% up to 50% in case it is properly designed, installed and operated compared to surface irrigation, and it can also enable increasing crop yields and crop quality. In order to get the highest benefits using drip irrigation, some soil data (infiltration rate, soil texture and soil structure), crop characteristics (row space, plant density, canopy cover, root system, crop species, crop variety) and water resources properties (water quality, surface or well water) must be considered in drip system design, management and operation. Fertigation is basically an agricultural technique and application together with water and fertilizer to soil and/or plants. It increases both yield and fertilizer use efficiency; therefore, leaching of nutrients is prevented. In order to utilize fertigation successfully, the four main factors must be considered: (i) the consumption rate of water and nutrients throughout the growth season that result in optimal yields, (ii) response in uptake of different crops to nutrient concentration in the soil and soil solutions, (iii) monitoring for total soil water potential, nutrients concentration in soil solution and % elements in plants as a function of time and (iv) root mass and distribution in the soil for given irrigation regimes and soil types.

Keywords: nutrient use efficiency, water use efficiency, water saving, sustainability

Water is essential to grow crops, to provide food and to decrease drought risks. Irrigated agriculture globally uses more than 70% of water (Khokhar, 2017; Anonymous, 2019a). Thus, it places increasing pressure on freshwater resources, especially in developing countries. Considering demand of industrial and domestic water, the ways of efficient water use must be practiced in irrigated agriculture. Use of surface irrigation methods in the world, especially in developing countries, is still preponderant. In general, these conventional irrigation methods use water excessively. This situation is mainly dependent on the nature of these methods and farmers' conditions.

In semiarid and arid climatic conditions, increasing agricultural production is mainly dependent on irrigation. As known, the conventional irrigation methods (surface irrigation) use much more water compared to the pressurized irrigation systems such as sprinkler and drip irrigation. Increasing food demand and decreasing water resources have composed a kind of pressure to find new technologies for efficient use of water and fertilizer for agriculture. In addition, protection of soil and water resources and environmental sustainability are other crucial factors to be considered. Thus, efficient and less water and fertilizer use is significantly important in terms of environmental protection (Hagin et al., 2003).

A considerable amount of water is lost as leakage and/or evaporation during storage and transport to the fields where the crops are grown in irrigated agriculture. The runoff is also an important loss considering surface irrigation (Wallace, 2000). Thus, the most important issue on use of water resources is to minimize the amount of water used in irrigated agriculture.

In order to increase water use efficiency and to shift to a more sustainable use of water in agriculture, improvement in water use efficiency is required (Barua, Kumar and Singh, 2018). This aim can be reached by: use of water efficient irrigation systems, appropriate irrigation scheduling, watershed management development, growing drought-tolerant crops, dry farming, rotational grazing, use of mulch and compost, cover crops, conservation tillage, and organic agriculture. One of the most important ways is to shift to the pressurized irrigation systems such as drip and sprinkler irrigation. The plant root zone receives water directly into the root zone by means of these systems. However, reducing the evaporation that happens with sprinkler irrigation systems is another important issue. Therefore, the adoption of drip irrigation, low-pressure sprinkler systems, and other water saving technologies and practices, has been becoming more widespread (Üzen, Çetın and Karaer, 2013; OECD, 2010).

The aim of this review paper is to give some basic benefits, gains and rules of drip irrigation and fertigation in case those are used in irrigated agriculture.

Increasing water use efficiency in irrigated agriculture: Use of drip irrigation

Drip irrigation is a method/kind of pressurized irrigation in which water is in form of portions slowly delivered to the plant root zone using less amount of water. Studies in many countries have shown that drip irrigation can save

Contact address: Öner Çetın, Prof. Dr., Dicle University, Agricultural Faculty, Department of Agricultural Structures and Irrigation, Diyarbakır, Turkey, phone: +90 412 241 10 00, e-mail: oner_cetin@yahoo.com

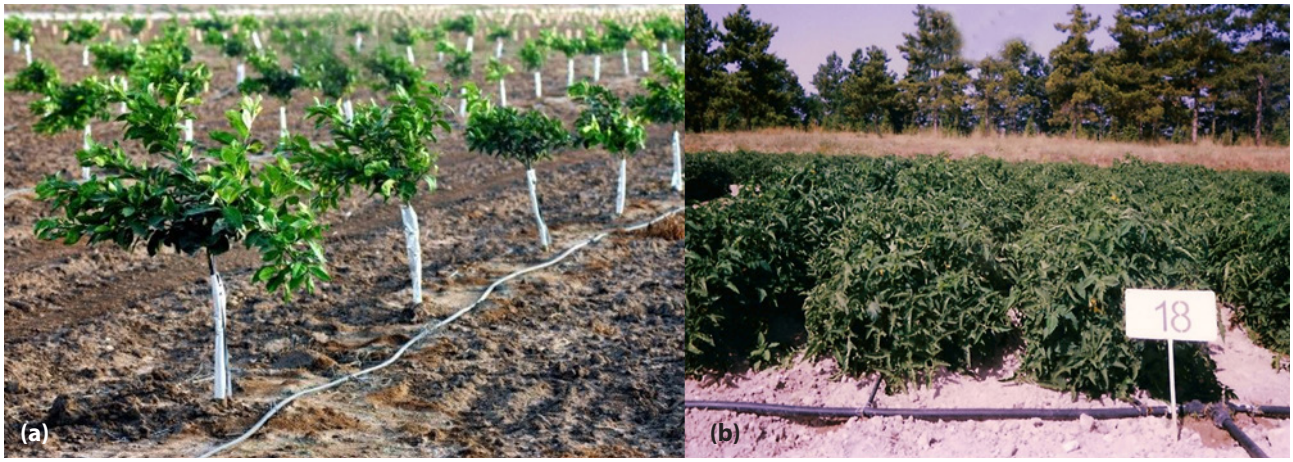

Figure 1 Use of drip irrigation for different horticultural crops. Young orange trees (a), field tomatoes (b)
Source: (a) – anonymous, 2019b; (b) – Çetın and Uygan, 2008

water use by 30% to 70% and raises crop yields by 20% to 90% depending on soil, climatic and crop characteristics, and farmers practices if it is properly designed, installed and operated (Postel et al., 2001; Çetın and Bilgel, 2002). In addition, considering water savings and higher yields by drip irrigation, water use efficiency also increases at least by 50% (Chartzoulakis and Bertaki, 2015).

At first, drip irrigation was mainly started to be used for horticultural (Fig. 1) and ornamental plants (Fig. 2). Then, it has been used for all kind of crops including field crops (Fig. 3), landscape and forest plants. (Stein, 2019). Drip irrigation enables a way of making sure each plant gets exactly the amount of water it needs, because it uses flexible tubing and/or pipes such as PE connected to individual drippers, or emitters. The drippers are placed at the root zone of each plant and apply a specific or certain amount of water in every irrigation cycle.

Table 1 shows how much irrigation water could be saved compared to the surface irrigation. The resulting efficiency, of course, depends on climatic, soil and crop characteristics and farmer practices. Thus, water saving ratio can vary depending on these conditions.

The advantages of drip irrigation could be specified as water saving (30–50%), higher crop yield, maximum utilization of available water, no water being available for weeds, high efficiency in the use of fertilizers, less weed growth, lower labour, no soil erosion, possible sophisticated automatic control, no runoff, no leaching of fertilizers into ground water, and less evaporation losses compared to surface irrigation. However, drip irrigation has some limitations such as clogging, salinity hazards at the top of soil profile for arid and semi-arid regions, higher investment costs compared to surface irrigation, higher skills and

Table 1 Efficiency of drip irrigation when compared to surface irrigation

Crop	Yield (kg.ha^{-1})			Irrigation		
	surface	drip	increase (%)	surface	drip	saving (%)
Beet root	570	880	54	86	18	79
Bitter gourd	3,200	4,300	34	76	33	57
Potato	17,200	29,100	69	60	28	54
Cucumber	4,230	6,090	44	109	42	62
Broccoli	14,000	19,500	39	70	60	14
Chili	17,100	27,400	60	27	18	33
Pomegranate	3,400	6,700	97	21	16	24
Okra	15,500	22,500	45	54	24	56
Onion	28,400	34,200	20	52	26	50
Tomato	6,180	8,870	44	50	11	79
Sweet potato	4,240	5,890	39	63	25	60
Banana	57,500	87,500	52	176	97	45
Watermelon	8,210	50,400	514	72	25	65
Grapes	26,400	32,500	23	53	28	47

Source: Shah, 2011

Figure 2 Use of drip irrigation for ornamental plants
Source: Anonymous, 2019c

Figure 3 Use of subsurface (a) and surface drip (b) drip irrigation on field crops such as cotton
Source: Çetın et al., 2018

experiences required for its design, install, operation and management.

In order to get the highest benefits using drip irrigation, some soil data (infiltration rate, soil texture and soil structure), crop characteristics (row space, plant density, canopy cover, root system, crop species, crop variety) and water resources properties (water quality, surface or well water) must be considered for drip system design, management and operation. Among others, the lateral design, dripper discharge, dripper space and requirement of energy are the most important components of drip irrigation system design.

The main problems in the use of drip irrigation systems are physical (sand and suspended solids) biological (bacteria, fungi and algae, slime) and chemical causes (mineral precipitation,- lime content of water) of emitter clogging. The common elements are calcium, magnesium, iron and manganese that may clog drip emitters by precipitation and sedimentation.

The most important irrigation water parameters in use of drip irrigation systems are content of suspended solids, dissolved solids, iron, manganese and bacteria (total plant count/ml), pH, hardness (as $CaCO_3$).

Use of fertilizers together with irrigation: Fertigation

Fertigation is basically defined as an application of fertilizers in irrigation water by means of irrigation systems. Fertigation has become a common practice in modern irrigated agriculture. Localized irrigation systems such as drip irrigation enable higher efficiency of water and fertilizer use. Considering the conventional fertilizing, this technique has got many advantages and is a kind of modern technology. Thus, the combined irrigation and fertilization has been widely used for the cultivation of crops and fruit orchards all over the world (Yan, Dai and Jia, 2018). Drip irrigation is more appropriate for applying fertigation. Thus, the soluble fertilizers at any concentrations needed by crops can be applied through irrigation systems to wetted zones of soil (Chartzoulakis and Bertaki, 2015).

Fertigation can be practiced for any irrigation system. However, fertilizers applied by surface irrigation and open canals might be inappropriate for nutrient distribution in the field. Fertigation can be applied as an integral part of

plant nutrient management and specifically under micro-irrigation, because such systems provide a concentrated and space-limited root system within the wetted soil volume and fertigation can ensure the optimum plant nutrition. On the other hand, soluble N fertilizers such as urea, ammonium sulphate, ammonium nitrate, and liquid urea are easily injected and applied through drip and microsprinkler systems and are commonly used for fertigation in vine and tree fruit crops (Schwankl, Hanson and Prichard, 1998; Bar-Yosef, 1999; Kafkafi and Tarchitsky, 2011).

The advantages of fertigation could be mentioned such as healthier plants, quick delivery of nutrients to plant roots, nutrient requirements can be adjusted with immediate effects, uniform distribution and precision application for nutrients, less labour, less water use, reduced runoff, increasing fertilizer use efficiency and nutrient availability, saving about 20–40% of fertilizer without affecting growth and yield of crops, saving labour and energy in application of fertilizer, reducing environmental contamination and leaching of nutrients. Additionally, fertigation prevents losses of nitrogen due to the fact that there is no leaching, because nutrients are directly supplied to root zone in available forms in the form of portions. Thus, nutrient concentration in soil solution can be controlled and application cost decreased.

Possible disadvantages and/or limitations of fertigation are higher initial investment cost, some inappropriate chemical reactions in the equipment of drip irrigation and fertigation, corrosion and precipitation of fertilizer and clogging of emitters. In addition, some other limitations can occur such as non-uniform fertilizers/nutrients distribution, the over-fertilization in case that irrigation is not based on actual crop requirements and the excessive use of soluble fertilizers (Chartzoulakis and Bertaki, 2015).

Fertigation is associated and/or considered together with irrigation engineering, soil science, plant nutrition, fertilization (soil physics, soil chemistry, soil biology, plant nutrition, soil fertility and fertilizer) and plant physiology. Thus, affecting factors of fertigation can be specified such as soil texture, plant root system, dripper discharge and dripper space, irrigation time, wetting area, fertigation injection rate, water quality, crop canopy cover and crop yield. In the case that all these conditions are taken into consideration, an appropriate and/or desirable quality and benefits could be provided by fertigation.

In addition, in order to utilize fertigation successfully, the four main factors must be considered:

a) the consumption rate of water and nutrients throughout the growth season that results in optimal yields;
b) response in uptake of different crops to nutrient concentration in the soil and soil solutions;
c) monitoring of total soil water potential, N concentration in soil solution and amount of elements in plants as a function of time;
d) root mass and distribution in the soil for given irrigation regimes and soil types.

Application methods and devices of fertigation

The application of fertilizers in fertigation can occur:

a) with gradual decrease;
b) constantly during the entire irrigation;
c) during a part of irrigation;
d) with intermitted chemical concentration (Manor et al., 1983).

Thus, different injection equipment can be used such as by-pass (closed tank) system, venturi (suction) and a hydraulic or external pump to apply different fertigation application methods. Fig. 4 shows the trend of fertilizer concentration in irrigation water during irrigation according to the application methods of fertigation.

The application devices of fertigation have got some different advantages and disadvantages. The advantages in use of the by-pass (closed tank) system are:

a) very simple operation;

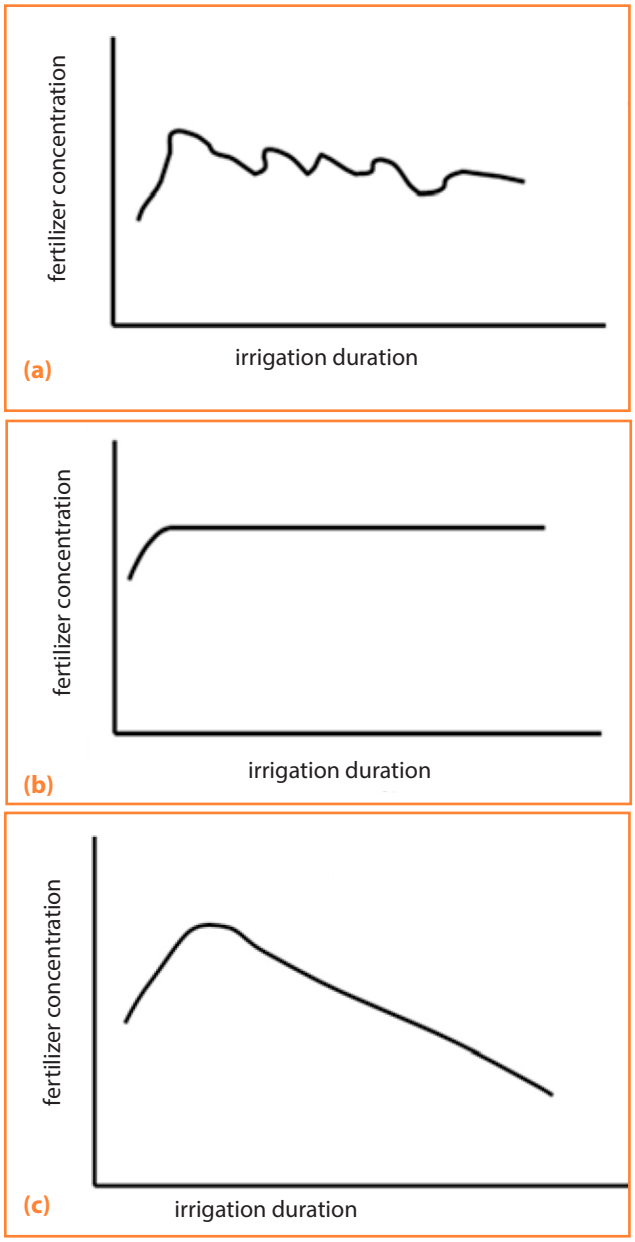

Figure 4 Distribution of fertilizer concentration in irrigation water during irrigation according to the application devices of fertigation
(a) venturi (suction) (b) external pumps and (c) pressure differential injection (closed tank, by-pass)

b) the stock solution does not need to be pre-mixed;
c) easy to install and not much maintenance needed;
d) it is not difficult to change fertilizers;
e) suitable for dry formulations;
f) no need of another energy source such as electricity or fuel.

The limitations in use of by-pass tank system are:

a) decreasing fertilizer concentration as fertilizer dissolves;
b) accuracy of application is not high.

There is some pressure loss in main irrigation line, proportional fertigation and equal concentration maintenance during irrigation is not possible, it is not suitable for automation. This system has been used commonly because of some advantages given above. The system was used successfully in different field crops such as silage corn and cotton (Yolcu and Çetın, 2015; Üzen and Çetın, 2016). Venturi (suction) device does not need an external energy (pressure) source to operate, its cost is relatively lower compared to other fertigation devices and it is easily connected to computer systems. However, its limitations include pressure loss in main irrigation line and the difficulty of quantitative fertigation and automation. The external pumps provide very accurate and proportional fertigation. There is no pressure loss in irrigation line and it is very suitable for automation. Disadvantages of this device are complicated design, it is expensive and requires more skills and experiences.

Basic rules for fertigation

Some basic rules for fertigation could be specified as below (Burt, 1998):

– Fill the mixing tank (container) with about 50–75% of the required amount of water to be used in the mix for dry and soluble fertilizers.
– Add the liquid fertilizers to the water in the mixing container before adding dry and soluble fertilizers. The additional fluid will create some heat in case the dry fertilizers have the characteristic of making solutions cold.
– Add the dry materials slowly with dispersion or shaking to prevent the formation of large, insoluble or slowly soluble lumps.
– Do not put water into acid, put acid into water.
– When chlorinating water with chlorine gas, chlorine is added into water.
– An acid or acidified fertilizer with chlorine is never mixed, whether the chlorine is in the gas form or the liquid form such as sodium hypochlorite. A toxic chlorine gas will form. Never store acids and chlorine together in the same room.
– Do not attempt to mix either anhydrous ammonia or aqua ammonia directly with any kind of acid. The reaction is violent and immediate.
– Do not attempt to mix concentrated fertilizer solutions directly with other concentrated fertilizer solutions.
– Do not mix a compound containing sulfate with another compound containing calcium. The result will be a mixture of insoluble gypsum.
– Always check with the chemical supplier for information about insolubility and incompatibility.
– Be extremely cautious about mixing urea sulfuric fertilizers with most other compounds. Urea sulfuric is incompatible with many compounds.
– Many incompatibility problems tend to disappear if chemicals are spoon-fed.
– Do not mix phosphorus containing fertilizers with another fertilizer containing calcium without first performing the jar test.
– Extremely hard water (containing relatively large amounts of calcium and magnesium) will combine with phosphate, neutral polyphosphate or sulfate compounds to form insoluble substances.

Conclusion

It can be assumed that because of its advantages, mainly drip irrigation systems should be used for conservation and sustainability management of soil and water resources. Drip irrigation provides more crops per drop and it saves about 30–50% of water. Thus, a major increase in water use efficiency and reduction in land and water degradation is essential. All researches, studies and approaches showed that increasing water use efficiency in irrigated agriculture is inevitable considering climatic change, drought conditions and decreasing water resources. This could be achieved mainly by use of drip irrigation. However, drip irrigation systems must be designed and installed considering soil and crop characteristic, and if operated appropriately, higher water use efficiency and higher benefits can be obtained. In addition, fertilizers and chemicals can be applied in safe and desired concentrations. Taking into account fertigation and drip irrigation, both of them could markedly improve availability and absorption of water and nutrients in soil, resulting in substantial increase of crop production and quality. Design, management, operation and maintenance of drip irrigation and fertigation need much more data on soil and crops, and higher skills and experiences. If all these conditions are taken into consideration, the maximum benefit can be obtained by use of drip irrigation and fertigation.

References

ANONYMOUS. 2019a. Water and agriculture. [online], cit. [2019-08-10]. Available at: https://blogs.worldbank.org/opendata/chart-globally-70-freshwater-used-agriculture

ANONYMOUS. 2019b. [online], cit. [2019-08-10]. Available at: oxfarmorganic.com

ANONYMOUS. 2019c. [online], cit. [2019-08-10]. Available at: greenmylife.in

BARUA, S. – KUMAR, R. – SINGH, S.P. 2018. Water saving techniques in agriculture. [online], cit. [2019-03-19]. Available at: https://www.indiawaterportal.org/articles

BAR-YOSEF, B. 1999. Advances in fertigation. In Adv. Agron, 199, no. 65, pp. 1–77.

BURT, M.C. 1998. Fertigation Basics. Irrigation Training and Research Center (ITRC), ITRC Paper 98-001. San Luis Obispo, CA, USA : California Polytechnic University, 1998.

ÇETIN, Ö. – ÜZEN, N. – TEMIZ, M.G. – BAŞBAG, S. 2018. Comparison

of surface and sub-surface drip irrigation and real-time irrigation scheduling based on FAO-56-Penman-Monteith for cotton. Final Project Report, Project No: TUBITAK 115O600, Ankara, Turkey (with an English abstract in Turkish).

ÇETIN, O. – UYGAN, D. 2008. The effect of drip line spacing, irrigation regimes and planting geometries of tomato on yield, irrigation water use efficiency and net return. In Agric. Wate. Manage., vol. 95, 2008, no. 8, pp. 949–958.

ÇETIN, O. – BILGEL, L. 2002. Effects of different irrigation methods on shedding and yield of cotton. In Agric. Wate. Manage, vol. 54, 2002, no. 1, pp. 1–15.

CHARTZOULAKIS, K. – BERTAKI, M. 2015. Sustainable water management in agriculture under climate change. In Agriculture and Agricultural Science Procedia, 2015, no. 4, pp. 88–98.

HAGIN, J. – SNEH, M. – LOWENGART-AYCICEGI, A. 2003. Fertigation, Fertilization through Irrigation. International Potash Instituıte, IPI Research Topics, Basel, Switzerland, 2003, no. 23.

KAFKAFI, U. – TARCHITSKY, J. 2011. Fertigation. A tool for efficient fertilizer and water management. Intl. Fert. Ind. Assn., Paris, France and Intl. Horgen, Switzerland : Potash Inst. 2011.

KHOKHAR, T. 2017. Globally, 70% of freshwater is used for agriculture. Available at: https://blogs.worldbank.org/opendata/chart-globally-70-freshwater-used-agriculture

MANOR, S. – LOWENGART, A. – BRUM, M. – HAZAN, A. – BAR, I. – GEVA, S. 1983. The technology of chemigation: Uniformity of Distribution in the Irrigation. In 3rd International Conference on Irrigation, Tel-Aviv, Israel, 3–6 October, 1983.

OECD. 2010. Sustainable Management of Water Resources in Agriculture. ISBN 978-92-64-08345-5 (print). DOI 10.1787/9789264083578-en

POSTEL, S. – POLAK, P. – GONZALES, F. – KELLER J. 2001. Drip irrigation for small farmers. A new initiative to alleviate hunger and poverty. In Water Intern., vol. 26, 2001, no. 1, pp. 3–13.

SCHWANKL, L. – HANSON, B. – PRICHARD, T. 1998. Micro-irrigation of trees and vines: A handbook for water managers. Publ. 3378. Oakland, CA : Div. Agr. Natural Resources, Univ. Calif., 1998.

SHAH, S.K. 2011. Towards Adopting Nanotechnology in Irrigation. Micro Irrigation Systems. Karnataka, India : India Water Portal, 2011.

STEIN, L.A. 2019. Drip irrigation: Salvation for the gardener. Texas AgriLife Extension Service. Texas, USA : Texas A & M University, College Station, 2019.

ÜZEN, N. – ÇETIN, Ö. – KARAER, M. 2013. Micro Irrigation for Modern Agriculture. 1st Central Asia Congress on Modern Agricultural Techniques and Plant Nutrition, Bishkek, Kyrgyzstan, 01–03 October, 2013, pp. 2131–2138.

ÜZEN, N. – ÇETIN, Ö. 2016. Effects of nitrogen fertigation frequency on yield and nitrogen retention in drip-irrigated cotton. In Journal of Plant Nutrition, vol. 39, 2016, no. 14, pp. 2126–2135.

WALLACE, J.S. 2000. Increasing agricultural water use efficiency to meet future food production. In Agriculture, Ecosystems and Environment, 2000, no. 82, pp. 105–119.

YAN, X.L. – DAI, T.F. – JIA, L.M. 2018. Evaluation of the cumulative effect of drip irrigation and fertigation on productivity in a poplar plantation. In Annals of Forest Science, 2018, no. 75, p. 5.

YOLCU, R. – ÇETIN, Ö. 2015. Nitrogen fertigation to improve nitrogen use efficiency and crude protein on silage corn. In Turk J Field Crops, vol. 20, 2015, no. 2, pp. 233–241.